Imperial College London

Synchronisation Phenomena with Time Delay

A thesis presented for the degree of

Doctor of Philosophy of Imperial College London

and the

Diploma of Imperial College

by

Seng Cheang

Department of Mathematics

Imperial College

180 Queen's Gate, London SW7 2BZ

JULY 18, 2014

I certify that this thesis, and the research to which it refers, are the product of my own work, and that any ideas or quotations from the work of other people, published or otherwise, are fully acknowledged in accordance with the standard referencing practices of the discipline.

Signed: S Cheang

Copyright

To my loving parents,

and my dear friends for their encouragement and support.

Abstract

I study a simple model of synchronisation proposed by Jensen (2008). The relevant degrees of freedom are expected to be strictly increasing functions of time, such as the total angle swept out by an oscillator. The model is rooted in Winfree's mean-field model for spontaneous synchronisation; some of Winfree's basic assumptions, such as identical or nearly identical dynamics and identical couplings, are therefore retained. I investigated the behaviour of the present model with respect to synchronisation without and in the presence of time delay.

The mathematical treatment focuses on characterising the synchronised state as either attractive or repulsive, producing a theory (which ultimately leads to a phase diagram) that compares well with numerics. I employed a perturbative approach, linearising in small time delays and small phase differences. The interaction between individual oscillators is captured by an interaction matrix, which does not require further approximation, i.e. lattice structure enters exactly. To link with established results in the literature, a mean field theory, however, is also studied.

The main result is that these typically systems synchronise due to a time delay.

Acknowledgements

I would like to express my gratitude to Dr. Gunnar Pruessner for his continuous support, guidance and enormous patience. I have been very fortunate to work with him in various aspects of Mathematics, especially in Complexity. It is my pleasure to have worked under his tutelage in such exciting field. I am deeply grateful for all the time we have spent together that I have learnt many invaluable lessons. My association with Dr. Pruessner has helped me grew not only as a researcher but also as an individual.

I would like to express my thanks to Prof. Henrik J. Jenson for his kindness to have spent time on many deep and intrinsic discussions we had. Prof. Jenson also introduced me to the Complexity group, where many other researches around the world discuss and collaborate, at Imperial College London which had definitely helped me become a better individual researcher.

I would like to thank Prof. Chew Lock Yue (Nanyang Technological University, Singapore) for hosting an exchange between Nguyen Huynh and myself so that we have different experience in similar fields under different environment and culture.

I would like to thank the staff at Mathematics department, especially Prof. John Elgin, Prof. Darryl Holm, Dr. Dan Moore, Prof. Andy Parry for their patience and help from time to time; Chris Sisson for giving me opportunity to be a great teaching assistant; Andy Thomas for his endless help on computing issues across different operating systems; also Mary Harvey and Tina Senkiw for theirs lifesharing talks and laughs which had made my life at Imperial remarkable and more interesting.

I also would like to thank my dear friends whom have given me support and strength throughout these years.

Last but not least, I want to thank my loving parents for their enormous support and their belief in me. When I face any hurdles, it was their support and love took me through them. I would have never accomplished this without them.

Seng

Table of contents

List of Figures

List of Tables

List of Publications

[13] Cheang S. and Pruessner G. *The Edwards–Wilkinson equation with drift and Neumann boundary conditions* J. Phys. A: Math. Theor. 44 (2011) 06503.

[54] Pruessner G., Cheang S. and Jensen H. *Doppler synchronization of pulsating phases by time delay*, in preparation. A copy can be found on http://arxiv.org/abs/1212.2746.

Abstract:

"Synchronization by exchange of pulses is a widespread phenomenon, observed in flashing fireflies, applauding audiences and the neuronal network of the brain. Hitherto the focus has been on integrate-and-fire oscillators. Here we consider entirely analytic time evolution. Oscillators exchange narrow but finite pulses. For any non-zero time lag between the oscillators complete synchronization occurs for any number of oscillators arranged in interaction networks whose adjacency matrix fulfils some simple conditions. The time to synchronization decreases with increasing time lag."

Chapter 1

Introduction

The first four paragraphs of this section are a summary of the introduction of the book "*Synchronisation : A universal concept in nonlinear science*." by Pikovsky et al. [51]. Originating from the Greek words $\sigma\upsilon\nu$ (syn), meaning together, and $\chi\rho\upsilon\nu\sigma\varsigma$ (chronos), meaning time; the word "synchronisation" means "together in common time". Synchronisation is defined as the state when a system of oscillating objects operates in unison by adjusting their frequencies due to their weak interaction.

Dating back as far as the seventeenth century, the synchronisation phenomenon was first observed and described by the Dutch researcher Christiaan Huygens, who became aware of the synchronous behaviour between two clocks on his wall while he was sick in bed. This discovery can be found in a collection of his letters and papers, which were reprinted in 1967 [26]. In one of his letters to his father, Constantyn Huygens, of 26 February 1665, Christiaan Huygens [27] wrote: "The two clocks, while hanging [on the wall] side by side with a distance of one or two feet between, kept in pace relative to each other with a precision so high that the two pendulums always swung together, and never varied." (translation from Pikovsky et al. [51].)

For centuries, synchronisation was also known to occur in biological systems. In 1729, the first observation of biological synchronisation was made by Jean-Jacques d'Ortous de Mairan [17], who discovered that the leaves of haricot beans will move up and down in unison despite the change of environment. This phenomenon was further developed into

a formal study of circadian rhythm, which is now well known as biological clocks in living systems.

Over half a century ago, a synchronisation phenomenon in acoustical systems was observed by John William Strutt [Lord Rayleigh] - successor of Maxwell as the Cavendish professor of experimental physics at Cambridge. Rayleigh [56] had not only observed mutual synchronisation or unison in sound in two distinct but similar pipes, he also discovered the effect of quenching, or oscillation death, which is when the coupling of the interacting system actually suppresses the oscillations. Further investigations of synchronisation were done by various mathematicians and physicists, including Engelbert Kaempfer [32], Edward Appleton [3, 4] and Balthasar van der Pol [3, 68].

A theoretical breakthrough came about in 1966 when A. Winfree pointed out that the oscillators will remain in the vicinity of their limit cycles at all times if the oscillators are weakly coupled. Therefore, one may ignore the amplitude variations and only consider the oscillator phase variations. In order to coalesce the oscillators are identical and the difference among the oscillators, Winfree assumed that the natural frequencies of the oscillators are drawn from a narrow probability density.

In recent decades, scientists have discovered many more populations of chemical and biological oscillators that display mutual synchronous behaviour, and realised that synchronisation phenomena are abundant in science and nature. Many of these authors also looked into the stability analyses of synchronisation. These analyses are based on Hopf bifurcation as Hopf bifurcation gives a good description of the transition when the system is driven away from its rest point. Frequently, one finds the rest state splits into two branches, namely the unstable rest state and the stable oscillation.

In particular, in 1975, Peskin proposed a highly schematic model on a cluster of 10,000 sinoatrial nodes symbolising the heart's natural pacemaker. Peskin stated two provocative conjectures about his model: (i) the system will always turn out in synchrony; (ii) synchronisation will occur even when the oscillators are not identical. However, Peskin was able to prove only his first claim in the simplest possible case of considering two identical oscillators, via an idea introduced by Henri Poincaré. Later on, Strogatz and

Mirollo [66] invested their time in Peskin's work and they were able to show numerically that the system will end up synchronised. From their numerical results, Strogatz and Mirollo reviewed Peskin's work and suggested a more abstract model for the individual oscillators. They proved that for any given initial condition and any arbitrary number of oscillators, their generalised system will always become synchronised via the absorption method, which means a sequence of absorptions will eventually lock all the oscillators.

Other examples, mostly mentioned and cited by Strogatz [43], include collective properties in clusters of pancreatic beta-cells [61, 62], the pacemaker cells of the heart [29, 42, 50], menstrual synchrony [30, 57] and kinematic cues [16, 60]. One of the most spectacular examples of synchronisation in nature is the flashing in synchrony of fireflies on an unbroken line of mangrove trees in the middle of the night in Thailand [63].

1.1 The Winfree Model

It was not until 1967 that the mathematical aspect of mutual synchronisation or collective behaviour of limit-cycle oscillators was formulated by Winfree. Winfree studied numerical synchronisation of a population of coupled phase oscillators with different natural frequencies by modelling the interaction strength with a coupling constant [70, 71]. Winfree observed that, for the spread of natural frequencies under certain critical values, coherent behaviour emerged for some couplings.

The Winfree model [70], which describes collective locking in an ensemble of oscillators to a single frequency, is defined as

$$\dot{\theta}_i = \omega_i + \frac{K}{N} \sum_{j=1}^{N} P(\theta_j) R(\theta_i) \tag{1.1}$$

for $i = 1, ..., N$, where $N \gg 1$. $\theta_i(t)$ is regarded as the phase of the i^{th} oscillator at time t; and ω_i is the corresponding natural frequency of the i^{th} oscillator drawn from a symmetric, unimodal density $g(\omega_i)$. K is the coupling strength, which is constant. The j^{th} oscillator makes its presence felt through as influence function $P(\theta_j)$ while the i^{th} oscillator responds to the average influence of the whole population according to a sensitivity function $R(\theta_i)$.

Recently, Ariaratnam and Strogatz [6] suggested an analytically solvable version of Winfree model by considering

$$P(\theta) = 1 + \cos(\theta), \quad R(\theta) = -\sin(\theta) \tag{1.2}$$

with $P(\theta)$ a smooth but pulse-like function. This type of pulse-like coupling is commonly found in biological systems such as flashing fireflies. In addition, Ariaratnam and Strogatz draw the natural frequencies ω_i from a symmetric, unimodal density $g(\omega_i)$ with mean equal to 1, and the width of $g(\omega_i)$ is characterised by a parameter γ. The particular form of $R(\theta_i)$ is chosen for its mathematical tractability [6].

Ariaratnam and Strogatz performed bifurcation analysis of the Winfree model by

characterising the collective behaviour and the bifurcations of the Winfree model as a function of two parameters, namely the coupling strength and the spread of natural frequencies. Ariaratnam and Strogatz [6] found that there exists states of oscillators other than incoherence, frequency locking, and oscillator death; which are the hybrid states combining two or more of the three mentioned. Ariaratnam and Strogatz also found analytically the boundaries of these hybrid states, namely the partial locking and the partial death states.

In order to classify the oscillators being frequency locked or not, they define p_i, the rotation number $p_i = \lim_{t\to\infty} \frac{\theta_i(t)}{t}$. If two or more oscillators have the same rotation number the oscillators are frequency locked. From the analysis of bifurcation, Ariaratnam and Strogatz [6] found that (i) the long-term behaviour of the system was independent of the initial conditions; (ii) the partial death state, where the slower oscillators having their frequencies and amplitudes suppressed and faster oscillators remain incoherent, bifurcates from incoherence along the straight line $\kappa = 1 - \gamma$, which holds for all symmetric or asymmetric frequency distribution $g(\omega)$; (iii) the boundary between death, when coupled oscillators approaching a stable rest state, and partial death corresponds to an endpoint bifurcation; (iv) a saddle-node bifurcation is responsible on the separation of death from full and partial locking, where some coupled oscillators are frequency locked but faster oscillators remain incoherent; (v) the boundary between locking and partial locking is determined numerically.

If we consider the analytically solvable Winfree model as suggested by Ariaratnam and Strogatz [6]; we can write the governing equation as

$$\dot{\theta}_i(t) = \omega_i + \sigma(t)\sin(\theta_i(t)) \tag{1.3}$$

where $\sigma(t) = K(1 + X(t))$ is the effective coupling with the order parameter $X(t) = \frac{1}{N}\sum_{j=0}^{N}\cos(\theta_j(t))$. According to Basnarkov and Urumov [10] the order parameter $X(t)$ is an appropriate macroscopic observable for the state of the population. One can see that if there is no ordering established, the effective coupling is K and the effective coupling approaches $2K$ as coherence develops.

If we now consider the system in steady state [1], where the effective coupling $\sigma(t) = \sigma_0$ is constant, we introduce the density function, $\rho(\theta, t, \omega)$, of drifting oscillators as the probability to find a drifting oscillator at θ at time t conditional to it having frequency ω. In the limit $N \to \infty$ we express the population using this density function. For example the order parameter can be expressed as

$$X(t) = \int \int \rho(\theta, t, \omega) g(\omega) \cos(\theta) \mathrm{d}\theta \mathrm{d}\omega \ . \tag{1.4}$$

Consider the continuity equation with velocity $u = \omega - \sigma_0 \sin(\theta)$. The distribution ρ is trivially stationary if the velocity u is zero, otherwise if the distribution ρ is stationary if $\rho u = C$ where C is a constant, which implies

$$\rho(\theta, \omega) = \frac{C}{u} = \frac{C}{\omega - \sigma_0 \sin(\theta)}$$

and quantify the normalisation constant C, we solve for C with the normalisation condition using tangent half-angle substitution and the substitution $X = \frac{1}{A}\left[\omega \tan\left(\frac{\theta}{2}\right) - \sigma_0\right]$, then $\mathrm{d}X = \frac{\omega}{2A}\left[1 + \tan^2\left(\frac{\theta}{2}\right)\right] \mathrm{d}\theta$ where C subjects to the condition that $A^2 = \omega^2 - \sigma_0^2$ the integral is then

$$\begin{aligned}
1 &= C \int_{-\pi}^{\pi} \frac{1}{\omega - \sigma_0 \sin(\theta)} \mathrm{d}\theta = C \int \frac{1}{\omega - \sigma_0 \frac{2\tan\left(\frac{\theta}{2}\right)}{1+\tan^2\left(\frac{\theta}{2}\right)}} \frac{2A}{\omega} \frac{1}{1 + \tan^2\left(\frac{\theta}{2}\right)} \mathrm{d}X \\
&= C \int \frac{2A \mathrm{d}X}{\omega^2\left[1 + \tan^2\left(\frac{\theta}{2}\right)\right] + 2\omega\sigma_0 \tan\left(\frac{\theta}{2}\right)} = C \int \frac{2A \mathrm{d}X}{(AX - \sigma_0)^2 + \omega^2 + 2\sigma_0 (AX - \sigma_0)} \\
&= \frac{2C}{\sqrt{\omega^2 - \sigma_0^2}} \left[\lim_{\theta \to \pi} \arctan\left(\frac{\omega \tan\left(\frac{\theta}{2}\right) - \omega}{\sqrt{\omega^2 - \sigma_0^2}}\right) - \lim_{\theta \to -\pi} \arctan\left(\frac{\omega \tan\left(\frac{\theta}{2}\right) - \omega}{\sqrt{\omega^2 - \sigma_0^2}}\right)\right] \\
&= \frac{2\pi C}{\sqrt{\omega^2 - \sigma_0^2}}
\end{aligned}$$

yields normalised distribution

$$\rho(\theta, \omega) = \frac{1}{2\pi} \frac{\sqrt{\omega^2 - \sigma_0^2}}{\omega - \sigma_0 \sin(\theta)} \ . \tag{1.5}$$

[1] A more detailed explanation will be stated in the Kuramoto section, Section 1.2.

1.1.1 Order parameter analysis in terms of coupling strength

A situation when the slower oscillators having their frequencies and amplitudes suppressed, *i.e.* stop moving altogether, and faster oscillators remaining incoherent, is referred to as partial death [6, 10, 46]. The corresponding phases of the phase-locked oscillators are $\theta^* = \arcsin\left(\frac{\omega}{\sigma_0}\right)$ where $\omega_{\min} \leq \omega \leq \sigma_0$. This is the case because if $\omega_{\min} > \sigma_0$ holds then the natural frequencies will always dominate and the oscillators will stay incoherent. The distribution of the phase-locked oscillators ρ_L is then given by a delta function [9]

$$\rho_L = \delta\left[\theta - \arcsin\left(\frac{\omega}{\sigma_0}\right)\right] . \tag{1.6}$$

Then we calcuate the contribution of these phase-locked oscillators to the order parameter by use of change of variables

$$X_L = \int\int \delta\left[\theta - \arcsin\left(\frac{\omega}{\sigma_0}\right)\right]\cos(\theta)g(\omega)\mathrm{d}\theta\mathrm{d}\omega = \int_{\omega_{\min}}^{\sigma_0}\sqrt{1-\frac{\omega^2}{\sigma_0^2}}g(\omega)\mathrm{d}\omega \ .$$

Now we consider the contribution of the drifting oscillators

$$\begin{aligned} X_D &= \int\int \frac{1}{2\pi}\frac{\sqrt{\omega^2-\sigma_0^2}}{\omega-\sigma_0\sin(\theta)}\cos(\theta)g(\omega)\mathrm{d}\theta\mathrm{d}\omega \\ &= \int \frac{\sqrt{\omega^2-\sigma_0^2}}{2\pi}g(\omega)\mathrm{d}\omega\int_0^{2\pi}\frac{\cos(\theta)}{\omega-\sigma_0\sin(\theta)}\mathrm{d}\theta = 0 \ . \end{aligned}$$

To understand the behaviour of the system near the critical point, we assume the difference between σ_0 and $\omega_{\min}$ is small, *i.e.* $\delta\sigma = \sigma_0 - \omega_{\min}$ [10]. Due to the fact that the drifting oscillators do not contribute to the order parameter, so if we let $\epsilon = \sigma_0 - \omega$, and by changing variables to ϵ

$$\begin{aligned} X = X_L &= \int_0^{\delta\sigma}\sqrt{1-\left(\frac{\sigma_0-\epsilon}{\sigma_0}\right)^2}g(\sigma_0-\epsilon)\mathrm{d}\epsilon = \frac{1}{\sigma_0}\int_0^{\delta\sigma}\sqrt{2\sigma_0\epsilon-\epsilon^2}g(\sigma_0-\epsilon)\mathrm{d}\epsilon \\ &\approx \frac{1}{\sigma_0}\int_0^{\delta\sigma}\sqrt{2\sigma_0\epsilon}g(\sigma_0)\mathrm{d}\epsilon = \frac{2\sqrt{2}g(\sigma_0)}{3\sqrt{\sigma_0}}(\delta\sigma)^{\frac{3}{2}} \end{aligned}$$

Therefore near the inception of partial death, the order parameter is

$$X \sim (\delta\sigma)^{\frac{3}{2}} g(\sigma_0) = (\sigma_0 - \omega_{\min})^{\frac{3}{2}} g(\sigma_0) \ . \tag{1.7}$$

In order to find the relationship between the order parameter X and the coupling parameter K, one considers the vicinity of inception of oscillation death, then $\sigma_c \approx K_c$ (subscript c refer to the critical value of the corresponding parameter), where oscillation death is caused by excessively strong coupling. In the steady state, if we consider a coupling strength which is slightly greater than the critical coupling strength, *i.e.* $K = K_c + \delta K$, then subsequently the effective coupling will also be increased, say $\sigma_0 = \sigma_c + \delta\sigma$. Using the relation that $\sigma(t) = K(1 + X(t))$ in conjunction with the fact that we are in the inception of oscillation death, then $\delta\sigma \approx \delta K$. Therefore

$$X \sim (K - K_c)^{\frac{3}{2}} g(\sigma_0) \ . \tag{1.8}$$

The ultimate simplication of the Winfree model is that each oscillator is influenced by the collective behaviour of the rest. Winfree found that the width of the frequency distribution governs the system's behaviour. The system deteriorates when the spread of the frequencies is large compared with the coupling, and the system will spring into synchrony if the spread decreases below a critical value. However, a surprising phenomenon was observed by Winfree [71] on an electrical firefly simulation which was established on an accumulative voltage until threshold then discharges abruptly. Winfree discovered that synchronisation will never be achieved if oscillators were coupled equally to one another through a common resistor, regardless of the strength of the coupling. This observation has established the foundation of pulse-coupled, or integrate-and-fire, biological oscillators and many other similar fields.

1.2 The Kuramoto Model

Despite Winfree model's historical importance the Winfree model has its limitations. It is complex enough not to grant a full treatment analytically, yet it is not sufficiently sophisticated to allow for the treatment of realistic systems. The former limitation overcame by Kuramoto [37, 39] by subsequently refining the Winfree model. This simplification, by introducing a mathematically tractable model, grants us access to understand populations of collective behaviour of coupled oscillators. The Kuramoto model, which can be solved analytically in the mean-field approximation, is a generic and powerful mathematical model which can be used to examine the theoretical effects of temporal organisation phenomenon in living systems, particularly in chemical, hydrodynamical, and mechanical processes.

In 1974 when Kuramoto and Tsuzuki [39] found that a temporarlly organised system may be represented by a population of N self-sustained oscillators Q_i with different natural frequencies ω_i satisfying the following equations of motion

$$\dot{Q}_i = (i\omega_i + \alpha)Q_i - \beta|Q_i|^2 Q_i \tag{1.9}$$

with $\alpha, \beta > 0$. In particular, they considered a distribution $g(\omega_i)$ of ω_i, where $g(\omega_i)$ is a Lorentzian

$$g(\omega_i) = \frac{1}{\pi\gamma\left[1 + \left(\frac{\omega_i - \omega_0}{\gamma}\right)^2\right]} = \frac{1}{\pi}\left[\frac{\gamma}{(\omega_i - \omega_0)^2 + \gamma^2}\right] \tag{1.10}$$

with the peak at ω_0 and width γ.

Kuramoto later [37] introduced pairwise interactions $\sum_{j\neq i}\kappa_{ji}Q_j$ where κ_{ji} is the coupling strength between the j^{th} and i^{th} oscillators, the system of N self-sustained oscillators Q_i will now obey the equations of motion

$$\dot{Q}_i = (i\omega_i + \alpha)Q_i - \beta|Q_i|^2 Q_i + \sum_{j\neq i}\kappa_{ji}Q_j \ . \tag{1.11}$$

Kuramoto [37] assumed that

1. the coupling strengths are independent of j and i, $\kappa_{ji} = \frac{\kappa}{N}$ [2],

2. constants $\alpha, \beta \to \infty$, however the values of $\frac{\alpha}{\beta}, \omega_i$ and κ are finite, and

3. the population size tends to infinity, *i.e.* $N \to \infty$.

Similar to the Winfree model [70], $\theta_i(t)$ is regarded as the phase of the i^{th} oscillator at time t. By considering $Q_i = \rho_i e^{i\theta_i}$ and by setting all the amplitudes $\rho_i = \sqrt{\frac{\alpha}{\beta}}$, Eq. (1.11) becomes

$$i\rho_i e^{i\theta_i}\dot{\theta}_i = i\omega_i \rho_i e^{i\theta_i} + \frac{\kappa}{N}\sum_{j\neq i}^{N} \rho_j e^{i\theta_j} \tag{1.12}$$

Since $\rho_i = \rho_j = \sqrt{\frac{\alpha}{\beta}}$ and by considering the imaginary part of (1.12), we simplify to yield the Kuramoto model

$$\dot{\theta}_i = \omega_i + \frac{\kappa}{N}\sum_{j=1}^{N} \sin(\theta_j - \theta_i) \tag{1.13}$$

for $i = 1, ..., N$, where $N \gg 1$. In the following sections we will retrace the theoretical work on Kuramoto model owing to Kuramoto's incredible intuition and symmetry arguments.

1.2.1 Remarks on Kuramoto's derivation

Kuramoto [37] found that mutual synchronisation, or self-entrainment, depends on a threshold condition $\eta \equiv |\frac{2\gamma}{\kappa}|$, where η is the width of the distribution of the natural frequencies. However, letting $Q_i = \sqrt{\frac{\alpha}{\beta}} e^{i\theta_i}$ constrains the original degrees of freedom to lie on a circle on the complex plane with radius $\sqrt{\frac{\alpha}{\beta}}$. In fact, considering the real part of (1.12) gives

$$0 = \frac{\kappa}{N}\sum_{j\neq i}^{N} \cos(\theta_j - \theta_i) \tag{1.14}$$

Looking at the right-hand side of Eq. (1.14),

$$\frac{\kappa}{N}\left(\sum_{j=1}^{N} \cos(\theta_j - \theta_i) - 1\right) = -\frac{\kappa}{N}$$

[2] $\kappa \geq 0$, in order to ensure the model is well behaved as $N \to \infty$, the factor $\frac{1}{N}$ is required.

which is generally unattainable. A natural question to ask is whether Q_i can generally be restricted on a circle.

1.2.2 Q_i constraints on a circle

By considering the simplest form of (1.12) with interactions with two chemical oscillators

$$\dot{Q}_1 = i\omega_1 Q_1 + \kappa_{21} Q_2 \tag{1.15a}$$

$$\dot{Q}_2 = i\omega_2 Q_2 + \kappa_{12} Q_1 \tag{1.15b}$$

with real couplings κ_{ij}. By using linear algebra, we can write the system as

$$\dot{\boldsymbol{Q}} = \begin{pmatrix} \dot{Q}_1 \\ \dot{Q}_2 \end{pmatrix} = \begin{pmatrix} i\omega_1 & \kappa_{12} \\ \kappa_{21} & i\omega_2 \end{pmatrix} \begin{pmatrix} Q_1 \\ Q_2 \end{pmatrix} = \boldsymbol{M}\boldsymbol{Q} \ . \tag{1.16}$$

Using the fact that $\boldsymbol{M} |e_i\rangle = m_i |e_i\rangle$, where m_i are the eigenvalues of $\boldsymbol{M}$ and $\langle e_i|$, $|e_i\rangle$ are the corresponding left-hand and right-hand eigenvectors, if we assume $|e_i\rangle$ are the basis of $\boldsymbol{M}$ then one may write $\boldsymbol{Q} = q_1 |e_1\rangle + q_2 |e_2\rangle$ and therefore

$$\dot{q}_1 |e_1\rangle + \dot{q}_2 |e_2\rangle = \dot{\boldsymbol{Q}} = \boldsymbol{M}\boldsymbol{Q} = q_1 m_1 |e_1\rangle + q_2 m_2 |e_2\rangle \ . \tag{1.17}$$

By projecting Eq. (1.17) by $\langle e_i|$ we get $\dot{q}_i = m_i q_i$ which gives $q_i = A_i e^{m_i t}$ and therefore

$$\boldsymbol{Q} = A_1 e^{m_1 t} |e_1\rangle + A_2 e^{m_2 t} |e_2\rangle \tag{1.18}$$

where m_1 and m_2 are the roots of $m^2 - im(\omega_1 + \omega_2) - \omega_1\omega_2 - \kappa_{12}\kappa_{21} = 0$, so

$$m_{1,2} = \frac{1}{2}\left[i(\omega_1 + \omega_2) \pm \sqrt{4\kappa_{12}\kappa_{21} - (\omega_1 - \omega_2)^2} \right] \ .$$

Therefore, the eigenvalues only have real parts if and only if $4\kappa_{12}\kappa_{21} > (\omega_1 - \omega_2)^2$. If the Q_i's are restricted on a circle, then we can write $Q_i = B_i e^{ib_i(t)}$ where B_i and $b_i(t)$ are

both real. By looking at Q_1, we have

$$e^{ib_1(t)} = \frac{A_1}{B_1} e^{m_1 t} e_{11} + \frac{A_2}{B_1} e^{m_2 t} e_{21} \ . \tag{1.19}$$

If m_1 and m_2 have different real parts, then the right hand side of Eq. (1.19) will either converge to 0 or diverge to infinity for $t \to \infty$ depending on the initial conditions. Hence we conclude Q_i constraints on a circle is only possible if m_1 and m_2 are purely imaginary. Similarly, if we consider Q_2 we get

$$e^{ib_2(t)} = \frac{A_1}{B_2} e^{m_1 t} e_{12} + \frac{A_2}{B_2} e^{m_2 t} e_{22} \ . \tag{1.20}$$

If we now substitute (1.19) and (1.20) into Eq. (1.15) we get

$$i\dot{b}_1 = i\omega_1 + \kappa_{12} \frac{B_2}{B_1} e^{i(b_2 - b_1)} \tag{1.21a}$$

$$i\dot{b}_2 = i\omega_2 + \kappa_{21} \frac{B_1}{B_2} e^{i(b_1 - b_2)} \ , \tag{1.21b}$$

and by separating the real and imaginary parts of Eq. (1.21a) give

$$\dot{b}_1 = \omega_1 + \kappa_{12} \frac{B_2}{B_1} \sin(b_2 - b_1) \tag{1.22}$$

$$0 = \kappa_{12} \frac{B_2}{B_1} \cos(b_2 - b_1) \ . \tag{1.23}$$

If we now assume that $A_2 = 0$ by initial condition, and let $\arg\left(\frac{A_1}{B_1} e_{11}\right) = \phi_1$ and $\arg\left(\frac{A_1}{B_2} e_{12}\right) = \phi_2$, for some constants ϕ_1 and ϕ_2 we can find expressions for $b_1(t)$ and $b_2(t)$ as

$$b_1(t) = \frac{m_1 t}{i} + \phi_1 \ , \quad b_2(t) = \frac{m_1 t}{i} + \phi_2 \tag{1.24}$$

which implies that $b_2(t) - b_1(t) = \phi_2 - \phi_1 = \frac{(2n+1)\pi}{2}$, $n \in \mathbb{N}$ which is a constant, by Eq. (1.23). This is necessary if we constraint Q_i on a circle. However, if we consider the

the modulo of Eq. (1.19) and Eq. (1.20)

$$1 = \left|e^{ib_1 - m_2 t}\right| = \left|\frac{A_1}{B_1} e^{m_1 t - m_2 t} e_{11} + \frac{A_2}{B_1} e_{21}\right|$$
$$1 = \left|e^{ib_2 - m_2 t}\right| = \left|\frac{A_1}{B_2} e^{m_1 t - m_2 t} e_{12} + \frac{A_2}{B_2} e_{22}\right|$$

then with the same initial condition $A_2 = 0$, we have

$$\left|\frac{A_1}{B_1} e_{11}\right| = 1 \ , \quad \left|\frac{A_1}{B_2} e_{12}\right| = 1 \ .$$

So in order to have Q_i constraint on a circle, there are two sets of conditions, namely

$$\frac{A_1}{B_1} e_{11} = 0 \quad \cup \quad \frac{A_2}{B_1} e_{21} = 0 \quad \cup \quad m_1 = m_2 \ ,$$
$$\frac{A_1}{B_2} e_{12} = 0 \quad \cup \quad \frac{A_2}{B_2} e_{22} = 0 \quad \cup \quad m_1 = m_2 \ .$$

However, this does not coincide with what we get from the previous method of analysis, namely that $b_2(t) - b_1(t)$ should be constant. Looking back to (1.19) and (1.20) with initial condition $A_2 = 0$, we find

$$e^{i(b_2 - b_1)} = \frac{\frac{1}{B_2} e_{12}}{\frac{1}{B_1} e_{11}} = \frac{B_1 e_{12}}{B_2 e_{11}} \ .$$

Now consider again the expression of $i\dot{b}_1$ (1.21a), and noting that $b_j = \frac{1}{i} m_1 t + \phi_j$ implies that $i\dot{b}_j = m_1$, the m_1 is purely imaginary, then

$$m_1 = i\dot{b}_1 = i\omega_1 + \kappa_{12} \frac{B_2}{B_1} e^{i(b_2 - b_1)} = i\omega_1 + \kappa_{12} \frac{B_2}{B_1} \frac{B_1 e_{12}}{B_2 e_{11}} = i\omega_1 + \kappa_{12} \frac{e_{12}}{e_{11}} \ . \tag{1.25}$$

Similarly if we consider the expression of $i\dot{b}_2$ (1.21b) then we obtain

$$m_1 \frac{e_{12}}{e_{11}} = i\omega_2 \frac{e_{12}}{e_{11}} + \kappa_{21} \ . \tag{1.26}$$

By using Linear Algebra, we write Eq. (1.25) and Eq. (1.26) in the form

$$\begin{pmatrix} i\omega_1 & \kappa_{12} \\ \kappa_{21} & i\omega_2 \end{pmatrix} \begin{pmatrix} 1 \\ \frac{e_{12}}{e_{11}} \end{pmatrix} = m_1 \begin{pmatrix} 1 \\ \frac{e_{12}}{e_{11}} \end{pmatrix} \Leftrightarrow \begin{pmatrix} i\omega_1 & \kappa_{12} \\ \kappa_{21} & i\omega_2 \end{pmatrix} \begin{pmatrix} \frac{e_{11}}{e_{12}} \\ 1 \end{pmatrix} = m_1 \begin{pmatrix} \frac{e_{11}}{e_{12}} \\ 1 \end{pmatrix}$$

which gives either $e_{12} = 0$ or $e_{11} = 0$ so that $\Re\left[\frac{e_{12}}{e_{11}}\right]$, or else $\Re\left[\frac{e_{11}}{e_{12}}\right]$, is zero, therefore $\cos(b_2(t) - b_1(t)) = \frac{(2n+1)\pi}{2}$ is not a constraint but it is a natural consequence of the setup.

The derivation above may therefore be seen solely as an attempt to motivate the Kuramoto model (1.13), rather than a derivation, as the parameterisation $Q_i = \sqrt{\frac{\alpha}{\beta}} e^{i\theta_i}$ is incompatible with the original problem (1.12).

1.2.3 Order Parameters

Assume we have a system of N coupled nonlinear oscillators governed by the equations of motion

$$\dot{\theta}_i(t) = \omega_i + \frac{\kappa}{N} \sum_{j=1}^{N} \sin(\theta_j(t) - \theta_i(t)) \ . \tag{1.27}$$

In order to understand the collective behaviour of the system, Kuramoto introduced the order parameter $r(t)$ via

$$r(t)e^{i\psi(t)} = \frac{1}{N} \sum_j e^{i\theta_j(t)} \tag{1.28}$$

where $r(t)$ measures the amount of collective behaviour in the system, *i.e.* the phase coherence, and $\psi(t)$ is the average phase. To visualise this, we can imagine all the oscillators are placed around the unit circle in the complex plane where the order parameter r varies along the radius and "points" at the centre of the oscillators and r rotates with phase ψ. The magnitude of $r(t)$ depends on the degree of clustering of the oscillators: if all oscillators are moving on the unit circle as a batch then $r \approx 1$, however, if all the oscillators drift around incoherently then $r \approx 0$.

Multiplying (1.28) by $e^{-i\theta_i(t)}$ one obtains

$$r(t)e^{i(\psi(t) - \theta_i(t))} = \frac{1}{N} \sum_j e^{i(\theta_j(t) - \theta_i(t))} \tag{1.29}$$

and by considering the imaginary parts

$$r(t)\sin(\psi(t)-\theta_i(t)) = \frac{1}{N}\sum_j \sin(\theta_j(t)-\theta_i(t)) \ . \tag{1.30}$$

Therefore, the Kuramoto model (1.13) can be rewritten as

$$\dot{\theta}_i(t) = \omega_i + \kappa r(t)\sin(\psi(t)-\theta_i(t)) \ . \tag{1.31}$$

This simplifies the system dramatically as the phase θ_i is now pulled towards the average phase ψ instead of the phases of other oscillators, and the effective coupling strength is proportional to the coherence $r(t)$. Strogatz [64] stated the importance of this proportionality. This proportionality constitutes a positive feedback loop between the coupling strength and coherence: if the system becomes more coherent, r grows and therefore the effective coupling strength κr increases, which results in more oscillators joining the synchronised batch. If the coherence is further increased by the newly joined oscillators then the process will continue; in the opposite scenario, the process becomes self-limiting.

The oscillators with equations of motion of the form (1.31) look as if they are uncoupled, however the oscillators are still coupled through $r(t)$ and $\psi(t)$, where $r(t) = \frac{1}{N}\sum_j e^{i(\theta_j(t)-\psi(t))}$ may be seen as the constraint.

In the present form, the analysis so far is applicable only to the mean field theory, where the coupling of one oscillator to the other oscillator is effectively given by the order parameter itself. If the κ_{ji} of Eq. (1.11) implement a lattice structure, the interaction term cannot generally be replaced by a multiple of $r(t)$.

1.2.4 Linear Stability Analysis

The key to Kuramoto's analysis is to consider the steady state solutions where the order parameter $r(t)$ is time independent and the phase $\psi(t)$ rotates uniformly at an angular frequency Ω, where

$$\Omega = \int_{\mathbb{R}} \omega g(\omega)\mathrm{d}\omega \tag{1.32}$$

is the population mean of the distribution $g(\omega_i)$, so that $\psi(t) = \Omega t + \psi_0$. This is reasonable only when the system has reached the steady state, because if the system is in the steady state, then the sample mean phase $\psi \approx \frac{1}{N}\sum_j \theta_j$ and $\sum_i \sin(\theta_i) \approx 0$. Hence $\dot{\psi} \approx \frac{1}{N}\sum_j \omega_j = \bar{\omega}$. By the Law of Large Numbers, in the limit of $N \to \infty$

$$\dot{\psi} \approx \bar{\omega} = \lim_{N\to\infty} \frac{1}{N}\sum_j \omega_j = \int_{\mathbb{R}} \omega g(\omega) \mathrm{d}\omega = \Omega \ . \tag{1.33}$$

In the steady state, when the transient behaviour has died off, if we set the frame of reference rotating with frequency Ω, $r(t)e^{i\psi(t)}$ will then be completely stationary. By performing a coordinate transform, $\dot{\tilde{\theta}}_i = \theta_i - \psi$ and $\tilde{\omega}_i = \omega_i - \Omega$, Eq. (1.31) becomes

$$\dot{\tilde{\theta}}_i + \dot{\psi} = \omega_i + \kappa r(-\sin(\tilde{\theta}_i)) \quad \Rightarrow \quad \dot{\tilde{\theta}}_i = \tilde{\omega}_i - \kappa r \sin(\tilde{\theta}_i) \ .$$

Assuming $\dot{\psi} = \Omega$, this is equivalent of setting $\psi = 0$ in Eq. (1.31) with the frame of reference rotating at angular frequency Ω. Keeping the coordinate transform in mind, to ease notation, we consider Eq. (1.31) with $\psi = 0$, which means:

$$\dot{\theta}_i = \omega_i - \kappa r \sin(\theta_i) \ . \tag{1.34}$$

We proceed to identify the fixed points given by the governing equation (1.34) above. Because $|\sin(x)| \leq 1 \ \forall x \in \mathbb{R}$, then for $\dot{\theta}_i = 0$, this implies the condition $|\omega_i| \leq \kappa r$. Therefore, we can split the system of oscillators into two groups, where the oscillators in each group exhibit different dynamics depending on the size of $|\omega_i|$ relative to κr.

Oscillators θ_i with $\dot{\theta}_i = 0$ are called frequency locked oscillators; while oscillators θ_i with $|\omega_i| > \kappa r$ are called drifting oscillators. Drifting oscillators cannot be frequency locked due to their nature, *i.e.* $|\omega_i| > \kappa r$ generally implies $\dot{\theta}_i \neq 0$. One crucial question to ask is whether the oscillators can neither be drifting nor be frequency locked. We shall address this in the following section. However, by having drifting oscillators, which cannot be frequency locked, seems to contradict the original assumption that $r(t) = r$ and $\psi(t) = \psi$ as these quantities cannot generally be constant in the presence of drifting

oscillators. For this reason, Kuramoto [38] demands the drifting oscillators to form a stationary distribution around the unit circle, albeit they are moving.

1.2.5 Frequency locked vs. drifting

In the steady state, are all oscillators either frequency locked or drifting? This is equivalent in asking whether a particular oscillator having $|\omega_i| < \kappa r$, *i.e.* not drifting, implies $\dot{\theta}_i \equiv 0$.

To answer that question we consider, in the steady state, the equation of motion of that oscillator

$$\dot{\theta}_i = \omega_i - \kappa r \sin(\theta_i)$$

with r constant and fixed, then all oscillators are effectively decoupled. If we assume there are a vanishing fraction of oscillators are adhered at the unstable fixed point, owing to the condition that $|\omega_i| < \kappa r$, in some course of time, these oscillators will pass through the stable fixed point and get stuck at the stable fixed point, *i.e.* in the cases of overdamped harmonic oscillators. Therefore, we can classify the oscillators into two class, frequency locked or drifting, depending on their dynamics.

1.2.6 Solving for κ_C Critical Coupling

In order to solve for the critical coupling κ_C in relationship with our order parameter r, Kuramoto [38] pointed out that self-consistency condition is the key. We introduce the density function, $\rho(\theta, t, \omega)$, of drifting oscillators as the probability to find a drifting oscillator at θ at time t conditional to it having frequency ω. From the continuity equation

$$\frac{\partial \rho}{\partial t} + \frac{\partial}{\partial \theta}(\rho u) = 0 \tag{1.35}$$

where $u = \dot{\theta}$ is the velocity of drifting oscillators located at θ at time t, then stationarity gives that $\dot{\theta}$ is constant in time. As we require the distribution remains constant in time, this implies $\frac{\partial \rho}{\partial t} = 0$. Therefore ρ is inversely proportional to the oscillators' frequencies

at θ, resulting in the form

$$\rho(\theta,\omega) = \frac{C}{\dot{\theta}} = \frac{C}{|\omega - \kappa r \sin(\theta)|} \tag{1.36}$$

which states clearly that ρ does depend on θ. Then, $\rho(\theta,\omega)\mathrm{d}\theta$ gives the fraction of oscillators with frequency ω that are found between θ and $\theta + \mathrm{d}\theta$. In order to quantify the normalisation constant C, we solve for C in

$$1 = \int_{-\pi}^{\pi} \rho(\theta,\omega)\mathrm{d}\theta = C\int_{-\pi}^{\pi} \frac{\mathrm{d}\theta}{\omega - \kappa r\sin(\theta)} \quad \Rightarrow \quad C = \frac{1}{2\pi}\sqrt{\omega^2 - (\kappa r)^2}\ .$$

As we have classified the oscillators into two groups, from Eq. (1.28) and having the frame of reference rotating at frequency Ω ($\psi = 0$), we have

$$re^{i\psi} = r = \left\langle e^{i\theta}\right\rangle = \left\langle e^{i\theta}\right\rangle_L + \left\langle e^{i\theta}\right\rangle_D \tag{1.37}$$

with subscripts L and D denote frequency locked and drifting oscillators correspondingly, and $\langle\cdot\rangle$ denotes the population average. Then

$$\left\langle e^{i\theta}\right\rangle = \int_{-\pi}^{\pi}\int_{W} e^{i\theta}\rho(\theta,\omega)g(\omega)\mathrm{d}\omega\mathrm{d}\theta \tag{1.38}$$

where W is the range of ω defined for corresponding dynamics. We first consider the contribution of the frequency locked oscillators. In the locked state $\dot{\theta} = 0$, we have $\sin(\theta) = \frac{\omega}{\kappa r}\ \forall|\omega| \le \kappa r$, which gives θ as a function of ω. Similar to Winfree model, then $\rho_L = \delta\left[\theta - \arcsin\left(\frac{\omega}{\kappa r}\right)\right]$. The distribution of ω is symmetric, *i.e.* $g(\Omega+\omega) = g(\Omega-\omega)$, equivalently $g(\omega) = g(-\omega)$, in the rotating frame of reference. In the limit of large N, as $N\to\infty$, the distribution of locked phases are symmetric about $\theta = 0$, therefore

$$\begin{aligned}\left\langle e^{i\theta}\right\rangle_L = \langle\cos(\theta)\rangle_L &= \int_{-\pi}^{\pi}\int_{-\kappa r}^{\kappa r}\cos(\theta(\omega))\rho(\theta,\omega)g(\omega)\mathrm{d}\omega\mathrm{d}\theta \\ &= \int_{-\frac{\pi}{2}}^{\frac{\pi}{2}}\cos(\theta)g(\kappa r\sin(\theta))\kappa r\cos(\theta)\mathrm{d}\theta = \kappa r\int_{-\frac{\pi}{2}}^{\frac{\pi}{2}}\cos^2(\theta)g(\kappa r\sin(\theta))\mathrm{d}\theta\ .\end{aligned}$$

If we now consider the contribution of the drifting oscillators, then

$$\begin{aligned}\left\langle e^{i\theta}\right\rangle_D &= \int_{-\pi}^{\pi}\int_{|\omega|>\kappa r} e^{i\theta}\rho(\theta,\omega)g(\omega)\mathrm{d}\omega\mathrm{d}\theta \\ &= \int_{-\pi}^{\pi}\int_{-\infty}^{-\kappa r} e^{i\theta}\rho(\theta,\omega)g(\omega)\mathrm{d}\omega\mathrm{d}\theta + \int_{-\pi}^{\pi}\int_{\kappa r}^{\infty} e^{i\theta}\rho(\theta,\omega)g(\omega)\mathrm{d}\omega\mathrm{d}\theta \\ &= -\int_{-\pi}^{\pi}\int_{\infty}^{\kappa r} e^{i\theta}\rho(\theta,-\omega)g(-\omega)\mathrm{d}\omega\mathrm{d}\theta + \int_{-\pi}^{\pi}\int_{\kappa r}^{\infty} e^{i\theta}\rho(\theta,\omega)g(\omega)\mathrm{d}\omega\mathrm{d}\theta\end{aligned}$$

by changing $\omega \to -\omega$ and using the property $g(\omega) = g(-\omega)$. By substituting $\hat{\theta} = \theta - \pi$ and $g(\omega) = g(-\omega)$, and using the fact that $\rho(\theta+\pi,-\omega) = \rho(\theta,\omega)$, then

$$\begin{aligned}\left\langle e^{i\theta}\right\rangle_D &= -\int_{-2\pi}^{0}\int_{\infty}^{\kappa r} e^{i\hat{\theta}}\rho(\hat{\theta}+\pi,-\omega)g(\omega)\mathrm{d}\omega e^{i\pi}\mathrm{d}\hat{\theta} + \int_{-\pi}^{\pi}\int_{\kappa r}^{\infty} e^{i\theta}\rho(\theta,\omega)g(\omega)\mathrm{d}\omega\mathrm{d}\theta \\ &= -\int_{-2\pi}^{0}\int_{\kappa r}^{\infty} e^{i\hat{\theta}}\rho(\hat{\theta},\omega)g(\omega)\mathrm{d}\omega\mathrm{d}\hat{\theta} + \int_{-\pi}^{\pi}\int_{\kappa r}^{\infty} e^{i\theta}\rho(\theta,\omega)g(\omega)\mathrm{d}\omega\mathrm{d}\theta \\ &= -\int_{-\pi}^{\pi}\int_{\kappa r}^{\infty} e^{i\hat{\theta}}\rho(\hat{\theta},\omega)g(\omega)\mathrm{d}\omega\mathrm{d}\hat{\theta} + \int_{-\pi}^{\pi}\int_{\kappa r}^{\infty} e^{i\theta}\rho(\theta,\omega)g(\omega)\mathrm{d}\omega\mathrm{d}\theta = 0\end{aligned}$$

Therefore, the self-consistency condition is reduced to

$$r = \kappa r\int_{-\frac{\pi}{2}}^{\frac{\pi}{2}}\cos^2(\theta)g(\kappa r\sin(\theta))\mathrm{d}\theta\ . \tag{1.39}$$

This equation defines the solutions but restrained to the fact that the order parameter r is constant. The trivial solution of $r = 0$, regardless of the value of κ, corresponds to the completely incoherent state where $\rho(\theta,\omega) = \frac{1}{2\pi}$ for all values of θ and ω, *i.e.* it is equally likely to find an oscillator anywhere on the unit circle. The other solution branch bifurcates continuously from $r = 0$, corresponding to partially synchronised state, at the critical coupling $\kappa = \kappa_C$. These solutions are obtained by letting $r \to 0^+$

$$1 = \kappa_C\int_{-\frac{\pi}{2}}^{\frac{\pi}{2}}\cos^2(\theta)g(0)\mathrm{d}\theta = \frac{1}{2}\kappa_C\pi g(0)\ .$$

Therefore, the critical coupling [38, 64] of the Kuramoto model is found to be

$$\kappa_C = \frac{2}{\pi g(0)}\ .$$

1.2.7 Bifurcation near the critical coupling κ_C

In order to study the effect on r as the coupling strength κ increases and the bifurcation around the critical coupling κ_C, we expand the integrand of (1.39) about $r = 0$,

$$1 = \kappa \int_{-\frac{\pi}{2}}^{\frac{\pi}{2}} \cos^2(\theta) \left[g(0) + g'(0)\kappa r \sin(\theta) + \frac{1}{2} g''(0) \left(\kappa r \sin(\theta)\right)^2 + \cdots \right] \mathrm{d}\theta \ . \tag{1.40}$$

Since the distribution of ω is unimodal and symmetric, *i.e.* $g(\Omega + \omega) = g(\Omega - \omega)$ implies $\Omega = 0$ on the rotating frame of reference and therefore $g(\omega)$ has a maximum at 0. Integrating Eq. (1.40) gives

$$\begin{aligned} 1 &= \frac{1}{2}\kappa\pi g(0) + \frac{1}{16}\kappa^3 \pi r^2 g''(0) \\ \kappa_C &= \kappa + \frac{\kappa_C}{16}\kappa^3 \pi r^2 g''(0) = \kappa + \frac{1}{16}\kappa_C \left(\kappa - \kappa_C + \kappa_C\right)^3 \pi r^2 g''(0) \\ &\approx \kappa + \frac{1}{16}\kappa_C^4 \pi r^2 g''(0) + \mathcal{O}\left((\kappa - \kappa_C)^3\right) \end{aligned}$$

near the critical coupling. The normalised distance above the threshold is defined as μ where

$$\mu = \frac{\kappa - \kappa_C}{\kappa_C} \sim -\frac{1}{16}\kappa_C^3 \pi r^2 g''(0)$$

therefore

$$r \sim \sqrt{\frac{1}{-g''(0)} \frac{16\mu}{\kappa_C^3 \pi}} = \sqrt{\frac{1}{-g''(0)} \frac{16}{\kappa_C^4 \pi}} \sqrt{\kappa - \kappa_C} \tag{1.41}$$

which implies that r obeys the square-root scaling law near the critical coupling, and the bifurcation is supercritical if $g''(0) < 0$ and subcritical if $g''(0) > 0$. In particular case of a Lorentzian density $g(\omega) = \frac{\gamma}{\pi(\gamma^2 + \omega^2)}$, this gives $\kappa_C = 2\gamma$ and

$$r = \sqrt{1 - \frac{\kappa_C}{\kappa}} \ . \tag{1.42}$$

1.2.8 Remarks on the Kuramoto model

However, Kuramoto model is designed to synchronise. Firstly, the interaction ceases for $\theta_j = \theta_i$. Secondly, to linear order, synchronisation is essentially the exponential. This can be seen in the $N = 2$ and $\omega_i = \omega$ case where $\dot{\varphi} = \frac{1}{2}(\dot{\theta}_1 - \dot{\theta}_2) = -\frac{\kappa}{2}\sin(\varphi)$. This differential equation can be solved exactly and the solution is $\tan\left(\frac{\varphi}{2}\right) = \tan\left(\frac{\varphi_0}{2}\right)\exp\left(-\frac{\kappa t}{2}\right)$. So asymptotically, *i.e.* for $\kappa > 0$ and t large, $\varphi \approx 2\tan\left(\frac{\varphi_0}{2}\right)\exp\left(-\frac{\kappa t}{2}\right)$. If the initial difference φ_0 is small, the system will asymptotically behave like $\varphi \approx \varphi_0 \exp\left(-\frac{\kappa t}{2}\right)$. Lastly, the Kuramoto model is capable of accommodating some diversity of the eigenfrequencies ω_i. This is surprising as synchronisation requires $\dot{\theta}_i = \dot{\theta}_j$ and, to leading order, the net effect of the sine term cancels over time.

Kuramoto-type of synchronisation (or equivalently a system entrainment) is well studied under weak coupling between identical or nearly identical oscillators [5, 51]. The interactions in the Kuramoto model (1.13) depend, sinusoidally, on the phase difference between each pair of oscillators. Over the last century, enormous literature [1, 64] has been generated from the analysis of the Kuramoto model on synchronisation of large emsembles of oscillators, including time-delayed interactions [34, 75]. However, it was not until recently that Ariaratnam and Strogatz [6] unearthed the Winfree model in the continuum limit as $N \to \infty$ and showed that Winfree's model is also tractable under this limit by having just one single Fourier component, namely

$$P(\theta) = 1 + \cos(\theta), \quad R(\theta) = -\sin(\theta) \tag{1.43}$$

as discussed in Section 1.1. Then, in the limit of weak coupling and nearly identical natural frequencies suggested in the Kuramoto model, Winfree's model reduces to Kuramoto's, *i.e.* one can show that the averaged equation of Winfree's model is isomorphic to Kuramoto's model with coupling $K = \kappa/2$. Ariaratnam and Strogatz [6] also discovered that, without taking the limit of weak coupling and the assumption of nearly identical natural frequencies, the Winfree model displays collective behaviour not seen in Kuramoto's model such as quenching and various hybrid states combining incoherent,

dead and frequency-locked oscillators. The oscillators are said to be frequency-locked when they have the same average frequency (also known as the rotation number ρ_i, where $\rho_i = \lim_{t\to\infty}(\theta_i(t)/t)$). A connection is also emerged between the Kuramoto model and Landau damping when Strogatz, Mirollo and Mathews [66] studied the decay to incoherence in oscillator communities, in which the frequency distribution is too broad to support synchrony.

Amony all living beings, time plays a key role. The rhythmical activities of living beings are complex and may be rooted in their physical or biological origins. The ubiquity of synchronisation would be a key factor on governing their individual or social behaviour, of which are determinied by different cycles of duration. For example in physical system, typical cycles of such will emit a pulse when the physical variable reaches a threshold, the pulse is then transmitted across to the neighbourhood while the physical variable itself will relax to its original state. Thereon, a new cycle commences. The emitted pulse will alter the states of the system by lengthening or shortening the periods of the neighbouring variables.

1.3 Pulse-coupled Biological Oscillators

Winfree comprehended synchronisation as a threshold process among a population of oscillators. Providing that the coupling between the oscillators are strong enough then perceptible number of the oscillators will synchronise to a common frequency. Hence, pulse-coupled, or integrate-and-fire, biological models were analysed extensively by many authors interested in synchronisation of biological oscillators. In particular, Mirollo and Strogatz [43] studied a model consisting of a population of identical integrate-and-fire oscillators where the coupling between oscillators is pulsatile. They found that, for almost all initial conditions, the system will develop into a state that all the oscillators will fire synchronously. In their paper, they also discussed the moral and the implication of the model in the real communities of biological oscillators. The model that the dual studied was inspired by the idea proposed by Peskin [50], which was an augmentation on Winfree's work [70]. Winfree recognised that collective behaviour in biological or physical systems such as mutual synchronisation is a cooperative phenomenon causing the phase transitions encountered in statistical physics.

Peskin [50], on realising Winfree's work on biological oscillators [70], considered a self-synchronised cardiac pacemaker which consists of 10,000 sinoatrial nodes. Peskin prognosticated that [50] "(i) for arbitrary initial conditions, the system approaches a state in which all the oscillators are firing synchronously; (ii) this remains true even when the oscillators are not quite identical." Similar models have also been studied by Knight [36], Keener *et al.* [33]. Although Peskin was only able to prove his first claim in the simpliest possible case of considering two identical oscillators, his idea has triggered many others to contribute in the biology field [2, 11, 23].

Based on a more general version of Peskin's model [50] and keeping Peskin's assumptions that all the oscillators are identical and coupled to all others in the system. In addition, Mirollo and Strogatz [43] posed the condition that "the oscillators rise towards threshold with a time-course which is monotonic and concave down". They defined the

behaviour of the system into two maps, the firing map

$$h(\phi) = g(\epsilon + f(1 - \phi)) \tag{1.44}$$

and return map

$$R(\phi) = h(h(\phi)) \ , \tag{1.45}$$

where R has simple dynamics. Mirollo and Strogatz proved the system will always lead to synchrony as the system is driven monotonically towards $\phi = 0$ or $\phi = 1$. Similar argument has been posed for the N-oscillator case where synchronisation occurs via absorptions. Absorption [43], defined by Mirollo and Strogatz, occurs when two oscillators become synchronised, the system merges the two oscillators into one and amplify the pulse strength of the coalescence. Therefore, a sequence of absorptions will eventually lock all the oscillators. Mirollo and Strogatz proved that synchrony will be achieved as long as all the pulse strengths are non-negative and non-trivial.

1.3.1 Integrate-and-fire Hodgkin-Huxley Model

Pulse oscillatory systems or integrate-and-fire models are widely studied from a theoretical aspect [44, 51, 65], particularly in the fields of mathematical biology and neurosciences. Normally excitatory integrate-and-fire models may appear to be the natural cause of synchronisation while inhibitory ones would result in anti-synchrony. However Van Vreeswijk, Abbott and Ermentrout [69] showed that in some cases that frequent inhibitory, but not excitatory, synaptic couplings leads to synchronisation. Van Vreeswijk *et al.* considered the synchronisation of two Hodgkin-Huxley model neurons with excitatory and inhibitory synaptic couplings. The equations of motion are given by

$$\dot{x}_i(t) = X - x_i(t) + E_i(t) \tag{1.46}$$

where $E_i(t) \mapsto E_i(t) + E_s(t - t_j)$ with $i \neq j$ is the synaptic input to neuron i. Time t_j defines the firing time of the j^{th} neuron. They considered $E_s(t)$ to be a normalised, to

value g, alpha function $E_s(t) = g\alpha^2 t e^{-\alpha t}$ as

$$\lim_{t\to\infty}\left[\int_0^t E_s(t')\mathrm{d}t'\right] = g\alpha^2\int_0^\infty te^{-\alpha t'}\mathrm{d}t' = g\ .$$

We also note that the time taken by the function $E_s(t)$ to reach its maximum is proportional to $\frac{1}{\alpha}$ as $\dot{E}_s(t) = g\alpha^2\left[e^{-\alpha t} - \alpha t e^{-\alpha t}\right]$ for both excitatory and inhibitory synapses.

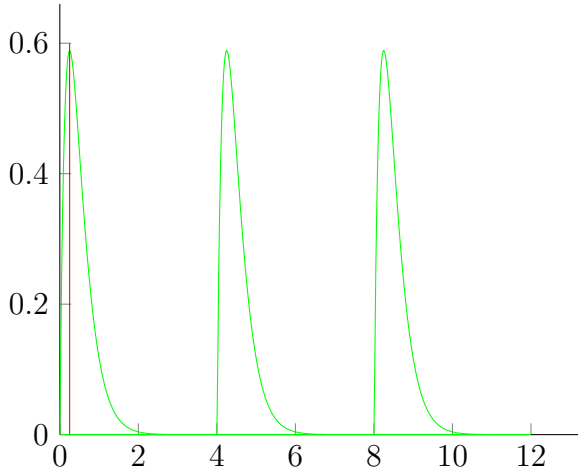

Figure 1.1: Time evolution of infrequent excitatory synapses, for inhibitory synapses are given by negative of these values. When the next firing occurs the cumulative effect of previous firing is almost negligible. The time taken to reach maximum per firing is proportional to $\frac{1}{\alpha}$.

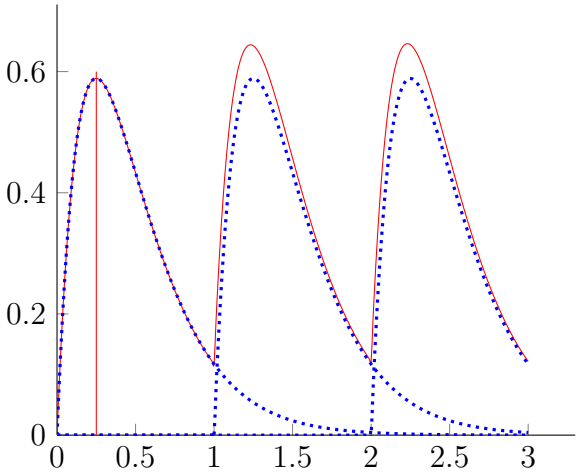

Figure 1.2: Time evolution of frequent excitatory synapses, for inhibitory synapses are given by negative of these values. When the consecutive firing times are close enough the effect of the firing accumulates. The blue (dotted) lines illustrate the effect of the individual firings whereas the red curve indicates the overall firing effect.The time taken to reach maximum per firing is proportional to $\frac{1}{\alpha}$.

Excitatory synapses are given by positive values of g while inhibitory synapses are

given by negative values of g, see Figure 1.1 and Figure 1.2. For excitatory synapses, the system will not be able to synchronise unless the neurons started off synchronised. This is because if one of the neurons is ahead of the other, the former one will push the latter one causing the latter to push the former ahead when threshold is reached, see Figure 1.3. Therefore the latter neuorn will not be able to catch up with the former and the two neurons will stay a finite distance apart. On the other hand, see Figure 1.4, inhibitory synapses will delay the firing time of the latter neuron compares to its own firing without feedback. Hence, the system allows the former neuron to be one period ahead of the latter and synchronisation is possible for certain values of α. This synchronisation phenomenon is consequences of the following properties:

Property 1 For the synaptic couplings being inhibitory, when the slow down of $x_2(t)$ due to $x_1(t)$'s firing reaches its maximum, $x_2(t)$ is closer to zero compared to $x_1(t)$ when its slow down due to $x_2(t)$'s firing reaches the maximum. Therefore the effect of the slow down on $x_2(t)$ will decrease more towards 0 by the time $x_2(t)$ reaches 1, compared to the slow down of $x_1(t)$ by the time $x_1(t)$ reaches 1.

Property 2 The response function $E_i(t)$ being augmented at a late stage in the life cycle of $x_i(t)$ has a greater effect than augmentation at an early stage.

In order to analyse the behaviour of the system and how the two oscillators will synchronise, in particular why inhibitory rather than excitatory synapses will result in synchronisation, we integrate the equation of motion

$$\begin{aligned} \dot{x}_i(t)e^t &= (X - x_i(t))e^t + E_i(t)e^t \\ \frac{\mathrm{d}}{\mathrm{d}t}\left[(x_i(t) - X)e^t\right] &= E_i(t)e^t \\ x_i(t) &= X(1 - e^{-t}) + x_i(0)e^{-t} + \int_0^t E_i(t')e^{t'-t}\mathrm{d}t' \ . \end{aligned}$$

The last integral represents the accumulated effect of firings depending on the time sequence of the other neuron reaching its threshold. Without loss of generality, we assume

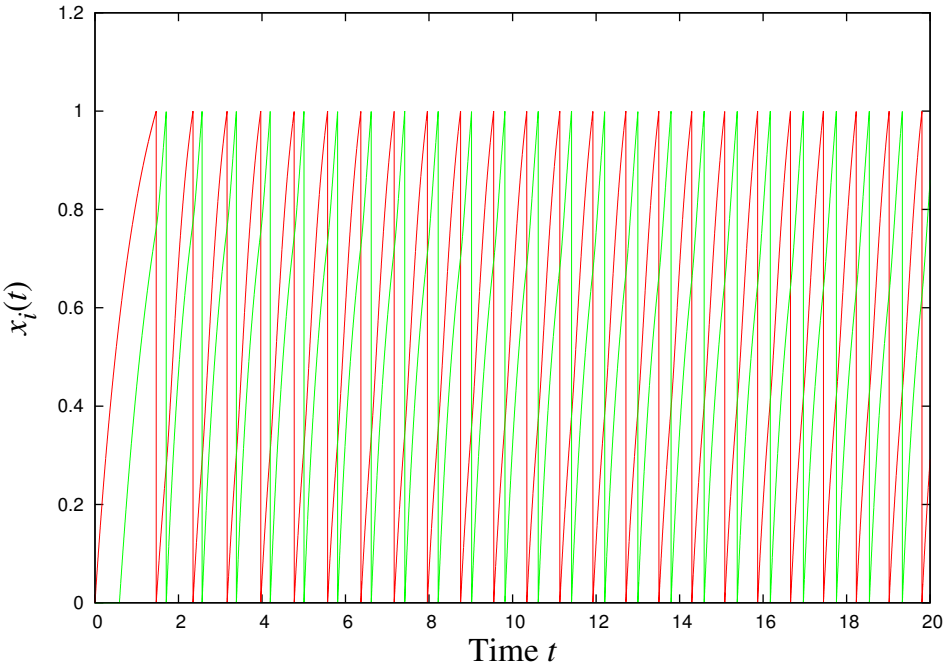

Figure 1.3: Time evolution of the system with excitatory synapses with neuron 1 (red) ahead of neuron 2 (green) at initialisation. Neuron 2 will never be able to catch up with neuron 1 and therefore they do not synchronise.

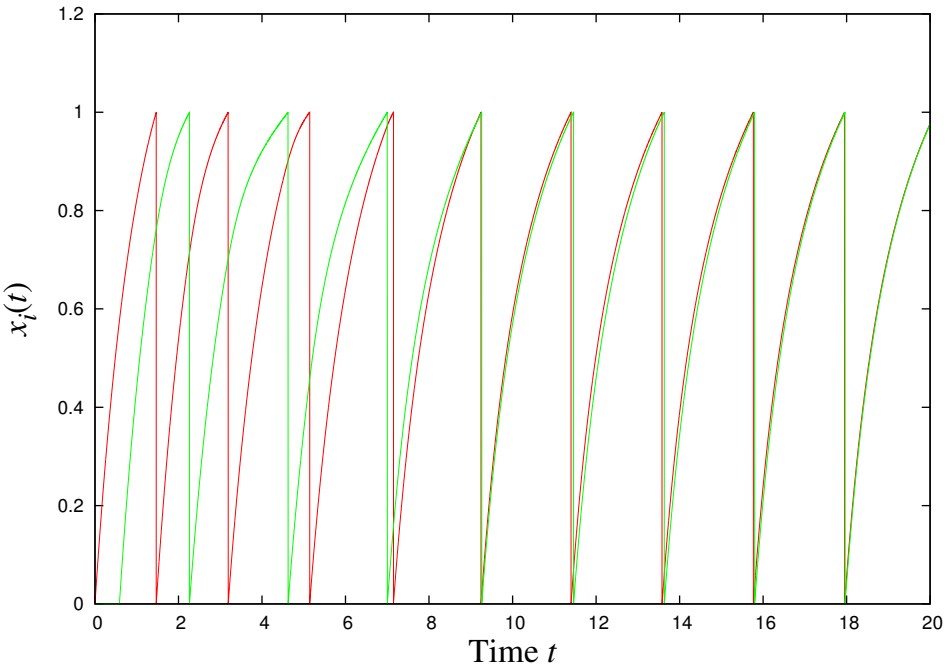

Figure 1.4: Time evolution of the system with inhibitory synapses with neuron 1 (red) ahead of neuron 2 (green) at initialisation. Neuron 2 effectively slows down relative to neuron 1 and therefore allows neuron 1 to advance a period ahead.

$x_1(t)$ is ahead of $x_2(t)$ at initialisation. If we only consider the effect of first firing of each neuron, *i.e.* the integral of $E_i(t)$ in the last equation above only get augmented once, then

$$\int_0^t E_i(t')e^{t'-t}\mathrm{d}t' = \int_{t_j}^t H[t'-t_j]E_s(t'-t_j)e^{t'-t}\mathrm{d}t' = \int_0^{t-t_j} E_s(t'')e^{t''+t_j-t}\mathrm{d}t'' \qquad (1.47)$$

where $H[\cdot]$ is a Heaviside step function, since $E_i(t)$ is yet to charge before first firing and $i \neq j$. If we have the system run for a considerable amount of time then we can approximate the upper limit of Eq. (1.47) by infinity, *i.e.* when t_j is much smaller compared to t. The effect of first firing is then

$$\int_0^t E_i(t')e^{t'-t}\mathrm{d}t' \approx e^{t_j-t}\int_0^\infty E_s(t'')e^{t''}\mathrm{d}t'' = e^{t_j-t}I \ .$$

Therefore, if neuron $x_1(t)$ is ahead of neuron $x_2(t)$ and neither $E_1(t)$ nor $E_2(t)$ is charged, then $t_1 < t_2$ where t_i indicates the first firing of the i^{th} neuron, gives

$$\int_0^t E_1(t')e^{t'-t}\mathrm{d}t' \approx e^{t_2-t}I > e^{t_1-t}I \approx \int_0^t E_2(t')e^{t'-t}\mathrm{d}t' \ ,$$

which is Property 2. From the analysis above we can readily deduce the relationship between the first firing time and the time the neuron reaches its threshold after receiving first response from the other neuron. Given that we know the solution of Eq. (1.46) is

$$x_i(t) = X\left(1-e^{-t}\right) + x_i(0)e^{-t} + e^{t_j-t}I \qquad (1.48)$$

where $I = \int_0^\infty E_s(t'')e^{t''}\mathrm{d}t''$ and $i \neq j$. If we started off the neurons at zero, *i.e.* $x_i(0) = 0$ for all i, and we denote the time the neuron first reaches its threshold after receiving first response from the other as $\tilde{t}_i$, then $x_i(\tilde{t}_i) = 1$. We obtain the following equation

$$1 = x_i(\tilde{t}_i) = X - \left(X - e^{t_j}I\right)e^{-\tilde{t}_i} \ .$$

By solving for $\tilde{t}_i$ we get

$$\tilde{t}_i = \ln\left(\frac{X - e^{t_j}I}{X-1}\right) \ .$$

Hence

$$\tilde{t}_2 = \ln\left(\frac{X - e^{t_1}I}{X - 1}\right) > \tilde{t}_1 = \ln\left(\frac{X - e^{t_2}I}{X - 1}\right)$$

as $t_1 < t_2$, meaning that the time taken for neuron behind $x_2(t)$ to reach its threshold is longer compared to the time taken for neuron ahead $x_1(t)$ to reach its threshold after receiving the first response from each other; of which, this is Property 1.

1.4 Synchronisation phenomena by time delay

"Kuramoto showed that as the coupling strength increased over a certain threshold, the model exhibits a spontaneous transition from incoherence to collective synchronisation" [38]. However, motivated by the significance of synaptic, dendritic and propagation delays in neural networks [45], Yeung and Strogatz [75] showed that perfect synchrony can be achieved in the Kuramoto model with time delay provided that all oscillators are identical. Yeung and Strogatz [75] generalised the Kuramoto model of coupled oscillators by introducing time-delayed interactions in presence of noise, which was originally developed as an analytically tractable version of Winfree's mean-field model for large populations of biological oscillators [70].

Yeung and Strogatz considered a system of N phase oscillators with noisy, randomly distributed intrinsic frequencies, and with delayed mean-field coupling [75]

$$\dot{\theta}_i = \omega_i + \xi_i(t) + \frac{K}{N}\sum_{j=1}^{N}\sin(\theta_j(t-\tau) - \theta_i(t) - \alpha) \tag{1.49}$$

where $\theta(t)$ is the phase of the i^{th} osciallator at time t, ω_i is the intrinsic frequency drawn randomly from a probability density $g(\omega_i)$ with mean ω_0. The frequency fluctuations are reflected in $\xi_i(t)$, a white noise with ensemble average $\langle\xi_i(t)\rangle = 0$ and $\langle\xi_i(s)\xi_j(t)\rangle = 2D\delta_{ij}\delta(s-t)$. The coupling strength is K where $K > 0$; $\tau > 0$ defines the time delay, and α is a phase frustration parameter. Sakaguchi and Kuramoto [58, 59] have studied the effects of frustration α and the noise correlator D separately without time delay, *i.e.* by setting $\tau = 0$ in the above model. In order to understand the macroscopic state of the system, Yeung and Strogatz [75] studied the case, *i.e.* the oscillators are identical, where $g(\omega) = \delta(\omega - \omega_0)$, and defined the complex order parameter

$$R(t)e^{i\psi(t)} = \frac{1}{N}\sum_{j=1}^{N} e^{i\theta_j(t)} \tag{1.50}$$

which measures the phase coherence of the system. Yeung and Strogatz [75] found that for $D = 0$, the continuous spectrum is pure imaginary, which corresponds to neutrally stable

rotating waves occuring in the full system. The fact that the continuous spectrum is pure imaginary implies that the incoherent state is never linearly stable; instead, depends on the (discrete) eigenvalues, the incoherent state is either unstable or neutral. If K and τ satisfy

$$K < \frac{\omega_0}{2m-1}, \quad \frac{(4m-3)\pi}{2\omega_0 - K} < \tau < \frac{(4m-1)\pi}{2\omega_0 + K} \tag{1.51}$$

for m being an arbitrary positive integer, then the incoherent state is neutrally stable. Yeung and Strogatz [75] also found that for given certain combinations of τ and K,

$$K < \frac{\omega_0}{2(2m-1)}, \quad \frac{(4m-3)\pi}{2\omega_0 - 2K} < \tau < \frac{(4m-1)\pi}{2\omega_0 + 2K} \tag{1.52}$$

for m being an arbitrary positive integer, where stable synchrony is impossible. Combining these results, one can find that for particular values of K and τ: (i) synchronisation - one or more synchronised stable states exists where the incoherent state is unstable; (ii) no synchronisation - incoherence is stable; and (iii) bistability - where one or more stable synchronised states coexist with stable incoherence. Although it has never be proven, numerics show that $R(t)$ approaches a constant if $g(\omega)$ is unimodal and symmetric as in the standard Kuramoto model. Yeung and Strogatz [75] later showed that if $g(\omega)$, *i.e.* the probability density, is Lorentzian, similar results are obtained but only the case of identical oscillators captures the essential features introduced by time delay.

1.4.1 Master stability equation with master stability function

In order to analyse and determine the stability of a synchronised state in chaotic and complex time delayed networks is of interests to many [18, 19, 35, 47, 48], in particular in terms of large time delayed couplings in laser applications [14, 20, 21]. Master stability function, first introduced by Pecora and Carroll [49], has been developed in order to determine the stability of a synchronous state at a given coupling strength.

Consider a system of N uncoupled identical nodes and they have the following equation of motion

$$\dot{\boldsymbol{x}}^i = \boldsymbol{F}(\boldsymbol{x}^i) \tag{1.53}$$

for each node, where $\boldsymbol{x}^i$ denotes a m-dimensional vector of dynamical variables of the i^{th} node. Given an arbitrary function $\boldsymbol{H} : \mathbb{R}^m \to \mathbb{R}^m$, which is the response function of each node's variables that is used in the coupling. The dynamics of the i^{th} node are given by

$$\boldsymbol{x}^i = \boldsymbol{F}(\boldsymbol{x}^i) + \sigma \sum_j G_{ij} \boldsymbol{H}(\boldsymbol{x}^j) \tag{1.54}$$

where σ is the coupling strength and G_{ij} is the coupling coefficient between the i^{th} and j^{th} node. Pecora and Carroll [49] defines the synchronisation manifold such that $\boldsymbol{x}^1 = \boldsymbol{x}^2 = \cdots = \boldsymbol{x}^N$ under the following assumptions:

1. the coupled nodes are all identical,
2. the same function of the components from each node is used to couple to other nodes,
3. the synchronisation manifold is an invariant manifold, and
4. the nodes are coupled in an arbitrary way which is well approximated near the synchronous state by a linear operator.

Under Pecora and Carroll's definition on synchronisation manifold and their assumption that this synchronisation manifold is invariant, this will imply that $\sum_j G_{ij} = g$ is constant, *i.e.* this sum is independent of i. Pecora and Carroll considered the matrix of coupling coefficients $\boldsymbol{G}$ where this constant is zero, *i.e.* $\sum_j G_{ij} = g = 0$.

Let $\boldsymbol{x} = \left(\boldsymbol{x}^1, \boldsymbol{x}^2, \cdots, \boldsymbol{x}^N\right)$, $\boldsymbol{F} = \left(\boldsymbol{F}(\boldsymbol{x}^1), \boldsymbol{F}(\boldsymbol{x}^2), \cdots, \boldsymbol{F}(\boldsymbol{x}^N)\right)$, and $\boldsymbol{H} = \Big(\boldsymbol{H}(\boldsymbol{x}^1), \boldsymbol{H}(\boldsymbol{x}^2), \cdots, \boldsymbol{H}(\boldsymbol{x}^N)\Big)$, and $\boldsymbol{G}$ be the coupling coefficients matrix, the system can be written as

$$\dot{\boldsymbol{x}} = \boldsymbol{F}(\boldsymbol{x}) + \sigma \boldsymbol{G} \otimes \boldsymbol{H}(\boldsymbol{x}) \tag{1.55}$$

where $\otimes$ is the Kronecker product. By assuming the collection of variation on each node is $\boldsymbol{\xi} = \left(\xi^1, \xi^2, \cdots, \xi^N\right)$, then the variational equation of Eq. (1.55) is then

$$\dot{\boldsymbol{\xi}} = \left[\mathbb{1}_N \otimes \mathrm{D}\boldsymbol{F} + \sigma \boldsymbol{G} \otimes \mathrm{D}\boldsymbol{H}\right] \boldsymbol{\xi} \tag{1.56}$$

with D$\boldsymbol{F}$ and D$\boldsymbol{H}$ are the Jacobian functions [49] and $\mathbb{1}_N$ is the N-dimensional identity matrix. Diagonalising the matrix $\boldsymbol{G}$ with unitary transformation $\boldsymbol{U}$ [3],

$$\text{diag}\left(\gamma_0, \gamma_1, \cdots, \gamma_{N-1}\right) = \boldsymbol{U}\boldsymbol{G}\boldsymbol{U}^{-1} \tag{1.57}$$

would decouple the system into

$$\dot{\xi}_k = \left[\text{D}\boldsymbol{F} + \sigma\gamma_k \text{D}\boldsymbol{H}\right]\xi_k \tag{1.58}$$

where γ_k is an eigenvalue of $\boldsymbol{G}$ with $k = 0, 1, 2, \cdots, N-1$. As we know that the independent row sums are equal and therefore $\sum_j G_{ij} = g = 0$ is always an, longitudinal, eigenvalue of $\boldsymbol{G}$ with eigenvector $(1, 1, \cdots, 1)$. Given that we know one eigenvalue is $\gamma_0 = 0$ and the corresponding eigenvector is $(1, 1, \cdots, 1)$ therefore if we let $\gamma_0 = g = 0$, then for $k = 0$ we obtain the variational equation for the synchronisation manifold with $\gamma_0 = 0$ as all systems are perturbed equally along this eigenvector. For variational equations with other values of k correspond to transversal pertubations to the synchronisation manifold. Therefore, the synchronisation manifold is stable if and only if all transversal pertubations die out. This is only possible if the maximum Lyapunov or Floquet exponent arising from Eq. (1.58) is negative for all transversal eigenvalues γ_k with $k = 1, 2, \cdots, N-1$. Consequently a divergence in the transverse direction means that the synchronised solulution is chaotic. Since we evaluate Eq. (1.58) on the synchronised state, the only difference in the transversal variational equation for each value of $k = 1, 2, \cdots, N-1$ will be the scalar multiplier $\sigma\gamma_k$. This has led Pecora and Carroll to the formulation of the master stability equation

$$\dot{\zeta} = \left[\text{D}\boldsymbol{F} + (\alpha + i\beta)\text{D}\boldsymbol{H}\right]\zeta \tag{1.59}$$

where $\lambda_{\max} \in \mathbb{C}$ is the associated master stability function which maps the complex number $\alpha + i\beta$ to the maximum Lyapunov exponent arising from Eq. (1.59) [49]. The master stability function will form a surface over the (α, β)-complex plane, see Figure 1.5,

[3] The unitary transformation does not affect the first term in Eq. (1.56) as it acts only on the matrix $\mathbb{1}_N$.

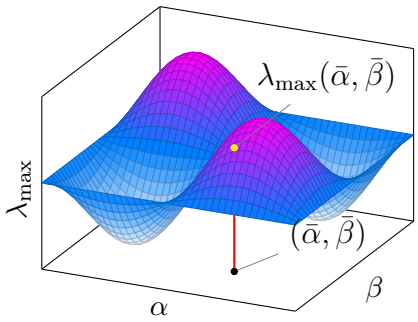

Figure 1.5: Graphical illustration of the master stability function $\lambda_{\max}$ above the (α, β)-complex plane from the generic variational equation Eq. (1.59). With a given value of scalar multiplier $\sigma\gamma_k = \bar{\alpha} + i\bar{\beta}$, one can locate the corresponding $\lambda_{\max}$ and therefore immediately reveal the stability of this particular scalar multiplier $\sigma\gamma_k$.

where the stability of a particular scalar multiplier $\sigma\gamma_k = \bar{\alpha} + i\bar{\beta}$ can be determined by the sign of $\lambda_{\max}$ of this particular point. In more general terms, once the sign of the master stability function is found for a particular coupling $\sigma\gamma_k$, we can tell whether the synchronised solution is stable or chaotic.

1.4.2 Master stability function with large time delay couplings

As master stability function was introduced by Pecora and Carroll [49], a lot of interests were paid towards the analyses of the complex network interactions [8, 12, 25, 28, 52, 67] and complex networks with time delays [18, 22, 35] with main application of chaos synchronisation in coupled semiconductor lasers where the time delay quantity $\tau \to \infty$ [20]. Kinzel *et al.* [35] first considered dynamical systems with time delay dependence and lately Flunkert *et al.* [22] considered synchronisation of delayed couplings in the large limit of time delay τ by use of master stability equation and master stability function.

Similar to the work of Pecora and Carroll, Flunkert [20] considered a system of N delayed coupled identical oscilators in a network, with $x^i \in \mathbb{R}^n$

$$\dot{x}^i(t) = f\left[x^i(t)\right] + \sum_{j=1}^{N} g_{ij} h\left[x^j(t-\tau)\right] \tag{1.60}$$

where the coupling matrix $g_{ij} \in \mathbb{R}$ determines the coupling topology and the corresponding coupling strength between each system. The non-linear function f describes the

dynamics of each individual isolated oscillator and h is a non-linear coupling function. The synchronised solution, which has the form,

$$\dot{\bar{x}}(t) = f\left[\bar{x}(t)\right] + \sigma h\left[\bar{x}(t-\tau)\right] \tag{1.61}$$

exists if and only if $\sigma = \sum_j g_{ij}$ [4]. In order to determine the stability of this synchronised solution, we perturb the synchronised solution by a small quantity $\xi^i(t)$ on each individual system

$$x^i(t) = \bar{x}(t) + \xi^i(t) \ . \tag{1.62}$$

Linearising Eq. (1.60) in ξ^i by using Eq. (1.62) and the synchronised solution (1.61) yields,

$$\dot{\xi}^i(t) = Df\left[\bar{x}(t)\right]\xi^i(t) + \sum_{j=1}^{N} g_{ij} Dh\left[\bar{x}(t-\tau)\right]\xi^i(t-\tau) \tag{1.63}$$

with Df and Dh the Jacobian functions. The linearised equation can be written in the form

$$\dot{\boldsymbol{\xi}}(t) = \mathbb{1}_N \otimes Df\left[\bar{x}(t)\right]\boldsymbol{\xi}(t) + \boldsymbol{G} \otimes Dh\left[\bar{x}(t-\tau)\right]\boldsymbol{\xi}(t-\tau) \tag{1.64}$$

with $\boldsymbol{\xi} = \left(\xi^1(t), \xi^2(t), \cdots, \xi^N(t)\right)$, the coupling matrix $\boldsymbol{G}$ and N-dimensional identity matrix $\mathbb{1}_N$. Similar to the procedure laid out in Section 1.4.1 [49], taking the unitary transformation $\boldsymbol{U}$

$$\mathrm{diag}\left(\sigma, \gamma_1, \gamma_2, \cdots, \gamma_{N-1}\right) = \boldsymbol{U}\boldsymbol{G}\boldsymbol{U}^{-1} \tag{1.65}$$

with $\sigma = \sum_j g_{IJ}$, yields the longitudinal variational equation

$$\dot{\xi}^0(t) = Df\left[\bar{x}(t)\right]\xi^0(t) + \sigma Dh\left[\bar{x}(t-\tau)\right]\xi^0(t-\tau) \tag{1.66}$$

and the set of $N-1$ transversal variational equations

$$\dot{\xi}^k(t) = Df\left[\bar{x}(t)\right]\xi^k(t) + \gamma_k Dh\left[\bar{x}(t-\tau)\right]\xi^k(t-\tau) \tag{1.67}$$

[4] A simple, yet sufficient, argument has been given in Section 3.3, see Property 1.

where $k = 1, 2, \cdots, N-1$. As Pecora and Carroll [49] summerised, this synchronised manifold is stable if and only if the maximum Lyapunov or Floquet exponent arising from Eq. (1.67) is negative for all γ_k and therefore the master stability equation has the form

$$\dot{\xi}(t) = Df\left[\bar{x}(t)\right]\xi(t) + (\alpha + i\beta)Dh\left[\bar{x}(t-\tau)\right]\xi(t-\tau) \tag{1.68}$$

where $\lambda_{\max}$, the master stability function, maps the complex number $\alpha + i\beta$ to the max Lyapunov or Floquet exponent arising from the master stability equation (1.68). This master stability function can be calculated numerically, however for more rigorous understanding of the dynamics of the system we discretise time [35] for the synchronised manifold (1.61) and the corresponding master stability equation (1.68)

$$x_{k+1} = f(x_k) + \sigma h(x_{k-\tau}) \tag{1.69}$$

$$\xi_{k+1} = A_k\xi_k + re^{i\psi}B_{k-\tau}\xi_{k-\tau} \tag{1.70}$$

where $A_k := Df(x_k)$, $B_{k-\tau} := Dh(x_{k-\tau})$, and $(\alpha + i\beta) = re^{i\psi}$ [20]. Delay differential equations of this type has been investigated widely with large time delay in literature [22, 41, 72, 74], where Lyapunov method for delay differential equations [55] has been recently generalised into the scaling of Floquet exponents or Floquet multiplier method [31, 73]. Assume ξ_k takes the form $\xi_k = z^k\xi_0$, taking the dynamics in the synchronised manifold to be a fixed point [20] we get the multiplier equation for z as

$$\det\left[\boldsymbol{A} - z\boldsymbol{I} + re^{i\psi}\boldsymbol{B}z^{-\tau}\right] = 0 \tag{1.71}$$

where $\boldsymbol{I}$ is the identity matrix. If $|z| < 1$ then $\xi_k \to 0$ as $k \to \infty$ then sychronisation is possible; on the other hand, if $|z| > 1$, in the limit of $\tau \to \infty$, z must be an eigenvalue of A in Eq. (1.71), then synchronisation is impossible. Let's now study explicitly the behaviour of z and therefore ξ_k in the limit of $\tau \to \infty$ where $z \approx 1$. Assume $z = \left(1 + \frac{\delta}{\tau}\right)e^{i\omega}$ then

$\lim_{\tau\to\infty} z = e^{i\omega}$ [20] and

$$\lim_{\tau\to\infty} z^{-\tau} = \lim_{\tau\to\infty} \left[\left(1 + \frac{\delta}{\tau}\right)^{-\tau} e^{-i\omega\tau} \right] = e^{-\delta} e^{-i\omega\tau} \ .$$

Multiplying Eq. (1.71) by the inverse of $\boldsymbol{B}$ and in the limit of large τ, we get

$$\det\left[-\boldsymbol{B}^{-1}\left(\boldsymbol{A} - \boldsymbol{I}e^{i\omega}\right) - re^{-\delta}e^{i(\psi-\omega\tau)}\right] = \det\left[-\boldsymbol{B}^{-1}\left(\boldsymbol{A} - \boldsymbol{I}e^{i\omega}\right) - \mu\right] = 0 \qquad (1.72)$$

gives a polynomial in eigenvalues μ in terms of ω, where $\mu(\omega) = re^{-\delta}e^{i(\psi-\omega\tau)}$. If $\boldsymbol{B}$ is not invertible, then we use Eq. (1.71) explicitly to calculate the eigenvalues $\mu(\omega)$ [20]. Then one can define the branches

$$\delta(\omega) = \ln\left[\frac{r}{|\mu(\omega)|}\right] = -\ln|\mu(\omega)| + \ln r \ .$$

If there exists an incident that $\omega = \omega_0$ where $\mu(\omega)$ admits zero values, then Eq. (1.72) tells us that this is corresponding to $\boldsymbol{A}$ having eigenvalues with $|z| = 1$, otherwise, $\mu(\omega)$ is bounded [22]. If no strongly unstable eigenvalue exists [7], then the sign of the corresponding branch determines the stability in the limit of large τ. The sign of $\delta(\omega)$ depends on the values of r where $r = \sqrt{\alpha^2 + \beta^2}$ in Eq. (1.68). As $\delta(\omega)$ increases if we increase r, so there exists a minimum radius r_0 where the branch changes its stability and therefore the master stability function $\lambda_{\max}$ changes its sign accordingly. Therefore one can determine the critical radius r_0, where stability changes, for a fixed point in the synchronisation manifold in limit of large values of τ.

We can see that the master stability function has a very simple structure in the limit of large coupling delays, therefore in dynamic systems with large delay couplings master stability function has been widely used [15, 24, 40].

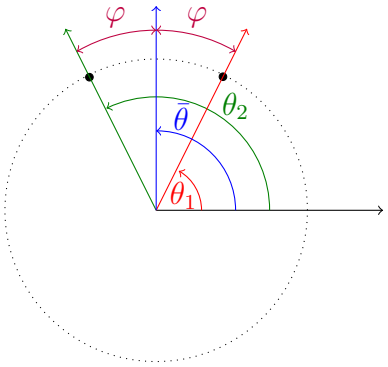

Figure 1.6: Graphical illustration of our system as oscillators on a circle.

1.5 Motivation

In this thesis, we are going to study a specific version of Winfree's model [70], first introduced by Prof. H. J. Jensen in 2008, and analyse the synchronous behaviour of non-time delay and time delay coupled systems for all values of N. Using the differential equation (1.1), we redefine the function $\frac{K}{N}R(\theta_i)$ to be the coupling strength or magnitude of feedback, J_{ij}, between the i^{th} and j^{th} oscillators.

Our non-time delay model is then

$$\dot{\theta}_i(t) = \omega_i + \sum_{j}^{N} \mathrm{J}_{ij}\sigma(\theta_j(t)) \tag{1.73}$$

and our corresponding time delay model, where the feedback function σ depends on some past values of θ, is

$$\dot{\theta}_i(t) = \omega_i + \sum_{j}^{N} \mathrm{J}_{ij}\sigma(\theta_j(t-\delta t)) \tag{1.74}$$

for $i = 1, ..., N$, where $N \gg 1$. Similar to Winfree's model (1.1) and Kuramoto's model (1.13), $\theta_i(t)$, the degree of freedom in the system, is regarded as the phase of the i^{th} oscillator at time t. The feedback $\sigma(\theta_j(t))$ is periodic, and ω_i is the corresponding initial frequency of the i^{th} oscillator.

In our systems, the oscillators are coupled via the coupling strength J_{ij}. We only make one further assumption that the phases of all oscillators are monotonically increasing,

i.e. the function $\theta_i(t)$ is monotonically increasing over time t [5]. However, we will retain Winfree's assumptions of identical or nearly identical dynamics, and each oscillator is coupled to all the others, but not to themselves, *i.e.* $\mathrm{J}_{ii} = 0$ for all i.

Definition 1.1. We define the synchronised state of our systems as $\theta_i = \bar{\theta} + n\xi$ for all i, that is, when all of the oscillators are moving in the same phase or phases differ by integer multiples of the period ξ of our function σ.

Since the equation of motion of our system is

$$\dot{\theta}_i(t) = \omega_i + \sum_j^N \mathrm{J}_{ij}\sigma(\theta_j(t)) \tag{1.75}$$

if the system synchronises, then $\theta_i = \bar{\theta}$ asymptotically and therefore $\dot{\theta}_i = \dot{\theta}_k$, which implies

$$\omega_i + \sigma(\bar{\theta}) \sum_j^N \mathrm{J}_{ij} = \omega_k + \sigma(\bar{\theta}) \sum_j^N \mathrm{J}_{kj} \ . \tag{1.76}$$

For this to hold for all values of t, and the effect of the ω terms cannot be cancelled by other terms and this implies $(\omega_i - \omega_k) = 0$ and $\left(\sum_j^n \mathrm{J}_{ij} - \sum_j^n \mathrm{J}_{kj}\right) = 0$, that is, we need $\omega_i = \tilde{\omega}$ and $\sum_j \mathrm{J}_{ij} = \tilde{\mathrm{J}}$. Therefore, $\bar{\theta}$ will also satisfy the same differential equation, namely

$$\dot{\bar{\theta}} = \tilde{\omega} + \tilde{\mathrm{J}}\sigma(\bar{\theta}) \tag{1.77}$$

where $\bar{\theta}$ is also a - strictly positive - monotonically increasing function in time t. However, the main motivation comes from the clash between the analytic solution (Section 2.1) and its numerical implementation using standard Euler scheme (Section 2.2) for the simplest model with $N = 2$ obeys the equations of motion given by Eq. (1.75). Yet, more sophisticated numerical schemes, such as Runge-Kutta, eliminates this pseudo synchronisation effect (Section 2.2.3). Due to the fact that standard Euler is based on a forward derivative and this hints to us that standard Euler scheme may have a self-implemented time delay effect.

[5] In order to achieve this, all parameters are to be chosen so that $\dot{\theta}_i > 0$ at all times. The easiest way to ensure we do not violate the monotonic manner of $\theta_i(t)$ is to choose $\sigma(\theta_i(t)) > 0$, therefore our choice of σ introduced in Section 1.5.2.

1.5.1 Two-oscillators Model with pulsating phases

To illuminate the effects of time delays, we first consider a system of two pulse oscillators with shock amplitude J and $\sigma(\theta(t))$ as periodic Dirac combs $\text{Ш}(\theta(t))$. This setup is our version of integrate-and-fire model with oscillators exchanging pulses according to time delayed interactions

$$\dot{\theta}_1(t) = \omega + J \sum_{n\in\mathbb{N}} \text{Ш}(\theta_2(t-\delta t) - n) \tag{1.78a}$$

$$\dot{\theta}_2(t) = \omega + J \sum_{n\in\mathbb{N}} \text{Ш}(\theta_1(t-\delta t) - n)) \ . \tag{1.78b}$$

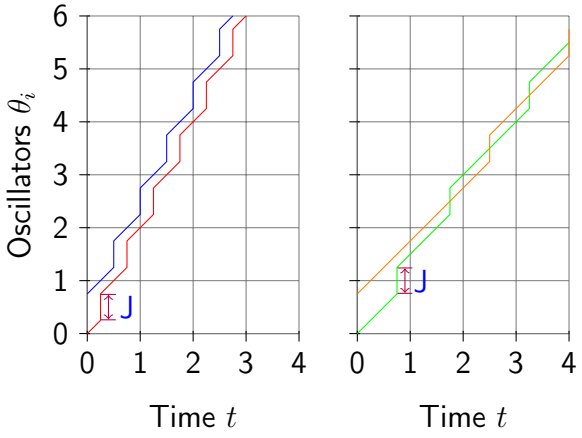

Figure 1.7: Time evolution of two oscillators exchanging pulses according to (1.78). Left panel: $\delta t = 0$ and right panel: $\delta t = 0.5$.

Integrating the set of Eq. (1.78) above, we can see that $\theta_1(t) \mapsto \theta_1(t) + J$ every time θ_2 passes through an integer value at a referenced time, depending on the value of the time delay δt. Similarly $\theta_2(t) \mapsto \theta_2(t) + J$ when every time θ_1 passes through an integer value at a referenced time. Without loss of generality, let $\theta_1(0) > \theta_2(0)$ and in the case of $\delta t = 0$, we can see from Figure 1.7 (left panel) that the two phases are unable to synchronise. In this particular case of $\delta t = 0$ at most we can get is a leap-frogging synchronisation - in fact, entrainment - if we increase the value of J. [6] Consequently if $\theta_1(0) - \theta_2(0) > J$ then

[6] Leap-frogging entrainment is only possible when the jump of one oscillator makes the other phase oscillator skips over an integer, therefore the former oscillator misses a jump from the latter. Without

leap-frogging entrainment will not be possible. Another property to note is that if the difference between $\theta_1(0)$ and $\theta_2(0)$ is out more than (and not equal to) $n\xi$, $n \in \mathbb{Z} \setminus \{0\}$; where ξ is the periodicity of $\text{Ш}(\theta(t))$, then the system does not eventually synchronise or entrain to less than $n\xi$. On the other hand, in the case of $\delta t \neq 0$, Figure 1.7 (right panel), we will get leap frogging entrainment independent of the value of J. An important note is that, if the function $\sigma(\theta(t))$ is a Dirac comb $\text{Ш}(\theta(t))$ the solution is strictly periodic. This fact contradicts our linearised solution of time delayed system in Section 2.4 where we only see asymptotic entrainment.

1.5.2 Choice of $\sigma(\bar{\theta}(t))$

Obviously periodic Dirac delta spikes are unrealistic in real systems. Pulse emitted will have a finite width and a smooth time dependence, therefore we have chosen our $\sigma(\bar{\theta}(t))$ to be a periodic, with period 1, gaussian of the form

$$\sigma(x) = \frac{1}{\sqrt{4\pi w^2}} \sum_{n=-\infty}^{\infty} \exp\left(\frac{-(x+n)^2}{4w^2}\right) \tag{1.79}$$

where $n \in \mathbb{R}$. The Poisson's summation formula may be stated as

$$\sum_{n=-\infty}^{\infty} f(n) = \sum_{n=-\infty}^{\infty} \hat{f}(n) \tag{1.80}$$

where $\hat{f}(n)$ is the Fourier Transform of $f(n)$, *i.e.* $\hat{f}(n) = \int_{-\infty}^{\infty} f(x) \exp(-2\pi i n x) \mathrm{d}x$. Applying Poisson's summation formula to our function,

$$F(x) = \sum_{n=-\infty}^{\infty} \frac{1}{\sqrt{4\pi w^2}} \exp\left(\frac{-(x+n)^2}{4w^2}\right)$$

gives

$$F(x) = \sum_{n=-\infty}^{\infty} \int_{-\infty}^{\infty} \frac{1}{\sqrt{4\pi w^2}} \exp\left(\frac{-(x+y)^2}{4w^2}\right) \exp(-2\pi i n y) \mathrm{d}y \ .$$

---

the presence of time delay, this is only possible if $J \geq \theta_1(0) - \theta_2(0)$ but it is a natural outcome in the time delayed integrate-and-fire systems.

Now if we complete the square, this will give

$$F(x) = \sum_{n=-\infty}^{\infty} \int_{-\infty}^{\infty} \frac{1}{\sqrt{4\pi w^2}} \exp\left(\frac{-(x+y+4\pi i n w^2)^2}{4w^2}\right) \exp(-4\pi^2 n^2 w^2) \exp(2\pi i n x) \mathrm{d}y$$

We now let $m = \frac{x+y+4\pi i n w^2}{2w}$ and using the fact that $\int_{-\infty}^{\infty} \exp(-z^2)\mathrm{d}z = \sqrt{\pi}$, this will imply

$$\begin{aligned} F(x) &= \sum_{n=-\infty}^{\infty} \exp(-4\pi^2 n^2 w^2) \exp(2\pi i n x) \int_{-\infty}^{\infty} \frac{1}{\sqrt{4\pi w^2}} \exp(-m^2) 2w \mathrm{d}m \\ &= \sum_{n=-\infty}^{\infty} \exp(-4\pi^2 n^2 w^2) \exp(2\pi i n x) \\ &= \vartheta_3(x\pi, \exp(-4\pi^2 w^2)) \end{aligned}$$

where, $\vartheta_3(z, q)$ is the Jacobi Theta Function. Therefore, we can write

$$\sum_{n=-\infty}^{\infty} \frac{1}{\sqrt{4\pi w^2}} \exp\left(\frac{-(x+n)^2}{4w^2}\right) = \vartheta_3(x\pi, \exp(-4\pi^2 w^2))$$

This would also mean that if $n \to n\xi$, where ξ defines the periodicity of σ, then we will have

$$\frac{1}{\xi} \sum_{n=-\infty}^{\infty} \frac{1}{\sqrt{4\pi \frac{w^2}{\xi^2}}} \exp\left(\frac{-(\frac{x}{\xi}+n)^2}{4\frac{w^2}{\xi^2}}\right) = \frac{1}{\xi} \vartheta_3\left(\frac{x}{\xi}\pi, \exp\left(-4\pi^2 \frac{w^2}{\xi^2}\right)\right) \tag{1.81}$$

Therefore, by means of Poisson's summation, we can rewrite our function in Jacobi Theta Function representation. This is useful when we want to examine multiples of period, or different periods, by considering different Jacobi Theta Functions.

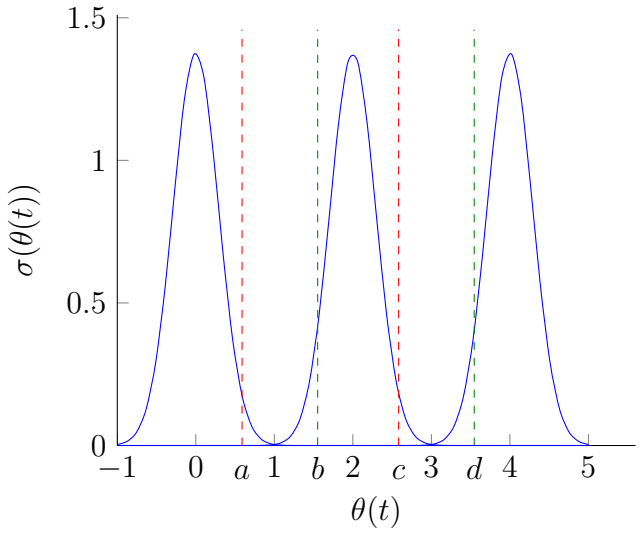

Figure 1.8: Periodic gaussian functions with period ξ, where $\xi = 2$. The distance between the red/green dotted lines is one period, *i.e.* $(c-a) = \xi$ and $(d-b) = \xi$. By graphical argument and the periodicity/properties of σ, we can show that $Area(a,b) + Area(b,c) = Area(a,c) = F(\xi) = Area(b,d) = Area(b,c) + Area(c,d)$. Therefore, this implies that $Area(a,b) = Area(c,d)$, and so if the value of C, in Eq. (2.3), is equal to $n\psi$ where $\psi = F(\xi)$. This would mean that the system would have started synchronised, where the phases for the two oscillators will differ by multiples of the period ξ.

Chapter 2

Two-oscillator Model

In this section, we consider two different types of systems. Firstly, we consider the non-time delay system for two-oscillator models [1], then we scrutinise the corresponding time delay system. Two-oscillator systems [2] consist of two oscillators which obey the equation of motion (1.73) introduced above, and we set $\omega_1 = \omega_2 = \omega$.

2.1 Non-time delay systems

For non-time delay two-oscillator systems, both θ_1 and θ_2 depend on the current time t. For simplicity, we assume the amplitudes of the coupling are symmetric, *i.e.* $\mathrm{J}_{12} = \mathrm{J}_{21} = \mathrm{J}$; and $\mathrm{J}_{ii} = 0$ as part of assumptions of the system. Therefore we have the set of equations of motion as

$$\dot{\theta_1} = \omega + \mathrm{J}\sigma(\theta_2) \tag{2.1}$$

$$\dot{\theta_2} = \omega + \mathrm{J}\sigma(\theta_1) \tag{2.2}$$

[1] This idea of two-oscillator models was introduced by Prof. H. J. Jensen., Imperial College London

[2] We lose a lot of detail by setting $\omega_i = \omega$ for all i. However, synchronisation in our system can mean $\theta_i = \tilde{\theta}$ for all i where $\tilde{\theta} \neq \bar{\theta}$ as defined in (3.2). For this to be true forever we require $\dot{\tilde{\theta}}_i = \omega_i + \sum_j \mathrm{J}_{ij}\sigma(\bar{\theta}) = \dot{\tilde{\theta}}$, which will imply $\omega_i = \omega$.

As both θ_1 and θ_2 are strictly positive, we can write

$$\frac{\dot{\theta}_2}{\dot{\theta}_1} = \frac{\mathrm{d}\theta_2}{\mathrm{d}\theta_1} = \frac{\omega + \mathrm{J}\sigma(\theta_1)}{\omega + \mathrm{J}\sigma(\theta_2)}$$

and therefore, we can deduce that

$$\int_{\theta_1(0)}^{\theta_1(t)} \omega + \mathrm{J}\sigma(\theta_1)\mathrm{d}\theta_1 = \int_{\theta_2(0)}^{\theta_2(t)} \omega + \mathrm{J}\sigma(\theta_2)\mathrm{d}\theta_2 \ .$$

By writing above integrals in the form of $F(\theta) = \int_0^{\theta} \omega + \mathrm{J}\sigma(\theta')\mathrm{d}\theta'$, we can express the above equation as

$$F(\theta_1) - F(\theta_2) = F(\theta_1(0)) - F(\theta_2(0)) = C \ . \tag{2.3}$$

where C is a constant. If we define time ψ as the time required for the oscillator θ_1 to travel one period ξ, *i.e.* $\theta_1(t+\psi) = \theta_1(t) + \xi$. From Eq. (2.3), we can rearrange the equation to get

$$F(\theta_1(t)) = C + F(\theta_2(t)) \tag{2.4}$$

which implies

$$\theta_1(t) = F^{-1}\left(C + F(\theta_2(t))\right) \ . \tag{2.5}$$

By substituting this into $\theta_1(t+\psi) = \theta_1(t) + \xi$, we have

$$F^{-1}(C + F(\theta_2(t+\psi))) = \theta_1(t+\psi) = \xi + \theta_1(t) = \xi + F^{-1}(C + F(\theta_2(t)))$$

and therefore

$$C + F(\theta_2(t+\psi)) = F(\xi) + C + F(\theta_2(t)) = C + F(\theta_2(t) + \xi)$$

which implies

$$\theta_2(t+\psi) = \theta_2(t) + \xi \ . \tag{2.6}$$

Note that $F(\theta)$ can be written as $F(\theta) = \theta\frac{\Theta}{\xi} + \tilde{F}(\theta)$, where $\tilde{F}(\theta)$ is a periodic function with period ξ,

$$F(\theta+\xi) = (\theta+\xi)\frac{\Theta}{\xi} + \tilde{F}(\theta+\xi) = \Theta + \theta\frac{\Theta}{\xi} + \tilde{F}(\theta) = \Theta + F(\theta)$$

where $\Theta = F(\xi) = \int_0^{\xi} \omega + J\sigma(x)\mathrm{d}x$. If $F(\theta)$ takes the form $F(\theta) = \int_0^{\theta} \omega + J\sigma(\theta')\mathrm{d}\theta'$, then $F(\theta)$ can be written as $F(\theta) = \frac{\Theta}{\xi}\theta + \tilde{F}(\theta)$, where $\tilde{F}(\theta)$ is a periodic function with period ξ. To see this, it will be sufficient to show whether $\tilde{F}(\theta) = F(\theta) - \frac{\Theta}{\xi}\theta$ is a periodic function. Therefore, we look at $\tilde{F}(\theta(t+\psi))$

$$\begin{aligned}\tilde{F}(\theta(t+\psi)) = \tilde{F}(\theta(t)+\xi) &= F(\theta+\xi) - \frac{\Theta}{\xi}(\theta+\xi) \\ &= \Theta + F(\theta) - \frac{\Theta}{\xi}\theta - \Theta = \tilde{F}(\theta)\ .\end{aligned}$$

Hence, we expect our $F(\theta)$ to be linear in θ, and therefore t [3], plus a periodic function. If we want to understand the dynamics of such a system, we would need to consider different values of C in the above expression (2.3) in order to analyse the behaviour of such a non-time delay two-oscillator system.

If the constant C is equal to 0, and since the integrand of F is monotonically increasing and strictly positive, this implies that $\theta_1(t) = \theta_2(t)\ \forall t$. Therefore the system would have been synchronised at the start, and vice versa.

If the constant $C = n\Theta$, where $n \in \mathbb{Z}$ and $\Theta = F(\xi)$ with ξ the period of the integrand of F (see Figure 1.8). We then can rewrite (2.3) as

$$F(\theta_1 - n\xi) - F(\theta_2) = 0 \tag{2.7}$$

by using the periodicity of the integrand of F, such that $F(\theta + n\xi) = F(\theta) + n\Theta$. From this, we can conclude that $\theta_1(t) - n\xi = \theta_2(t)\ \forall t$. Therefore, the system would have been synchronised at the start as well, and vice versa.

[3] Because θ is a monotonically increasing function in t, therefore there exists a bijection between θ and t.

This would leave us a final question of whether values of C, which are not equal to $n\Theta$, would lead to synchronisation in these kinds of non-time delay two-oscillator systems. This is equivalent of asking whether $F(\theta_1) - F(\theta_2) \neq n\Theta$ would imply $\theta_1 - \theta_2 \neq m\xi$, $\forall m, n \in \mathbb{Z}$ with $F(\theta) = \int_0^\theta \omega + \mathrm{J}\sigma(\theta')\mathrm{d}\theta'$. This can be proved by considering the contra-positive statement; which is, $\exists_{n\in\mathbb{Z}} F(\theta_1) - F(\theta_2) = n\Theta \Leftarrow \exists_{m\in\mathbb{Z}} \theta_1 - \theta_2 = m\xi$, namely when $m = n$. Therefore, we conclude that the system will not synchronise if the constant is not equal to $n\Theta$; and hence, the two-oscillator non-time delay systems should never synchronise.

It is instructive to study a linearised solution of the above system. Section 2.3 follows an analytic solution of a slight modification of our system with a concrete $\sigma(\theta)$. We define φ, the average difference of the two oscillators, and $\bar{\theta}$, the average of the two oscillators, we have

$$\varphi = \frac{1}{2}(\theta_1 - \theta_2) \tag{2.8}$$

$$\bar{\theta} = \frac{1}{2}(\theta_1 + \theta_2) \tag{2.9}$$

which gives, by substituting our equations of motion,

$$\dot{\varphi} = \frac{1}{2}\mathrm{J}(\sigma(\theta_2) - \sigma(\theta_1)) \tag{2.10}$$

$$\dot{\bar{\theta}} = \frac{1}{2}\mathrm{J}(\sigma(\theta_2) + \sigma(\theta_1)) + \omega \ . \tag{2.11}$$

For synchronisation, we require φ to converge to a constant as $t \to \infty$, which implies $\dot{\varphi} = 0$. By writing θ_1 and θ_2 in terms of φ and $\bar{\theta}$, and substituting to $\dot{\varphi}$ above gives $0 = \dot{\varphi} = \frac{1}{2}\mathrm{J}(\sigma(\bar{\theta} - \varphi) - \sigma(\bar{\theta} + \varphi))$. Therefore, $\varphi = 0$ is a fixed point as $\sigma(\bar{\theta} - \varphi) = \sigma(\bar{\theta} + \varphi)$. We now then consider the first order linearisation of this system by expanding in small values of φ, and the above equations become

$$\dot{\varphi} \approx -\mathrm{J}\varphi\sigma'(\bar{\theta}) \tag{2.12}$$

$$\dot{\bar{\theta}} \approx \mathrm{J}\sigma(\bar{\theta}) + \omega \ . \tag{2.13}$$

Since $\bar{\theta}$ is also strictly positive, we can write

$$\frac{\dot{\varphi}}{\dot{\bar{\theta}}} = \frac{\mathrm{d}\varphi}{\mathrm{d}\bar{\theta}} = \frac{-\mathrm{J}\varphi\sigma'(\bar{\theta})}{\mathrm{J}\sigma(\bar{\theta})+\omega} = -\varphi\frac{\mathrm{d}}{\mathrm{d}\bar{\theta}}[\ln(\mathrm{J}\sigma(\bar{\theta})+\omega)+c_1] \tag{2.14}$$

for some constants c_1. This gives,

$$\varphi(t) = \varphi_0\frac{[\mathrm{J}\sigma(\bar{\theta}(0))+\omega]}{\mathrm{J}\sigma(\theta(\bar{t}))+\omega} \tag{2.15}$$

Both analytic result (2.3) and linearised result (2.15) suggest synchronisation would not be observed in these kinds of non-time delay two-oscillator systems. However, when we numerically integrate this set of equations using the standard Euler method (in Section 2.2.1), synchronisation is attained. A question is then raised: why would the numerics show synchronisation while analytically there should not be any?

To check whether this is a numerical issue, we seek an improvement of integrating the set of equations numerically. Once we implement this slight improvement (see Section 2.2.2), the unpredicted synchronisation effect will disappear; however, for some sets of parameters, the system will still synchronise after a very long period of time. After this slight improvement on the standard Euler scheme, we want to investigate whether the numerics with higher order derivatives will match our analytical result. Therefore, we look into applying the Runge-Kutta method (see Section 2.2.3) to our differential equations, and indeed the system will no longer be synchronised. Further analysis and detail will be discussed in Section 2.2.

In summary, the analytics suggests that no synchronisation would be obtained, while the standard Euler numerics shows that the system would actually be synchronised. However if we slightly improve the standard Euler numerical scheme, the numerics only gives synchronisation after very long period of time; and if we go a step further by considering higher order derivatives and using the Runge-Kutta method, the numerics actually agrees with the analytics; that is, synchronisation will never take place in two-oscillator non-time delay systems if the systems were not synchronised at the beginning.

2.2 Numerics for Two-oscillator Non-time delay Model

In this section, we are going to find solutions of our systems by numerical integration. We concentrate on applying the standard Euler method, our version of the Euler method and Runge-Kutta integration on the two-oscillator non-time delay systems. The equation of motion of two-oscillator non-time delay system is

$$\dot{\theta}_i(t) = \omega_i + \sum_{j}^{N} \mathrm{J}_{ij}\sigma(\theta_j(t)) \ . \tag{2.16}$$

Same as we have introduced in the analytics, we set all the oscillators to have the same initial frequencies, *i.e.* $\omega_i = \omega$ for all i, and we also set the amplitudes of the coupling to be symmetric and equal, that is $\mathrm{J}_{ij} = \mathrm{J}_{ji} = \mathrm{J}$, but $\mathrm{J}_{ii} = 0$.

2.2.1 Standard Euler Integration

In order to approximate the solution of the initial value problem

$$\dot{\theta}(t) = f(t, \theta(t)), \qquad \theta(t_0) = \theta_0 \tag{2.17}$$

we apply linear approximation around the point $(t_0, \theta(t_0))$, that is, by using the first two terms of the Taylor expansion of θ. One step of the Euler method from t_n to $t_{n+1} = t_n + \Delta t$, with small values of time increment Δt, is then

$$\theta(t + \Delta t) \approx \theta + \Delta t\dot{\theta} \ . \tag{2.18}$$

By implementing this numerical scheme on the equations of motion of two-oscillator non-time delay systems as defined in Section 2.1, with $\sigma(\theta)$ a periodic gaussian function of the form $\sigma(\theta) = \frac{1}{\zeta\sqrt{2\pi}} \exp\left(-\frac{\theta^2}{2\zeta^2}\right)$, where $\zeta = w\sqrt{2}$ in Eq. (1.79) and the values of θ are modulo of the period ξ. Synchronisation is attained by standard Euler integration for such systems (see Figure 2.1). If we improve the resolution, by a factor of 20, on our integration time step Δt, the synchronisation phenomenon still exists (see Figure 2.3 inset), but after

a much longer time. However, the numerical results obtained from the standard Euler integration does not seem to agree with our analytical solution Eq. (2.3).

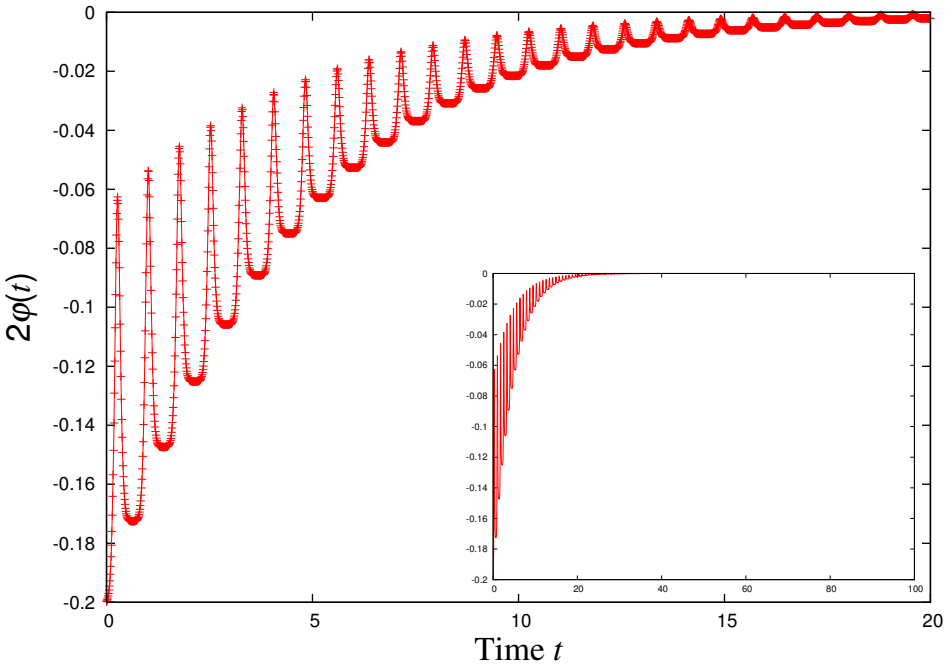

Figure 2.1: Trajectory of solution to the two-oscillator non-time delay systems using standard Euler scheme with $\Delta t = 0.01$, $\xi = 1.0$, $\omega = 1.0$ and $\zeta = 0.1$. Inset: trajectory between time 0 to 100.

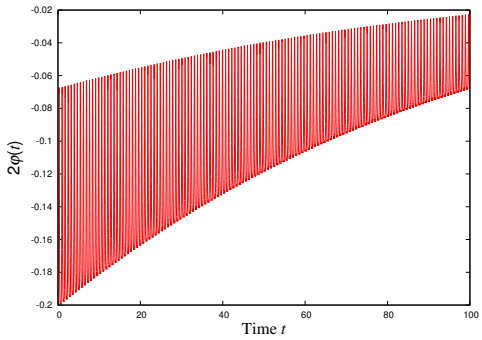

Figure 2.2: Trajectory of solution to the two-oscillator non-time delay systems using standard Euler scheme with $\Delta t = 0.0005$, $\xi = 1.0$, $\omega = 1.0$ and $\zeta = 0.1$.

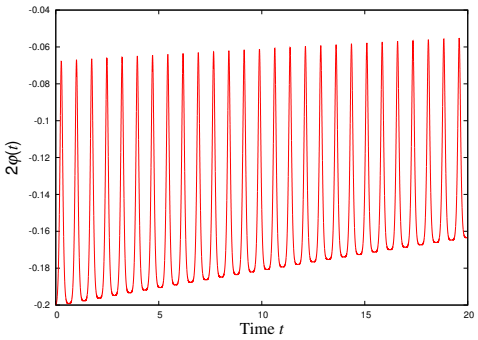

Figure 2.3: Same data as Figure 2.2 between time 0 to 20.

2.2.2 Improved Euler Integration

In this section we seek an improvement of the standard Euler method when integrating the two-oscillator non-time delay systems. The standard Euler method is relying on

forward derivatives

$$\dot{\theta} = \frac{\theta(t + \Delta t) - \theta}{\Delta t} \tag{2.19}$$

which has a broken symmetry and only depends on the current time t. Since $\dot{\theta}(t)$ is actually a function depends only on θ, we can write $\dot{\theta} = f(\theta)$. The standard Euler (2.18) becomes

$$\theta(t + \Delta t) \approx \theta + \Delta t\dot{\theta} = \theta + \Delta t f(\theta) = \theta + \Delta\theta_0 \ , \tag{2.20}$$

where θ_0 is the old approximation of θ. We introduce the better approximation by taking the average of current value of θ and a *bad* estimation of the future value of $\theta + \Delta\theta_0$, that is

$$\begin{aligned}
\Delta\theta_1 &= \frac{1}{2}\Delta t f(\theta) + \frac{1}{2}\Delta t f(\theta + \Delta\theta_0) \\
&\cong \frac{1}{2}\Delta t f(\theta) + \frac{1}{2}\Delta t(f(\theta) + \Delta\theta_0 f'(\theta)) \\
&= \Delta t\dot{\theta} + \frac{1}{2}(\Delta t)^2\dot{\theta}f'(\theta) \ .
\end{aligned}$$

Since $\dot{\theta} = f(\theta)$, then this implies $\ddot{\theta} = \dot{\theta}f'(\theta)$ and therefore, the new approximation by the improved Euler method is

$$\theta(t + \Delta t) \approx \theta + \Delta\theta_1 = \theta + \Delta t\dot{\theta} + \frac{1}{2}(\Delta t)^2\ddot{\theta} \tag{2.21}$$

which is effectively taking the second derivative of θ, with respect to t, into account when integrating. Similar to the standard Euler scheme, we take $\sigma(\theta)$ in form of a periodic gaussian function, *i.e.* $\sigma(\theta) = \frac{1}{\zeta\sqrt{2\pi}} \exp\left(-\frac{\theta^2}{2\zeta^2}\right)$. When we use this procedure to integrate the two-oscillator non-time delay systems, with $\Delta t = 0.0005$, the improved Euler scheme resolves the numerical discrepancy to some extent, *i.e.* the system will no longer synchronise (see Figure 2.4). However if we use a lower resolution of Δt, *i.e.* $\Delta t = 0.01$, the system would still synchronise after a comparatively long period of time (see Figure 2.6).

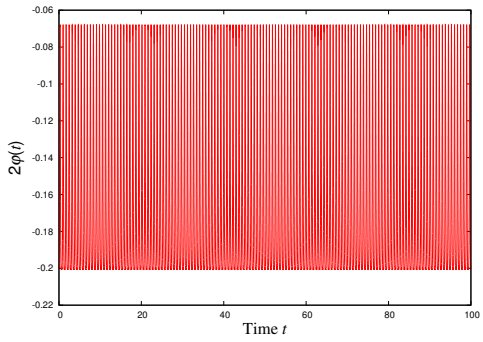

Figure 2.4: Trajectory of solution to the two-oscillator non-time delay systems using improved Euler scheme with $2\varphi_0 = 0.2$, $\Delta t = 0.0005$, $\xi = 1.0$, $\omega = 1.0$ and $\zeta = 0.1$.

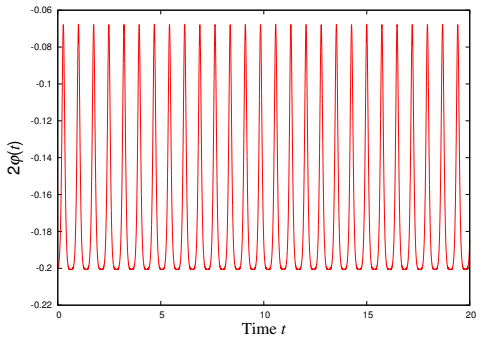

Figure 2.5: Same data as Figure 2.4 between time 0 to 20.

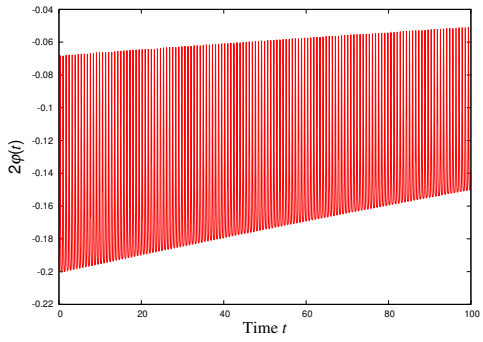

Figure 2.6: Trajectory of solution to the two-oscillator non-time delay systems using improved Euler scheme with $2\varphi_0 = 0.2$, $\Delta t = 0.01$, $\xi = 1.0$, $\omega = 1.0$ and $\zeta = 0.1$.

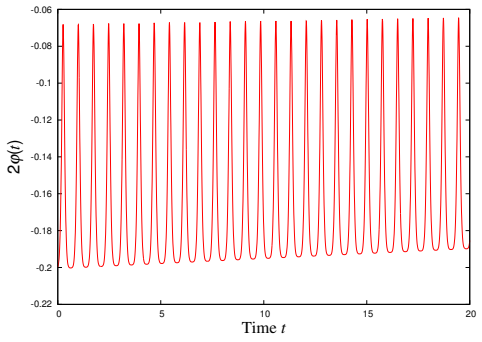

Figure 2.7: Same data as Figure 2.6 between time 0 to 20.

2.2.3 Interleaved integration with Runge-Kutta

After this slight improvement of the standard Euler scheme, we want to investigate whether higher derivatives will give us the correct numerical results. Therefore, we look into apply the Runge-Kutta forth-order method, more commonly known as RK4, to our differential equations.

If we have an initial value problem

$$\theta(t) = f(t, \theta(t)), \qquad \theta(t_0) = \theta_0 \ ,$$

the RK4 method [53] for the full system is given by

$$\begin{aligned} \theta_{n+1} &= \theta_n + \frac{1}{6}(k_1 + 2k_2 + 2k_3 + k_4) \\ t_{n+1} &= t_n + \Delta t \end{aligned}$$

where $\theta(t_{n+1})$ is approximated by θ_{n+1} using RK4; and,

$$\begin{aligned} k_1 &= (\Delta t) f(t_n, \theta_n) \\ k_2 &= (\Delta t) f\left(t_n + \frac{1}{2}\Delta t, \theta_n + \frac{1}{2}k_1\right) \\ k_3 &= (\Delta t) f\left(t_n + \frac{1}{2}\Delta t, \theta_n + \frac{1}{2}k_2\right) \\ k_4 &= (\Delta t) f(t_n + \Delta t, \theta_n + k_3) \end{aligned}$$

where k_1 is the slope at the beginning of the interval; k_2 and k_3 are the slopes at the midpoint of the interval, with the intermediate θ values determined at the point $t_n + \frac{\Delta t}{2}$ via Euler's method using slope k_1 and k_2 respectively; and k_4 is the slope at the end of the interval, using slope k_3 to determine its θ value.

The next value of θ_{n+1} is then determined by adding the current value of θ_n and the product of the size of interval, Δt, with estimated slope, s; where

$$s = \frac{1}{6}(k_1 + 2k_2 + 2k_3 + k_4) \tag{2.22}$$

is a weighted average of the slopes. Similar to other non-time delay systems, we take $\sigma(\theta) = \frac{1}{\zeta\sqrt{2\pi}} \exp\left(-\frac{\theta^2}{2\zeta^2}\right)$. We implement the RK4 method, via the numerical RK4 routine by Press et al. [53], to our differential equation and the unpredicted synchronisation effect will vanish, even with $\Delta t = 0.01$ (see Figure 2.8). This means that the numerics of the full system on N-oscillator non-time delay system will never synchronise, and this agrees with the linearised solution (2.15) we found.

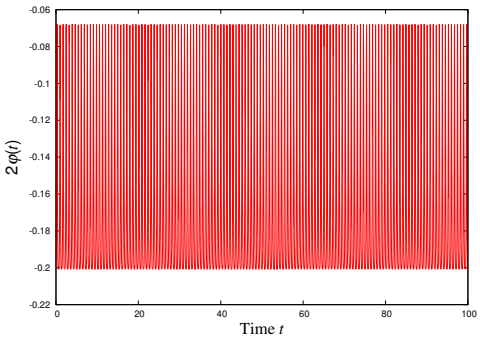

Figure 2.8: Trajectory of solution to the two-oscillator non-time delay systems using RK4 method with $2\varphi + 0 = 0.2$, $\Delta t = 0.01$, $\xi = 1.0$, $\omega = 1.0$ and $\zeta = 0.1$.

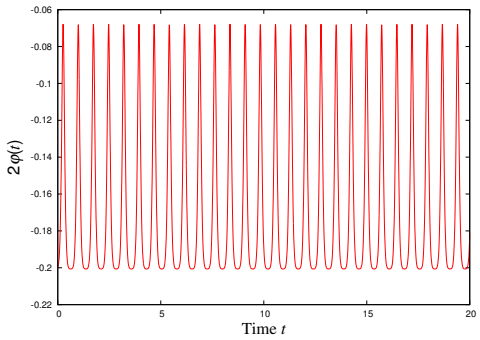

Figure 2.9: Same data as Figure 2.8 between time 0 to 20.

2.3 Analytical solution of a two-oscillator non-time delay system

In this section, we show how a coupled system, which consists of two non-time delay oscillators, can be solved analytically. This particular system has equations of motion

$$\dot{\theta}_1 = \omega + \sigma(\theta_2) - \sigma(\theta_1) \tag{2.23}$$

$$\dot{\theta}_2 = \omega + \sigma(\theta_1) - \sigma(\theta_2) \tag{2.24}$$

with $\sigma(x) = \frac{\kappa}{2}\sin(x)$. If we let φ be the average difference of the two oscillators, and let $\bar{\theta}$ be the average of the two oscillators, we have

$$\varphi = \frac{1}{2}(\theta_1 - \theta_2) \tag{2.25}$$

$$\bar{\theta} = \frac{1}{2}(\theta_1 + \theta_2)\ . \tag{2.26}$$

By writing θ_1 and θ_2 in terms of φ and $\bar{\theta}$, *i.e.* $\theta_1 = \bar{\theta} + \varphi$ and $\theta_2 = \bar{\theta} - \varphi$, we get

$$\dot{\varphi} = \sigma(\theta_2) - \sigma(\theta_1) = \sigma(\bar{\theta} + \varphi) - \sigma(\bar{\theta} - \varphi) \tag{2.27}$$

$$\dot{\bar{\theta}} = \omega \tag{2.28}$$

which gives $\bar{\theta}(t) = \omega t + \bar{\theta}(0)$ but we can always set $\bar{\theta}(0) = 0$ by having initially symmetric setup of the oscillators; and so,

$$\dot{\varphi} = \frac{\kappa}{2}\sin(\omega t - \varphi) - \frac{\kappa}{2}\sin(\omega t + \varphi) = -\kappa\sin(\varphi)\cos(\omega t)\ . \tag{2.29}$$

Using separation of variables, we can obtain the analytic solution as

$$\tan\left(\frac{\varphi}{2}\right) = \tan\left(\frac{\varphi_0}{2}\right)\exp\left(-\frac{\kappa}{\omega}\sin(\omega t)\right) \tag{2.30}$$

which gives,

$$\varphi(t) = 2\tan^{-1}\left[\tan\left(\frac{\varphi_0}{2}\right)\exp\left(-\frac{\kappa}{\omega}\sin(\omega t)\right)\ .\right] \tag{2.31}$$

From this equation, we can obtain the range of the system as

$$-\frac{\kappa}{\omega} \leq \ln\left(\frac{\tan(\frac{\varphi(t)}{2})}{\tan(\frac{\varphi_0}{2})}\right) \leq \frac{\kappa}{\omega} \ . \tag{2.32}$$

For this particular example, we can conclude that, the sign of $\tan\left(\frac{\varphi_0}{2}\right)$ will need to be the same as $\tan\left(\frac{\varphi(t)}{2}\right)$ since $\ln(x)$ is only defined for $x > 0$. On another note, if there was a change of sign of $\tan\left(\frac{\varphi(t)}{2}\right)$, we would think that it is possible on having $\varphi = 0$ but once that is reached, the system should stay there. From (2.31), we can also see that $\varphi(t)$ does not synchronise if $t \to \infty$, instead, it oscillates with frequency ω.

By comparing this particular model of two-oscillator non-time delay system to Kuramoto's model (1.13) of case $N = 2$ and $\omega_i = \omega$, that is

$$\dot{\theta}_1 = \omega + \frac{\kappa}{2}\sin(\theta_2 - \theta_1) \tag{2.33}$$

$$\dot{\theta}_2 = \omega + \frac{\kappa}{2}\sin(\theta_1 - \theta_2) \ . \tag{2.34}$$

Instead of considering the sine of the difference between the oscillators, as introduced in the Kuramoto model; we consider the difference of the sine of the oscillators in our model. We can see a fundamental difference of our model compared to Kuramoto's. The Kuramoto model suggests synchronisation whereas our model oscillates with frequency ω, *i.e.* our model does not synchronise. The reason of this fundamental difference is, although both models are solved by linearisation, when θ_1 and θ_2 become large, $\sin(\theta_2) - \sin(\theta_1) \neq \sin(\theta_2 - \theta_1) + \mathcal{O}(\sin)^2$.

2.4 Timedelay Systems

The difference between the standard Euler and improved Euler numerics is that, the standard Euler is based on the *past* values of t, but the improved Euler is based on an average of *past* and estimated *future* values of t. Our method for obtaining the estimated future values of t is discussed in Section 2.2.2. This slight change in the numerics suggests that time delay may play a role in such systems for synchronisation, as standard Euler only takes θ values at t to approximate the θ value at $t + \Delta t$. To verify this, we now look into the time delay systems. In order to implement the time delay, we introduce δt into the system, where δt is small but finite. The equations of motion are now

$$\dot{\theta_1} = \omega + \mathrm{J}\sigma(\theta_2(t - \delta t)) \tag{2.35}$$

$$\dot{\theta_2} = \omega + \mathrm{J}\sigma(\theta_1(t - \delta t)) \tag{2.36}$$

Similar to the non-time delay systems, we introduce φ and $\bar{\theta}$, such that

$$\varphi = \frac{1}{2}(\theta_1 - \theta_2)$$
$$\bar{\theta} = \frac{1}{2}(\theta_1 + \theta_2)$$

To investigate this kind of systems, we first apply Perturbation Theory by expanding about small values of δt. This gives

$$\dot{\theta_1} = \omega + \mathrm{J}[\sigma(\bar{\theta} - \varphi) - \delta t\dot{\theta_2}\sigma'(\bar{\theta} - \varphi) + ...]$$
$$\dot{\theta_2} = \omega + \mathrm{J}[\sigma(\bar{\theta} + \varphi) - \delta t\dot{\theta_1}\sigma'(\bar{\theta} + \varphi) + ...]$$

and we can rewrite $\dot{\varphi}$ and $\dot{\bar{\theta}}$ using our equations of motion, giving

$$\dot{\varphi} = \frac{1}{2}\mathrm{J}[\sigma(\theta_2(t - \delta t)) - \sigma(\theta_1(t - \delta t)]$$
$$\dot{\bar{\theta}} = \frac{1}{2}\mathrm{J}[\sigma(\theta_2(t - \delta t)) + \sigma(\theta_1(t - \delta t))] + \omega$$

At this point we consider small values of φ as we require φ to converage to a constant as $t \to \infty$ for synchronisation. Hence, for small values of φ, expanding in σ gives

$$\sigma(\theta_1) = \sigma(\bar{\theta}) + \varphi\sigma'(\bar{\theta}) + \frac{1}{2}\varphi^2\sigma''(\bar{\theta}) + ...$$
$$\sigma(\theta_2) = \sigma(\bar{\theta}) - \varphi\sigma'(\bar{\theta}) + \frac{1}{2}\varphi^2\sigma''(\bar{\theta}) + ...$$

This implies that our equation, in first order of δt, of $\dot{\varphi}$ becomes

$$\begin{aligned}\dot{\varphi} &= -\mathrm{J}\varphi(t-\delta t)\sigma'(\bar{\theta}(t-\delta t)) + \mathcal{O}(\varphi)^3 \\ &\approx -\mathrm{J}(\varphi - \delta t\dot{\varphi})\sigma'(\bar{\theta}(t-\delta t)) \\ &= -\mathrm{J}\varphi(\sigma'(\bar{\theta}) - \delta t\dot{\bar{\theta}}\sigma''(\bar{\theta})) + \mathrm{J}\delta t\dot{\varphi}\sigma'(\bar{\theta}) + \mathcal{O}(\delta t)^2\end{aligned}$$

which gives,

$$\dot{\varphi} \approx -\varphi\frac{\mathrm{J}(\sigma'(\bar{\theta}) - \delta t\dot{\bar{\theta}}\sigma''(\bar{\theta}))}{1 - \mathrm{J}\delta t\sigma'(\bar{\theta})} = -\varphi(\mathrm{J}\sigma'(\bar{\theta}) - \mathrm{J}\delta t\dot{\bar{\theta}}\sigma''(\bar{\theta}) + \mathrm{J}^2\delta t\sigma'^2(\bar{\theta}) + \mathcal{O}(\delta t)^2) \tag{2.37}$$

Similar to φ, our equation of $\bar{\theta}$, in first order of δt, becomes

$$\begin{aligned}\dot{\bar{\theta}} &= \mathrm{J}\sigma(\bar{\theta}(t-\delta t)) + \omega + \mathcal{O}(\varphi)^2 \\ &\approx \mathrm{J}\sigma(\bar{\theta}) - \mathrm{J}\delta t\dot{\bar{\theta}}\sigma'(\bar{\theta}) + \omega\end{aligned} \tag{2.38}$$

which gives,

$$\dot{\bar{\theta}} = \frac{\mathrm{J}\sigma(\bar{\theta}) + \omega}{1 + \mathrm{J}\delta t\sigma'(\bar{\theta})} = \omega + \mathrm{J}\sigma(\bar{\theta}) - \mathrm{J}\delta t\sigma'(\bar{\theta})(\omega + \mathrm{J}\sigma(\bar{\theta})) + \mathcal{O}(\delta t)^2 \tag{2.39}$$

Again, since $\bar{\theta}$ is strictly positive, in first order of δt, we can write

$$\varphi' = \frac{\mathrm{d}\varphi}{\mathrm{d}\bar{\theta}} \approx \frac{-\varphi(\mathrm{J}\sigma'(\bar{\theta}) - \mathrm{J}\delta t\dot{\bar{\theta}}\sigma''(\bar{\theta}) + \mathrm{J}^2\delta t\sigma'^2(\bar{\theta}))}{\omega + \mathrm{J}\sigma(\bar{\theta}) - \mathrm{J}\delta t\sigma'(\bar{\theta})(\omega + \mathrm{J}\sigma(\bar{\theta}))}$$

Considering the derivative of $\dot{\bar{\theta}}$ with respect to $\bar{\theta}$, we have

$$\dot{\bar{\theta}}' = \frac{\mathrm{d}}{\mathrm{d}\bar{\theta}}\dot{\bar{\theta}} = \mathrm{J}\sigma'(\bar{\theta}) - \mathrm{J}\delta t\dot{\bar{\theta}}\sigma''(\bar{\theta}) - \mathrm{J}^2\delta t\sigma'^2(\bar{\theta})$$

By substituting the approximation of $\dot{\bar{\theta}}$, (2.39), and using this expression of $\dot{\bar{\theta}}'$, we can simplify the equation of φ', up to first order of δt, as,

$$\varphi' = -\varphi\left(\frac{\mathrm{d}}{\mathrm{d}\bar{\theta}}\ln(\dot{\bar{\theta}}(\bar{\theta})) + \frac{2\mathrm{J}^2\delta t\sigma'^2(\bar{\theta})}{\dot{\bar{\theta}}(\bar{\theta})}\right) \tag{2.40}$$

By separation of variables, we get

$$\varphi(t) = \varphi_0\frac{\dot{\bar{\theta}}(0)}{\dot{\bar{\theta}}(t)}\exp\left(-2\mathrm{J}^2\delta t\int_{\bar{\theta}(0)}^{\bar{\theta}}\frac{\sigma'^2(\bar{\theta}')}{\dot{\bar{\theta}}(\bar{\theta}')}\mathrm{d}\bar{\theta}'\right),$$

containing $\bar{\theta}(t)$, which can be obtained by integrating (2.39). A more practical form of the equation above is found by considering $\bar{\theta}$ as the independent variable, consistent with $\dot{\bar{\theta}}$ in (2.39), which is best interpreted as a function of $\bar{\theta}$ as well

$$\varphi(t(\bar{\theta})) = \varphi_0\frac{\dot{\bar{\theta}}(0)}{\dot{\bar{\theta}}(t(\bar{\theta}))}\exp\left(-2\mathrm{J}^2\delta t\int_{\bar{\theta}(0)}^{\bar{\theta}(t(\bar{\theta}))}\frac{\sigma'^2(\bar{\theta}')}{\dot{\bar{\theta}}(\bar{\theta}')}\mathrm{d}\bar{\theta}'\right). \tag{2.41}$$

Clearly, from the linearised solution (2.41) above, the system will eventually be synchronised with the presence of time delay. $\varphi(t)$ goes to zero exponentially in δt. We can also note that, the larger value of the time delay, the quicker the system is going to be synchronised. If we turn off the time delay in (2.41), we recover the linearised solution (2.15) of the two-oscillator non-time delay system, *i.e.* no synchronisation if $\delta t \to 0$.

2.5 Numerics for Two-oscillator Timedelay Model

After we conclude that the non-time delay systems of our model will not synchronise, we want to investigate whether the time delay systems of our model agree with the analytics. In order to do this, we will implement time delay into our numerics. We will also apply the various numerical methods: standard Euler, our version of the Euler method and Runge-Kutta integration to our two-oscillator time delay systems. The reliability will then be checked against the linearised solution of the two-oscillator time delay model. The equation of motion of two-oscillator time delay system is

$$\dot{\theta}_i(t) = \omega_i + \sum_{j}^{N} \mathrm{J}_{ij}\sigma(\theta_j(t-\delta t)) \tag{2.42}$$

Similar to the non-time delay system, we set all the oscillators to have the same initial frequencies, *i.e.* $\omega_i = \omega$ for all i, and we also set the amplitudes of the coupling to be symmetric and equal, that is $\mathrm{J}_{ij} = \mathrm{J}_{ji} = \mathrm{J}$, but $\mathrm{J}_{ii} = 0$.

2.5.1 Standard Euler Integration

For two-oscillator time delay systems, our initial value problem is then

$$\dot{\theta}(t) = f(\theta(t-\delta t)), \qquad \theta(t_0) = \theta_0 \ . \tag{2.43}$$

We implement the time delay by introducing δt to our numerics such that our σ function depends on the *past* values of θ, that is $\sigma = \sigma(\theta(t-\delta t))$. For our two-oscillator time delay system, the numerics from the standard Euler scheme shows synchronisation (see Figure 2.10). By comparing the standard Euler numerics of two-oscillator non-time delay and standard Euler numerics of two-oscillator time delay systems (see Figure 2.11), we conclude that the standard Euler scheme does indeed have a self-implemented time delay feature; however, the tendency to synchronise in the standard Euler scheme is now mixed with the effect of the time delay.

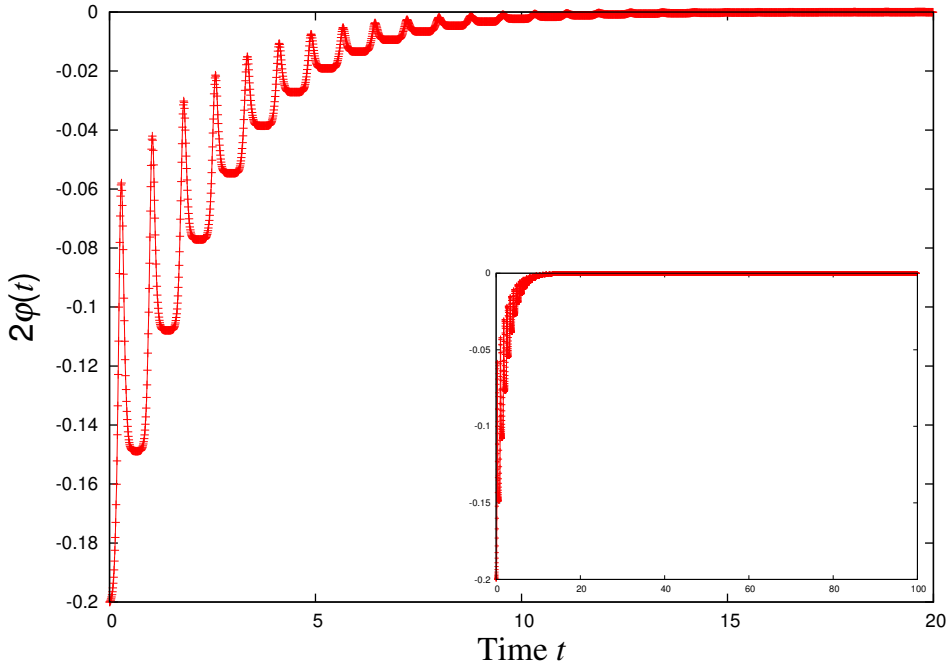

Figure 2.10: Trajectory of the two-oscillator time delay systems using Euler method. Parameters used: $2\varphi_0 = 0.2$, $\Delta t = 0.0005$, $\xi = 1.0$, $\omega = 1.0$, $\zeta = 0.1$ and $\delta t = 0.05$. Inset: Trajectories between time 0 and 100.

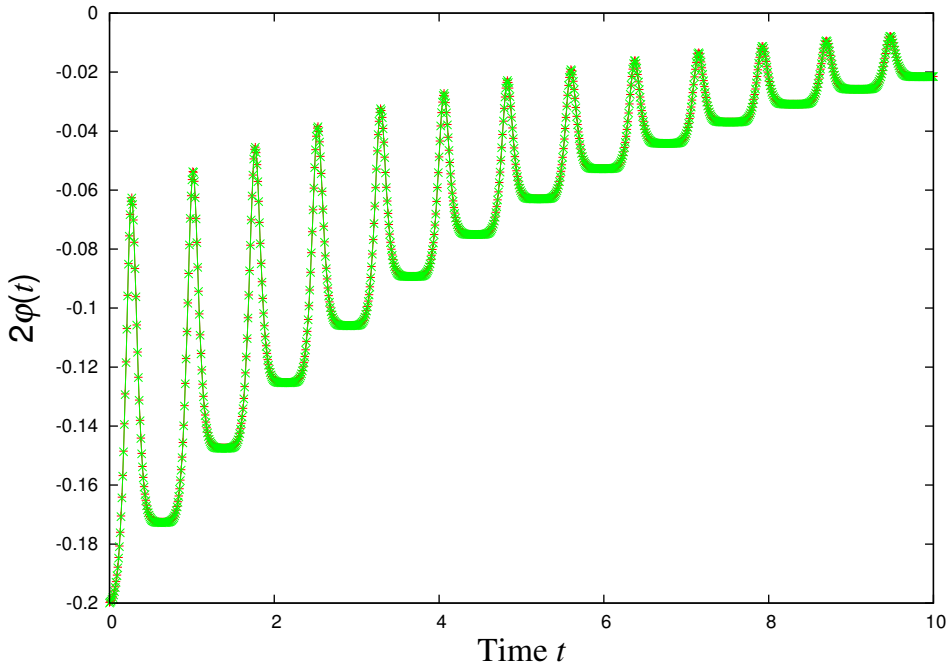

Figure 2.11: Trajectory comparisons of of non-time delay (Figure 2.1, red) and corresponding time delay systems (green) on top of each other, both numerics are based on the standard Euler scheme. Parameters used: $2\varphi_0 = 0.2$, $\Delta t = 0.01$, $\xi = 1.0$, $\omega = 1.0$, $\zeta = 0.1$ and $\delta t = 0.01$. The two numerics match precisely to each other suggesting that the standard Euler scheme has a self-implemented time delay feature.

2.5.2 Improved Euler Integration

Since the standard Euler is not reliable for obtaining the correct numerical results for two-oscillator non-time delay system, in order to verify whether our time delay systems will synchronise numerically we look into our version of the Euler scheme, *i.e.* the improved Euler integration method introduced in Section 2.2.2. Again, we implement the time delay by introducing the variable δt into our numerics, such that our feedback function σ depends on *past* values of θ.

Both the numerics from the standard Euler scheme and the improved Euler scheme (see Figure 2.13) match closely with each other. Therefore, we expect our time delay systems to synchronise with presence of time delay.

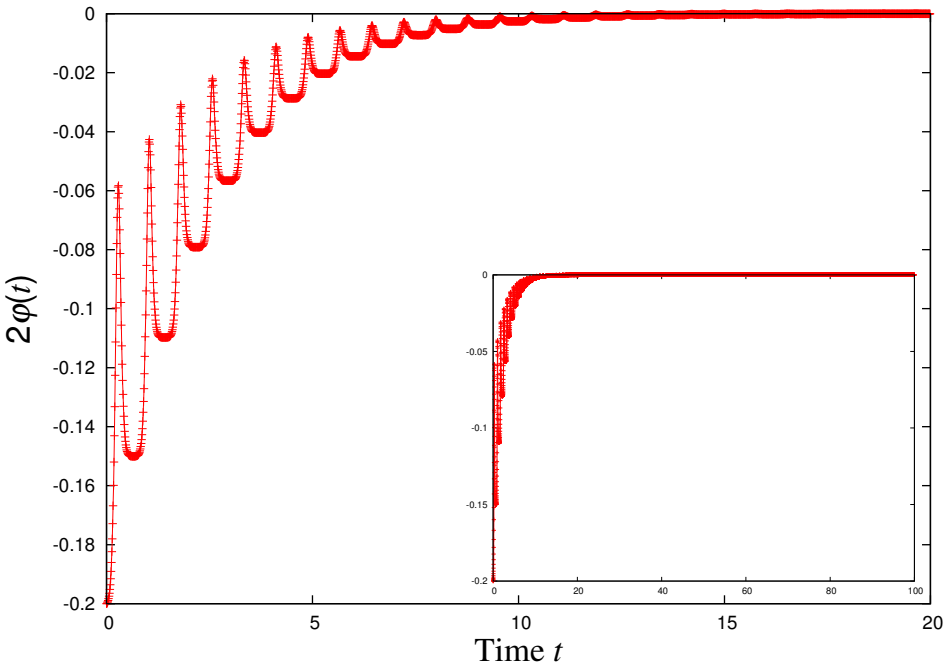

Figure 2.12: Trajectory outputs of the two-oscillator time delay systems using improved Euler integration. Parameters used: $2\varphi_0 = 0.2$, $\Delta t = 0.0005$, $\xi = 1.0$, $\omega = 1.0$, $\zeta = 0.1$ and $\delta t = 0.05$. Inset: Trajectories between time 0 and 100.

2.5.3 Interleaved integration with Runge-Kutta

Since both Euler's method and the improved Euler scheme agree closely to each other, we would want to confirm whether with higher order derivatives the numerics of our time delay system will synchronise with the presence of time delay. Again, we apply the

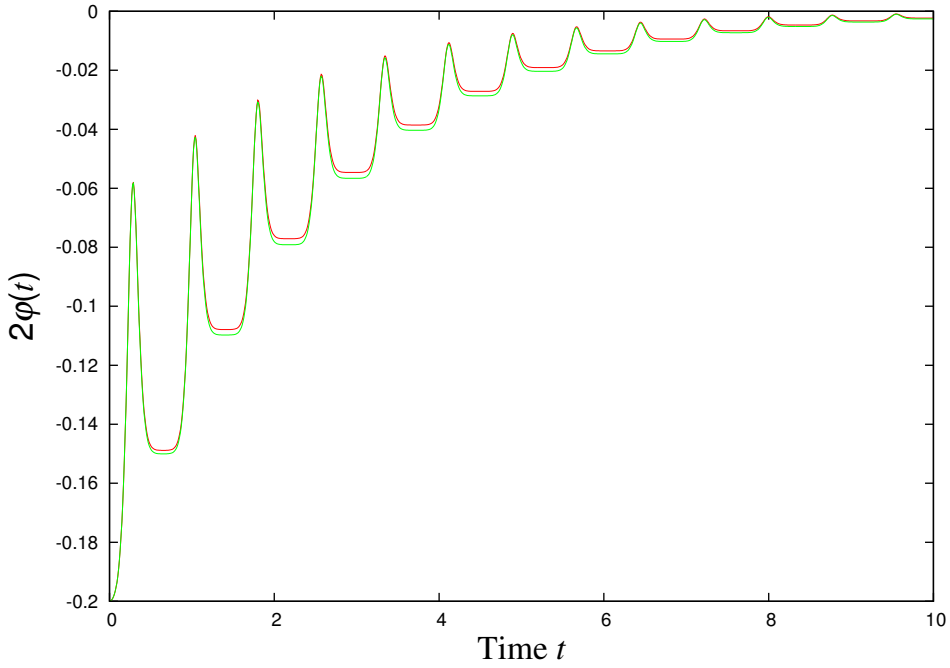

Figure 2.13: Trajectory outputs of standard Euler (red) scheme and improved Euler (green) scheme match very closely on the two-oscillator time delay system. Parameters used: $2\varphi_0 = 0.2$, $\Delta t = 0.0005$, $\xi = 1.0$, $\omega = 1.0$, $\zeta = 0.1$ and $\delta t = 0.01$

numerical RK4 routine by Press et al. [53], to our full time delay system (see Figure 2.14). We can see that the three numerics all show synchronisation and they match very closely to each other (see Figure 2.15). Note that the Euler scheme deviates little compared to the improved Euler scheme due to the self-implemented time delay feature in the Euler scheme.

Since the RK4 method is the most reliable, we go on to investigate the synchronisation behaviours of the systems and we look into draw a phase diagram of the system. In order to cope with the large history data we are going to use, we introduce and utilise a circular piece of memory so that we only go back as far as we need, *i.e.* one time step, and therefore the history size of the circular piece memory is the ratio of time delay to the integration time step, *i.e.* $\frac{\delta t}{\Delta t}$. Most importantly the time delay therefore has to be an integer multiple of the integration time step.

When we start to look into different values of initial phase difference between the two oscillators, all time delay systems will indeed synchronise; however, we discover that our time delay system may synchronise to different states, namely multiples of periods of ξ (see Figure 2.16), depending on the initial phase difference. For convenience on

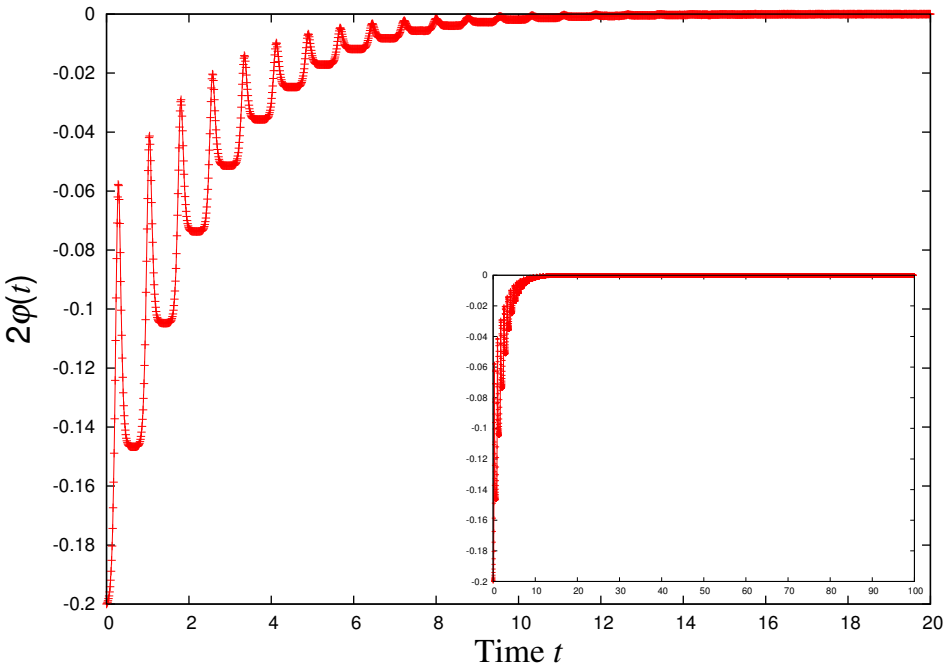

Figure 2.14: Trajectory outputs of the two-oscillator time delay systems using RK4 method with interpolation approximation. Parameters used: $2\varphi_0 = 0.2$, $\Delta t = 0.0005$, $\xi = 1.0$, $\omega = 1.0$, $\zeta = 0.1$, and $\delta t = 0.05$. Inset: Trajectories between time 0 and 100.

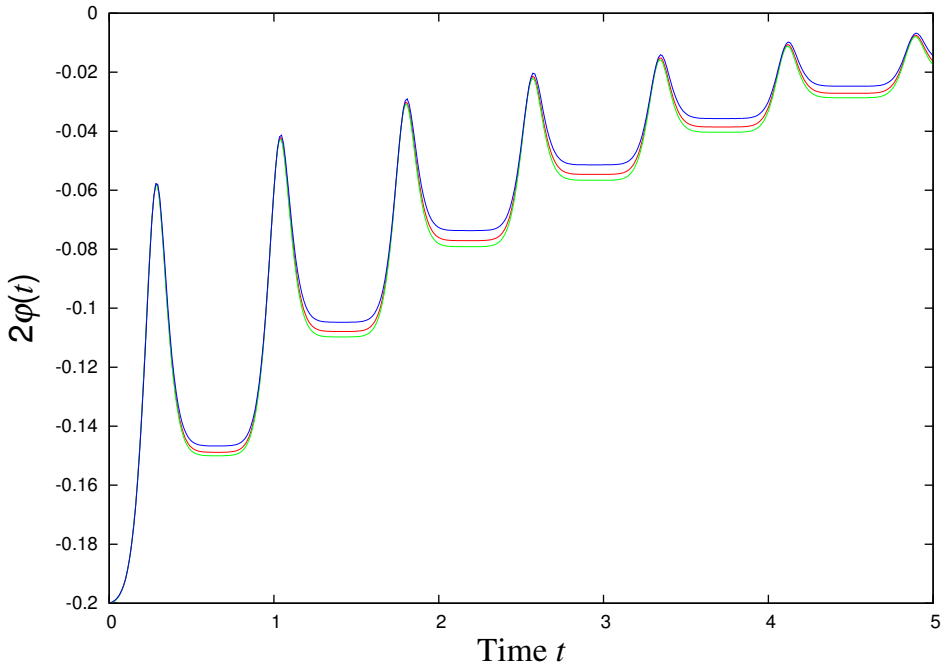

Figure 2.15: Trajectories outputs of the standard Euler scheme (red), the improved Euler scheme (green) and RK4 method (blue) match very closely to one another of the two-oscillator time delay system. Parameters used: $2\varphi_0 = 0.2$, $\Delta t = 0.0005$, $\xi = 1.0$, $\omega = 1.0$, $\zeta = 0.1$ and $\delta t = 0.01$.

understanding the effect graphically, we consider $\theta_2(t) - \theta_1(t)$ in see Figure 2.16, because initially $\theta_2(0) > \theta_1(0)$ in our setup. If $(\theta_2(0) - \theta_1(0)) \in (0, n\xi - \frac{\xi}{2} + \epsilon)$ with $\epsilon = 0.004$, the system will synchronise to $(n-1)\xi$ while if $(\theta_2(0) - \theta_1(0)) \in (n\xi - \frac{\xi}{2} + \epsilon, n\xi)$, the system will then synchronise to $n\xi$. This is due to the stability of our unstable node of the system, that is, at half of a period $n\xi + \frac{\xi}{2}$ for $n \in \mathbb{Z}$. Numerically, the unstable node of the system appears to be $n\xi - \frac{\xi}{2} + \epsilon$ rather than the analytic boundary $n\xi - \frac{\xi}{2}$ is due to the fact that we have no historic values of $\theta_i(t)$ for the first $\frac{\delta t}{\Delta t}$ steps, *i.e.* when the circular piece of memory is still empty.

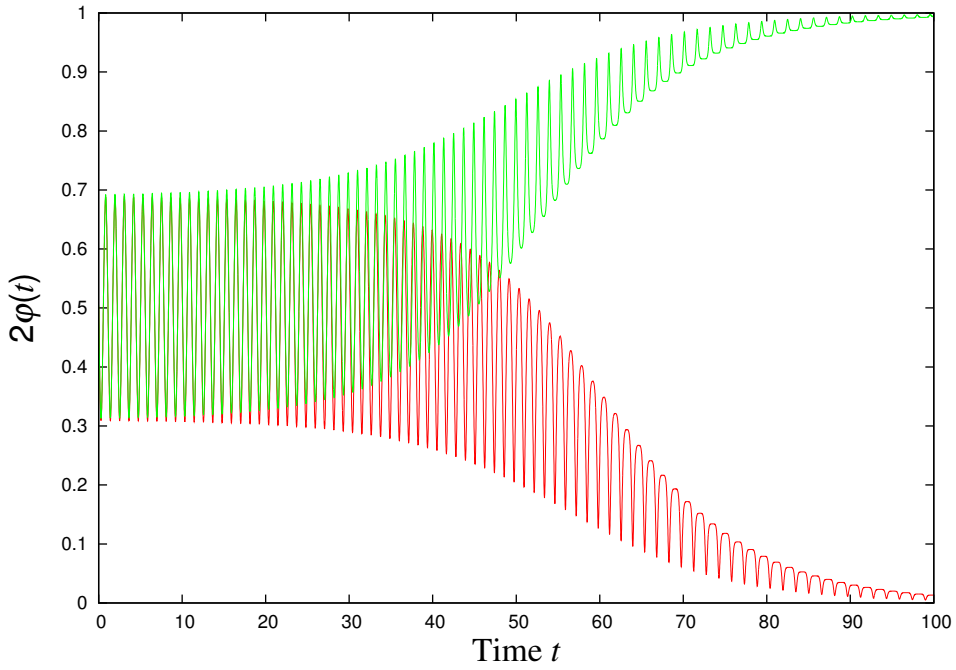

Figure 2.16: Trajectories of 2-oscillator full system with different initial phase difference $\theta_2(0) - \theta_1(0)$. The system will synchronise to two different states. With initial difference of 0.503 (red) the system synchronises to 0, while with initial difference of 0.505 (green) the system synchronises to 1, which is one period of ξ. We have applied RK4 routine with $\Delta t = 0.0001$, $\xi = 1.0$, $\omega = 1.0$, $\zeta = 0.1$, $\delta t = 0.004$.

We also find that if we allow fast synchronisation, that is, for large values of time delay δt, some systems will desynchronise (see Figure 2.17). We thought at first that this was caused by the numerical precision of the program, *e.g.* the resolution of Δt, or accumulative errors in the history of the values of θ_i. However this issue will still remain macroscopic even if we apply the highest precision available at the time and having a fresh history halfway through the system [4]. In fact, the issue is caused by the bias of how

[4]We reset all histories of $\theta_i(t)$ for a particular time while the programming is running. The macroscopic

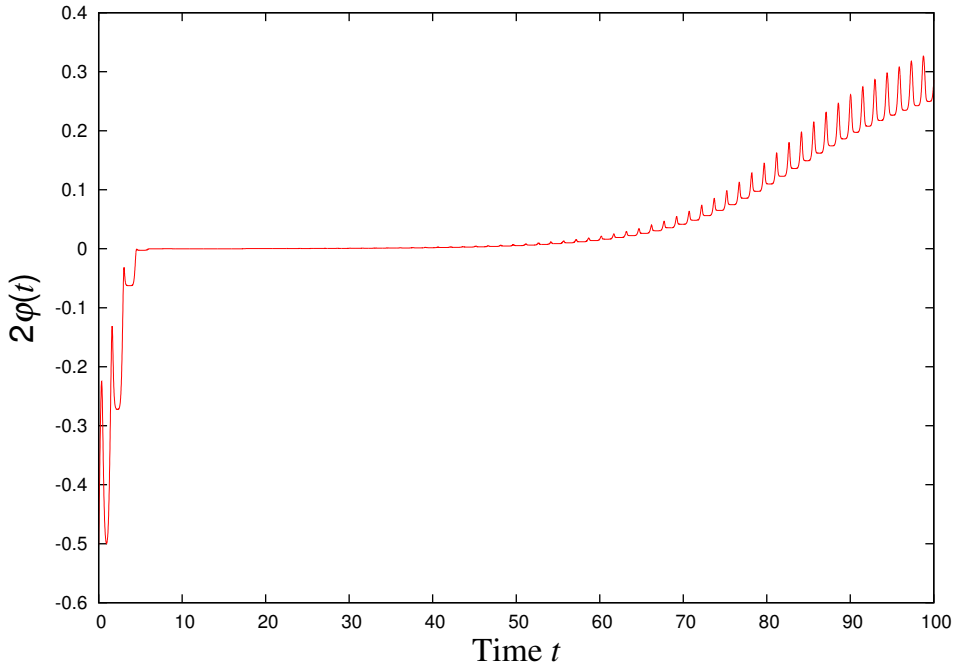

Figure 2.17: Trajectory output of RK4 with interleaved integration. After some time, the system will desynchronise itself. We apply the RK4 routine with $\Delta t = 0.0001$, $\xi = 1.0$, $\omega = 1.0$, $\zeta = 0.1$, $\delta t = 0.05$ and $2\varphi_0 = (\theta_1(0) - \theta_2(0)) = 0.503$

Figure 2.18: Assume that we are on the, say, even timeline with whole Δt increments, then the timeline with $\frac{1}{2}\Delta t$ will be the odd timeline. If we want to calculate $t + 2\Delta t$ from $t + \Delta t$, then we require historical values (with a δt shift) on the timelines of $t+\Delta t$ which are $t-\delta$ (from even timeline), $t-\delta t+\frac{\Delta t}{2}$ (from odd timeline) and $t - \delta t + \Delta t$ (from even timeline). This bias causes the errors accumulate unevenly and therefore the system will desynchronise.

Interpolation points	Weighing of evenly spaced points
2	$\frac{1}{2}, \frac{1}{2}$
4	$-\frac{1}{16}, \frac{9}{16}, \frac{9}{16}, -\frac{1}{16}$
6	$\frac{3}{256}, -\frac{25}{256}, \frac{150}{256}, \frac{150}{256}, -\frac{25}{256}, \frac{3}{256}$

Table 2.1: Table of interpolation points and corresponding weighing

RK4 is implemented into our program, see Figure 2.18. For the RK4 routine to calculate the value of θ_{n+1}, the program itself will require the value of θ_n and asks for a function for an intermediate value of θ at $n + \frac{1}{2}$. The way we implement the algorithm is to treat all *half*-points as full points on the timeline [5]. Therefore, we move in time steps of two for the values we want to calculate numerically and move one time step back to obtain the intermediate values, *i.e.* an interleaved scheme. In this case, we will need to rescale the output by a factor of $\frac{1}{2}$. This suggests that the interleaved RK4 scheme is then biased on calculating future values of θ as it either takes two half-points and one full point, or two full points and one half-point; which will cause the errors accumulate unevenly and hence the system desynchronises. In order to resolve this issue, we introduce the RK4 method with interpolation approximation.

desynchronisation effect still remains. By having all histories of $\theta_i(t)$ reset will certainly affect the system, at least for time δt, since our system depends on the historical values of $\theta_i(t)$. However the purpose of doing so is to check whether this particular desynchronisation effect is a numerical artefact or it is due to accumulation of errors.

[5] We rescale the timeline by factor of 2, and therefore effectively making the "distance" between $\frac{\Delta t}{2}$ and Δt one integration time step. We then require to move in steps of two to get to the values with the original integration time step. Moving forwards or backwards for step of one gives the intermediate values.

2.5.4 RK4 method with Interpolation Approximation

Since RK4 is biased on calculating the future values of θ, we first take our timeline back in steps of one and then we approximate the intermediate points via interpolation. Interpolation means that we estimate the intermediate point by means of weighted average over history of θ (see Table 2.1).

These values of weighing are determined by coefficients of a interpolation polynomial. For the polynomial p to interpolate our data means to have $p(x_j) = y_j, \forall i \in \{0, 1, ..., n\}$, and the polynomial interpolation has the form

$$p(x) = a_0 + a_1 x + a_2 x^2 + \cdots + a_n x^n \ . \tag{2.44}$$

We will then get a system of linear equations in the coefficients a_i,

$$y_j = \sum_i^n a_i x_j^i, \qquad \forall j \in \{0, 1, ..., n\} \tag{2.45}$$

which can be represented in matrix form

$$\begin{bmatrix} 1 & x_0 & x_0^2 & \cdots & x_0^n \\ 1 & x_1 & x_1^2 & \cdots & x_1^n \\ \vdots & \vdots & \vdots & & \vdots \\ 1 & x_n & x_n^2 & \cdots & x_n^n \end{bmatrix} \begin{bmatrix} a_0 \\ a_1 \\ \vdots \\ a_n \end{bmatrix} = \begin{bmatrix} y_0 \\ y_1 \\ \vdots \\ y_n \end{bmatrix} \tag{2.46}$$

The x_j^i matrix on the left is commonly known as a Vandermonde matrix [53]. We write the above equation, (2.46), as $\boldsymbol{V}\vec{a} = \vec{y}$. In order to find the weighing of each given points, *i.e.* our coefficients of the interpolation polynomial, we would need to find the inverse of $\boldsymbol{V}$. The interpolation polynomial is then

$$p(x) = \sum_i^n a_i x^i = \sum_i^n \left[\boldsymbol{V}^{-1}\vec{y}\right]_i x^i \ . \tag{2.47}$$

When we use this interpolation polynomial to approximate the mid-points required for

the RK4 method, then the desynchronisation effect will disappear (Figure 2.19). Note that in order to compare the trajectories for RK4 with and without interpolation, we will need to rescale time by $\frac{1}{2}$ for RK4 without interpolation as we are moving in steps of two (interleaved) on our timeline.

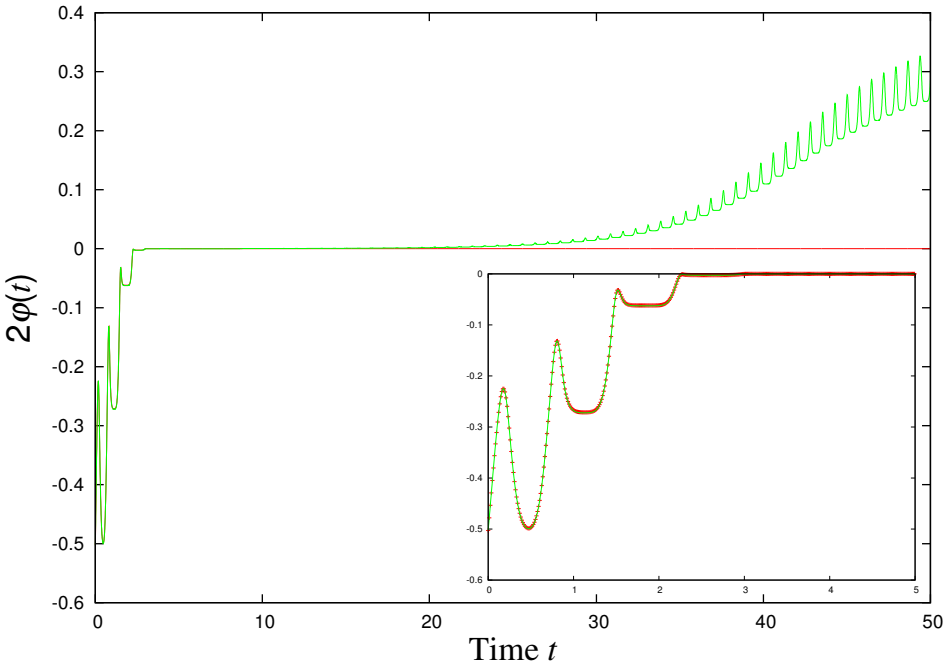

Figure 2.19: Trajectory comparisons of solutions to the two-oscillator time delay systems using RK4 method with $\Delta t = 0.0001$, $\xi = 1.0$, $\omega = 1.0$, $\zeta = 0.1$, $\delta t = 0.05$ and $2\varphi_0 = 0.503$. Main: with interpolation (red) and without (green). Inset: Trajectories between time 0 and 6.

2.5.5 Interpolation approximation for four given points

We are going to demonstrate how we approximate the mid-point by interpolation polynomial of four given points, say y_{-1}, y_0, y_1, y_2; and we want to approximate the mid-point, *i.e.* $y_{\frac{1}{2}}$. The Vandermode matrix is then

$$\boldsymbol{V} = \begin{bmatrix} 1 & -1 & 1 & -1 \\ 1 & 0 & 0 & 0 \\ 1 & 1 & 1 & 1 \\ 1 & 2 & 4 & 8 \end{bmatrix} \Rightarrow \boldsymbol{V}^{-1} \begin{bmatrix} 0 & 1 & 0 & 0 \\ -\frac{1}{3} & -\frac{1}{2} & 1 & -\frac{1}{6} \\ \frac{1}{2} & -1 & \frac{1}{2} & 0 \\ -\frac{1}{6} & \frac{1}{2} & -\frac{1}{2} & \frac{1}{6} \end{bmatrix} \tag{2.48}$$

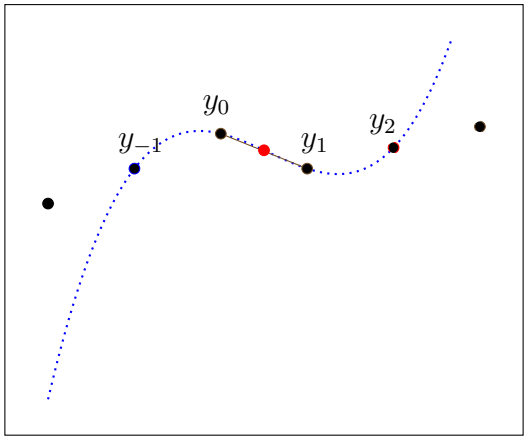

Figure 2.20: Graphical illustration of the interpolation polynomial with four given points (2.50).

and the coefficients of the interpolation polynomial will be

$$\vec{a} = \boldsymbol{V}^{-1}\vec{y} = \begin{bmatrix} 0 & 1 & 0 & 0 \\ -\frac{1}{3} & -\frac{1}{2} & 1 & -\frac{1}{6} \\ \frac{1}{2} & -1 & \frac{1}{2} & 0 \\ -\frac{1}{6} & \frac{1}{2} & -\frac{1}{2} & \frac{1}{6} \end{bmatrix} \begin{bmatrix} y_{-1} \\ y_0 \\ y_1 \\ y_2 \end{bmatrix} = \begin{bmatrix} y_0 \\ -\frac{1}{3}y_{-1} - \frac{1}{2}y_0 + y_1 - \frac{1}{6}y_2 \\ \frac{1}{2}y_{-1} - y_0 + \frac{1}{2}y_1 \\ -\frac{1}{6}y_{-1} + \frac{1}{2}y_0 - \frac{1}{2}y_1 + \frac{1}{6}y_2 \end{bmatrix} \tag{2.49}$$

The interpolation polynomial is then $p(x) = \sum_0^3 a_i x^i$, see Figure 2.20. As we want to approximate the mid-point $y_{\frac{1}{2}}$, we set $x = \frac{1}{2}$ and simplify the expression to get

$$y_{\frac{1}{2}} = p\left(\frac{1}{2}\right) = -\frac{1}{16}y_{-1} + \frac{9}{16}y_0 + \frac{9}{16}y_1 - \frac{1}{16}y_2 \tag{2.50}$$

and hence the weighings are $-\frac{1}{16}, \frac{9}{16}, \frac{9}{16}, -\frac{1}{16}$ correspondingly. If we want to estimate the half-point value $\theta\left(\frac{1}{2}\right)$, then $\theta\left(\frac{1}{2}\right) = -\frac{1}{16}\theta(-1) + \frac{9}{16}\theta(0) + \frac{9}{16}\theta(1) - \frac{1}{16}\theta(2)$, where in our case $\theta(i)$ with $i \in \mathbb{Z}$ are the corresponding historical values. Similarly we can obtain the expressions for six-point or other interpolation polynomials.

2.6 Phase diagram for Two-oscillator Timedelay systems

In our numerics, we define our system as synchronised if the phase difference between the two oscillators drops below a certain value of threshold H. Due to the behaviour of our systems, we define the first time that a whole period is below this threshold as the synchronisation time $\tau(t)$ of our system. In order to understand how the initial phase differences relates to the time delays δt, we look into the phase diagram of the system of these two parameters, for a given fixed synchronisation time. In this section, we will also compare the numerics of our full system, by using the RK4 method with interpolation approximation, to the numerics of our linearised solution, by integrating (2.41) numerically; and to what extend the linearised solution agrees with the full system.

2.6.1 Phase diagram by RK4 with interpolation approximation

Our current piece of program of RK4 with interpolation approximation returns a value of synchronisation time $\tau(t)$ by a particular value of time delay δt. In order to plot the phase diagram of the system, we implement an (naïve) root finding algorithm so that we tune our values of time delay to obtain a particular synchronisation time, up to certain error, for a given value of initial phase difference. We also need to implement our program so that it returns the synchronisation time based on our criterion.

When we are trying to use our RK4 with interpolation approximation scheme to plot the different initial phase differences against the time delays required to have the system synchronised under certain values of threshold, we encounter a problem that a small difference, of order 1.4×10^{-5}, in the time delay will cause a massive difference of 0.424 in the synchronisation time (see Table 2.2). We think that this is a matter of resolution and therefore, instead of having $\Delta t = 0.0001$, we increase the resolution by a factor of 200, *i.e.* $\Delta t = 5 \times 10^{-7}$, and we see an increase of 15% in the estimated time delay. The values of time delays and corresponding synchronisation times are different suggesting that this is indeed a matter of resolution of Δt. However, the difference in the synchronisation times are yet massive.

Integration Time-step Δt	Time delay δt	Synchronisation time τ
0.0001	0.00289066	10.413 600 00
0.0001	0.00290438	9.989 200 00
5×10^{-7}	0.00345337	10.306 121 00
5×10^{-7}	0.00345354	9.967 583 50

Table 2.2: Table of time delay δt, via root finding algorithm, with target synchronisation time $\tau = 10$.

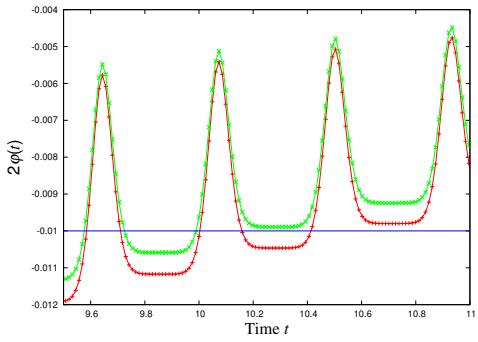

Figure 2.21: Trajectories of the two-oscillator time delay system with two different time delay, namely 0.00289066 (red) and 0.00290438 (green). Other parameters of the system are $\Delta t = 0.0001$, $\xi = 1.01$, $\omega = 2.0$, $\zeta = 0.1$, $2\varphi_0 = 0.5$, $\tau = 10$ and $H = 0.01$.

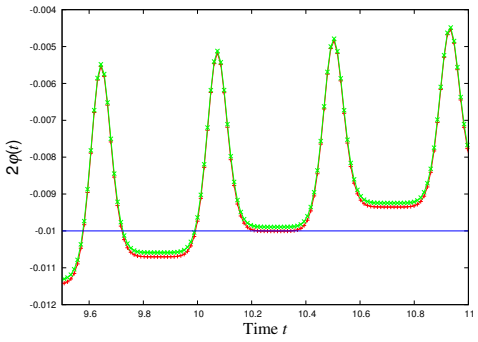

Figure 2.22: Trajectories of the two-oscillator time delay system with two different time delay, namely 0.00289066 (red) and 0.00290438 (green). Other parameters of the system are $\Delta t = 0.00002$, $\xi = 1.01$, $\omega = 2.0$, $\zeta = 0.1$, $2\varphi_0 = 0.5$, $\tau = 10$ and $H = 0.01$.

In order to investigate why the synchronisation time is so sensitive to the value of time delay, we look into the trajectories of the two systems with threshold $H = -0.01$ (see Figure 2.21 and Figure 2.22), or $H = 0.01$ if you consider $\theta_2(t) - \theta_1(t)$. We can see that, with $\Delta t = 0.0001$, the trajectory of $\delta t = 0.0028906$ sits above the threshold around $t = 10$ while the trajectory of $\delta t = 0.0029043$ sits below. Although we increase the resolution to $\Delta t = 2 \times 10^{-5}$ and the two trajectories sit much closer to each other, the massive difference in synchronisation time still persists, as one trajectory still sits above and one sits below the threshold H. One may notice that the difference of the trajectories of $\theta_2(t) - \theta_1(t)$ in Figure 2.21 and Figure 2.22 with $\delta t = 0.00289066$ is much more affected compared to those with $\delta t = 0.00290438$, despite the change in integration time steps Δt. The reason of this is because our memory size is an integer given by $\frac{\delta t}{\Delta t}$. Therefore with $\Delta t = 0.0001$ the effective time delay implemented numerically by the memory is 0.0028 and 0.0029 as opposed to 0.00288 and 0.00290 with $\Delta t = 0.00002$. Hence, the visible difference between $\Delta t = 0.0001$ and $\Delta t = 0.00002$ for $\delta t = 0.00289066$ but not for

$\delta t = 0.00290438$.

From these figures, we find that the enormous difference in synchronisation time is actually a result of how we define synchronisation in our numerical systems. Therefore, we will need to redefine the synchronisation criterion of our numerics.

Since the phase difference has a (somewhat periodic) trend of decreasing values over time, we consider our synchronisation time as a function of φ, where $\varphi = \frac{1}{2}(\theta_1 - \theta_2)$. This means that now the function τ is $\tau = \tau(t(\theta_i))$. Therefore, we redefine our criterion for our numerical systems as when the average over a window size of historical values of φ reaches below the threshold H, as the average over this window size of φ is a monotonically decreasing function in time. This particular value of window size $\hat{t}$ is define by

$$\bar{\theta}(t) - \xi = \bar{\theta}(t - \hat{t}) \tag{2.51}$$

where ξ is the period of the function σ. Then $\tilde{\varphi}$, our window averaged φ, has the form

$$\tilde{\varphi} = \frac{1}{\hat{t}} \int_{t-\hat{t}}^{t} \varphi(t')\mathrm{d}t' = \frac{1}{\hat{t}} \int_{\bar{\theta}(t)-\xi}^{\bar{\theta}(t)} \frac{\varphi(\bar{\theta}')}{\dot{\bar{\theta}}(\bar{\theta}')}\mathrm{d}\bar{\theta}' \ ,$$

where $\hat{t}$ is determined by Eq. (2.51). Numerically, $\hat{t}$ is simply equal to $t - t(\bar{\theta}(t) - \xi)$.

By use of this new definition of synchronisation, we can obtain the phase diagram by the RK4 method with interpolation approximation (see Figure 2.23) with threshold $H = 0.05$ [6]. This phase diagram makes sense because the two oscillators *see* each other on a periodic ξ-track. This means that if θ_1 is at $n\xi$ and θ_2 is at $m\xi + a$ where $\forall m, n \in \mathbb{Z}$ and $a \in (0, \xi)$, the system synchronises the same way as if θ_1 is at $n\xi$ and θ_2 is at $m\xi - a$; however, the systems synchronise to different periods of ξ. This is why the time taken for initial phase difference of 0.11 to synchronise is similar to the time taken for initial phase difference of 0.9 to synchronise (our period $\xi = 1.01$). We can also see that the trajectories of our phase diagram only start around 0.12. This is because our initial phase difference $2\varphi_0 = (\theta_2(0) - \theta_1(0))$, and therefore, if $2\varphi_0 = (\theta_2(0) - \theta_1(0)) < 2H$, *i.e.* the

[6] It does not really matter for the two-oscillator case if we consider $\theta_2(0) - \theta_1(0)$ or $\theta_1(0) - \theta_2(0)$ as the initial phase difference, but for consistency to previous arguments, for the rest of this section we will take $\theta_2(0) - \theta_1(0)$ as the initial phase difference, and therefore consider positive values of H.

initial phase difference $\theta_2(0) - \theta_1(0)$ is less than twice of the value of the threshold, then our criterion of synchronisation is already satisfied and so the numerics sees this as a violation, that is, any values of time delay will make the system synchronised. Hence, our trajectories of the phase diagram only starts at around those values where the initial phase difference is larger than twice of the value of the threshold. [7] Therefore, although our systems with time delay will always synchronise, we require certain (or *valid*) initial condition, *i.e.* $2H < 2\varphi_0 = \theta_2(0) - \theta_1(0)$, for us to obtain the corresponding value of time delay achieve synchronisation in a particular time t.

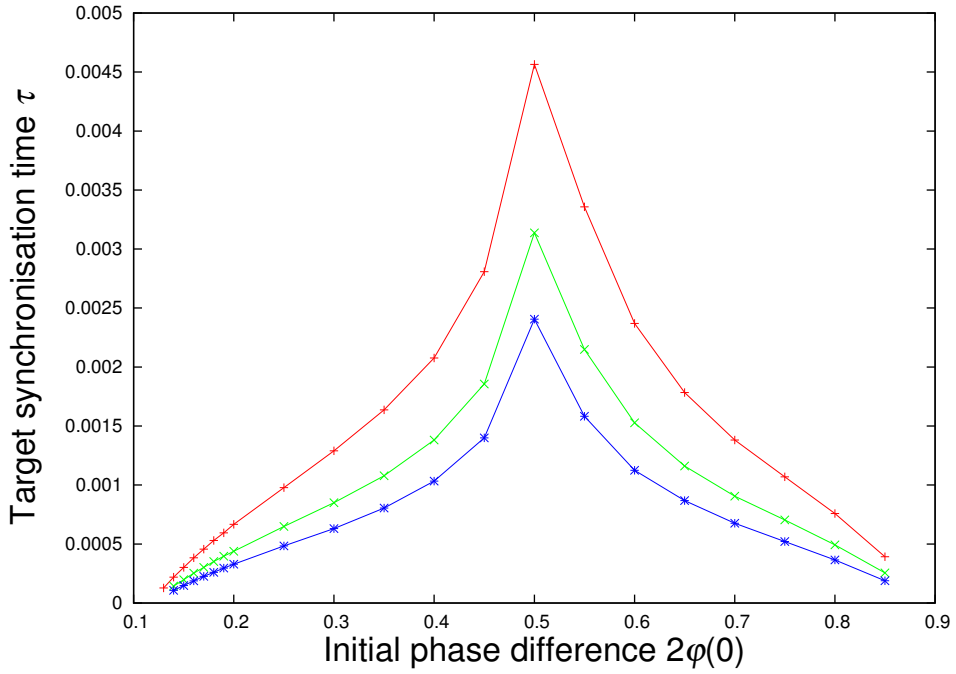

Figure 2.23: Full system phase diagram for time delay found, for particular synchronisation time τ to a certain threshold $H = 0.05$, versus various values of inital phase differences $2\varphi_0$. Parameters used: $\Delta t = 1 \times 10^{-6}$, $\xi = 1.01$, $\zeta = 0.1$, $\omega = 2.0$, and J = 2. Phase diagram for initial phase differences between 0 and 1 using RK4 outputs: target synchronisation time $\tau = 5$ (red), $\tau = 7.5$ (green) and $\tau = 10$ (blue).

2.6.2 Phase diagram by linearised solution

In order to check our linearised solution (2.41) against the full system, we examine the linearised solution by numerically integrating (2.41).

When we try to integrate the linearised solution, we first apply the Romberg's in-

[7] This argument also applies to the phase diagram obtained from the linearised solution.

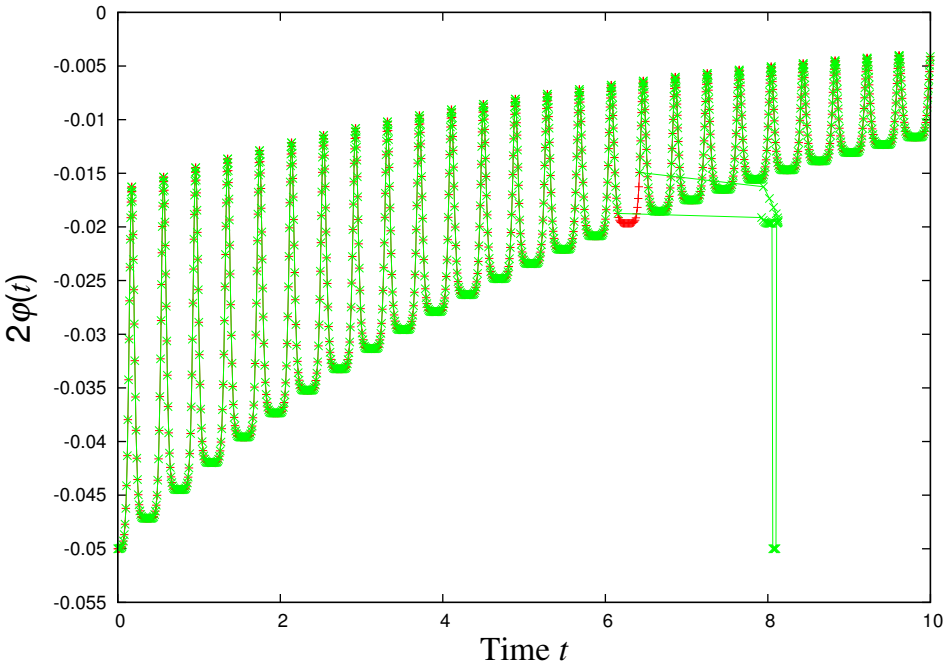

Figure 2.24: Trajectories outputs from the qsimp (red) and qromb (green) routines [53], where the qromb routine gives a numerical artefact at the 16^{th} period.

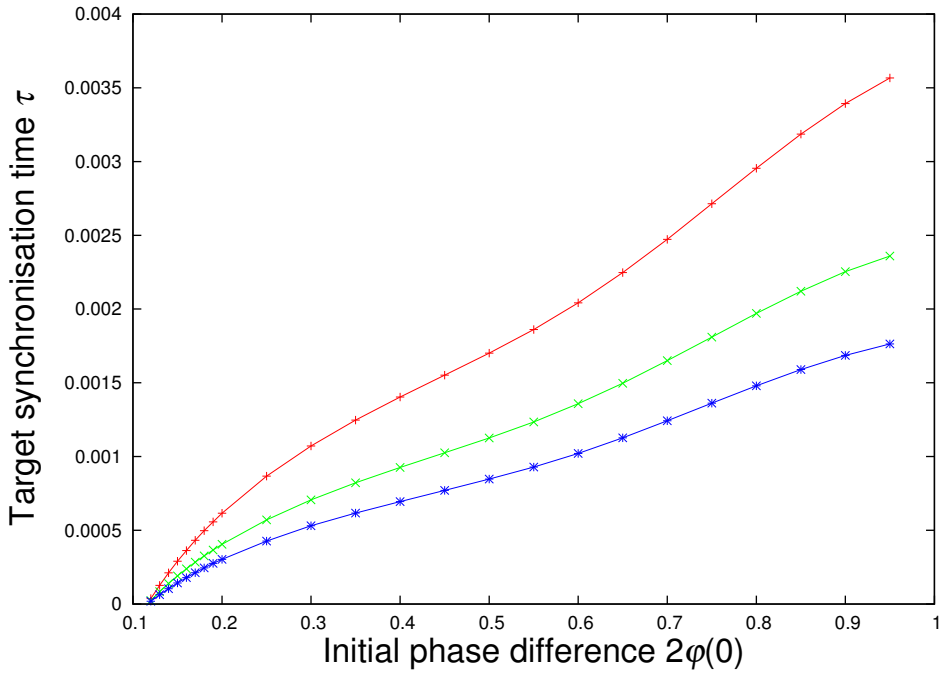

Figure 2.25: Linearised solution phase diagram for time delay found, for particular synchronisation time τ to a certain threshold $H = 0.05$, versus various values of initial phase differences $2\varphi_0$. Parameters used: $\Delta t = 1 \times 10^{-6}$, $\xi = 1.01$, $\zeta = 0.1$, $\omega = 2.0$, and $\mathrm{J} = 2$. Phase diagram for initial phase differences between 0 and 1 using Simpson's rule: target synchronisation time $\tau = 5$ (red), $\tau = 7.5$ (green) and $\tau = 10$ (blue).

tegration, the qromb routine by Press et al. [53], which can be treated as the natural generalisation of integration schemes that are of higher order than the Simpson's rule. Press [53] said, "The routine qromb is quite powerful for sufficiently smooth integrands, integrated over intervals which contain no singularities, and where the endpoints are also nonsingular." However it turns out our integrands are not as smooth as we think since the our sigma function peaks up sharply at half periods, *i.e.* at $\frac{(2n+1)\xi}{2}$ with $n \in \mathbb{Z}$, and the qromb routine will produce a numerical artefact on the trajectories of the system at powers of two (see Figure 2.24 for comparison). Therefore, instead of Romberg's integration, we apply the Simspson's rule, the qsimp routine [53], to our numerical integration of the linearised solution. The Simpson's rule is

$$\int_{x_1}^{x_3} f(x)\mathrm{d}x = h\left[\frac{1}{3}f_1 + \frac{4}{3}f_2 + \frac{1}{3}f_3\right] + \mathcal{O}(h^5 f^{(4)}) \tag{2.52}$$

where h is the integration time step and $f^{(4)}$ means the fourth derivative of the function f evaluated at an unknown place in the interval. We can also note that the formula gives the integral over an interval of size $2h$, so the coefficients add up to 2 [53]. If we apply (2.52) to successive, non-overlapping pairs of intervals, we get the extended Simpson's rule [53], namely

$$\int_{x_1}^{x_N} f(x)\mathrm{d}x = h\left[\frac{1}{3}f_1 + \frac{4}{3}f_2 + \frac{2}{3}f_3 + \frac{4}{3}f_4 + \cdots + \frac{2}{3}f_{N-2} + \frac{4}{3}f_{N-1} + \frac{1}{3}f_N\right] + \mathcal{O}\left(\frac{1}{N^4}\right)$$

By use of this qsimp routine [53], we can obtain the trajectories of the system. Similar to the RK4 method, for a given value of initial phase difference, we implement a root finding algorithm so that we can tune the values of the time delay to obtain a particular synchronisation time; again up to certain error. Then we will be able to obtain the phase diagram of the linearised system (see Figure 2.25). The phase diagram of linearised solution makes sense because the two oscillators do *not see* each other on the periodic ξ-track, instead they are two forever increasing objects that *talk* to each other via the coupling J. Therefore, the time taken for initial phase difference of 0.9 to synchronise is much longer than the time taken for initial phase difference of 0.11. For the same reason

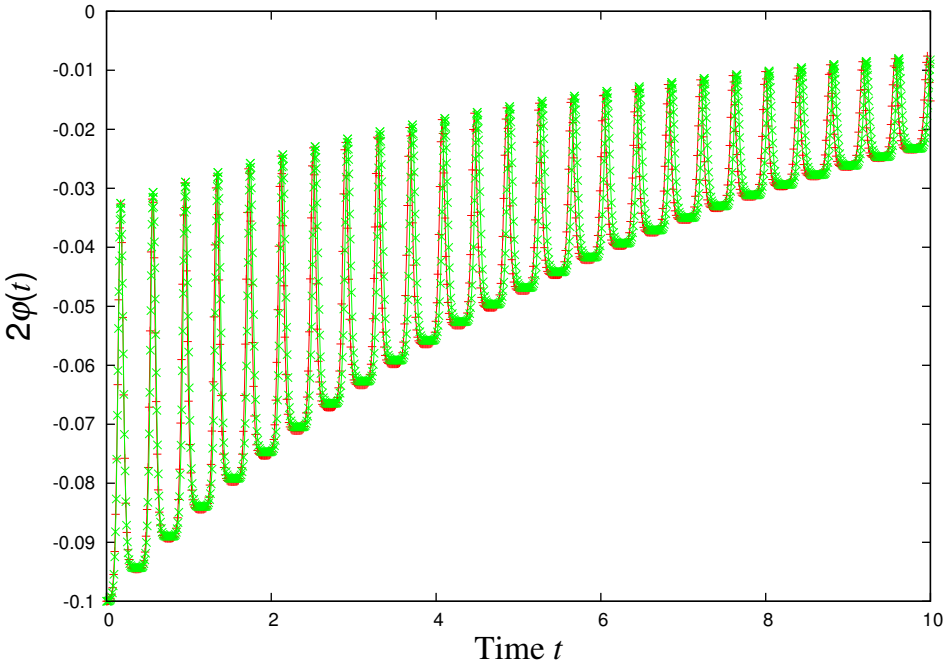

Figure 2.26: Trajectories of full system (RK4 with interpolation, red) and linearised solution (qsimp, green) according to the time delay found on each system respectively. Parameter used: $\Delta t = 0.000001$, $\xi = 1.01$, $\omega = 2.0$, $\mathrm{J} = 2$ and $\zeta = 0.1$

as the full system, the trajectories of the phase diagram only start if $2H < 2\varphi_0$ (see Section 2.6.1).

If we now set the target synchronisation time as $t = 10$ with initial phase difference of 0.1, *i.e.* the two oscillators are 0.1 apart when the system starts and the RK4 method with interpolation approximation will return a time delay of value 0.00082278 while the linearisation method gives 0.00081299 as the time delay for the same parameters. However we can see that the two trajectories match very closely to each other (see Figure 2.26). We then try to obtain the trajectory from the RK4 method with interpolation approximation by applying the time delay we found via the linearised solution (and vice versa). Again, the plots of these trajectories match very closely (see Figure 2.27 and Figure 2.28).

If we now look at the two phase diagrams of the full system and our linearised system, they agree fairly closely for initial phase difference less than or equal to 0.2. (see Figure 2.29 and inset). This is expected as our linearised solution is only valid for small values of φ.

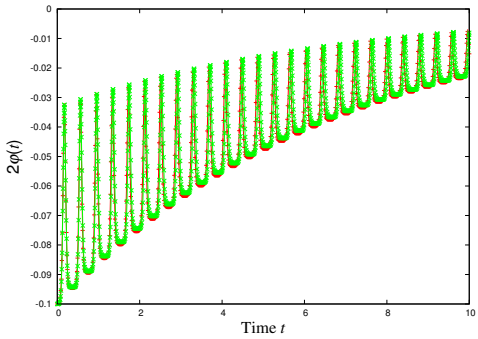

Figure 2.27: Trajectories of full system (RK4 with interpolation, red) and linearised solution (qsimp, green) according to the time delay found by RK4 method. Parameter used: $\Delta t = 0.000001$, $\xi = 1.01$, $\omega = 2.0$, J $= 2$ and $\zeta = 0.1$

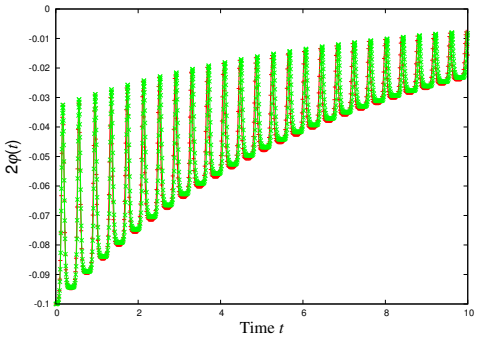

Figure 2.28: Trajectories of full system (RK4 with interpolation, red) and linearised solution (qsimp, green) according to the time delay found by qsimp routine. Parameter used: $\Delta t = 0.000001$, $\xi = 1.01$, $\omega = 2.0$, J $= 2$ and $\zeta = 0.1$

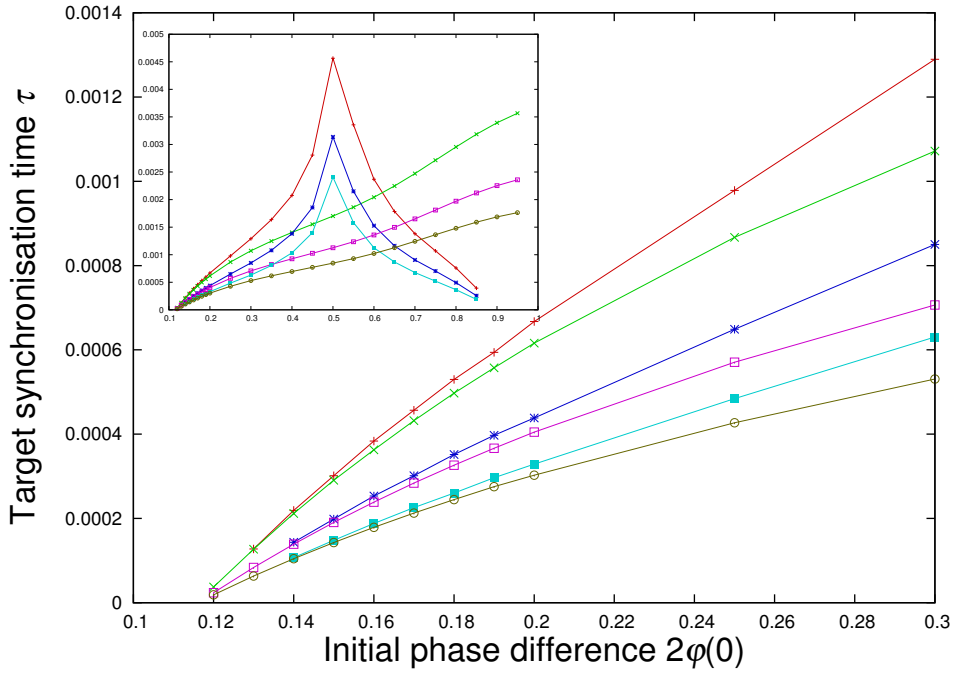

Figure 2.29: Phase diagram comparison for time delay found, for particular synchronisation time τ to a certain threshold $H = 0.05$, versus various values of inital phase differences $2\varphi_0$. Parameters used: $\Delta t = 1 \times 10^{-5}$, $\xi = 1.01$, $\zeta = 0.1$. Inset: phase diagram for initial phase differences between 0 and 1. RK4 outputs: target synchronisation time $\tau = 5$ (red), $\tau = 7.5$ (blue) and $\tau = 10$ (cyan). Linearised solution outputs: $\tau = 5$ (green), $\tau = 7.5$ (purple) and $\tau = 10$ (brown).

2.7 Discussion

We have showed that our linearised solution is a very good approximation of our system with equations of motion defined by Eq. (2.35) and Eq. (2.36). If we now define the quantities ψ and S such that

$$\psi = \int_0^{\xi} \frac{\mathrm{d}\bar{\theta}'}{\omega + \sigma(\bar{\theta}')} \approx \int_0^{\xi} \frac{\mathrm{d}\bar{\theta}'}{\dot{\bar{\theta}}(\bar{\theta}')} \tag{2.53}$$

$$S = \int_0^{\xi} \frac{\sigma'^2(\bar{\theta}')\mathrm{d}\bar{\theta}'}{\omega + \sigma(\bar{\theta}')} \tag{2.54}$$

where ψ is, to leading order, the time which takes σ to go through one period, *i.e.* $\bar{\theta}(t+\psi) \approx \bar{\theta}(t) + \xi$. Time t in our system is given by

$$t = \int_{\bar{\theta}(0)}^{\bar{\theta}(t)} \frac{\mathrm{d}\bar{\theta}'}{\dot{\bar{\theta}}(\bar{\theta}')} \approx \frac{\bar{\theta}(t) - \bar{\theta}(0)}{\xi}\psi \tag{2.55}$$

for large time t. Since our $\bar{\theta}$ can be written as $\bar{\theta} = \bar{\theta}(0) + n\xi - b$, where $0 \leq b < \xi$, then for large time t, we can approximate the integral in Eq. (2.41) by

$$\begin{aligned}\int_{\bar{\theta}(0)}^{\bar{\theta}(t)} \frac{\sigma'^2(\bar{\theta}')}{\dot{\bar{\theta}}(\bar{\theta}')}\mathrm{d}\bar{\theta}' &= \int_{\bar{\theta}(0)}^{\bar{\theta}(0)+n\xi} \frac{\sigma'^2(\bar{\theta}')}{\dot{\bar{\theta}}(\bar{\theta}')}\mathrm{d}\bar{\theta}' + \int_0^b \frac{\sigma'^2(\bar{\theta}')}{\dot{\bar{\theta}}(\bar{\theta}')}\mathrm{d}\bar{\theta}' \\ &= nS + \int_0^b \frac{\sigma'^2(\bar{\theta}')}{\dot{\bar{\theta}}(\bar{\theta}')}\mathrm{d}\bar{\theta}' = \frac{\bar{\theta}(t) - \bar{\theta}(0)}{\xi}S + \frac{b}{n}S + \mathcal{O}(S) \approx \frac{t}{\psi}S\ .\end{aligned}$$

Then Eq. (2.41) can be written as

$$\varphi(t) = \varphi(0)\frac{\dot{\bar{\theta}}(0)}{\dot{\bar{\theta}}(t)}e^{-\frac{t}{\tau}} \tag{2.56}$$

where τ is the characteristic synchronisation time, the time taken to reduce the amplitude of $\varphi(t)$ by a factor of $\frac{1}{e}$,

$$\tau = \frac{\psi}{2\mathrm{J}^2\delta t S} \tag{2.57}$$

which is inversely proportional to the time delay δt. The synchronisation time thus cannot be made arbitrarily small since this approximation is only valid for small values

of δt compared to ψ, the time taken over one period of σ. In the cases that our σ is constant, which implies $S = 0$, the characteristic synchronisation time diverges which corresponds to lack of interaction. Then, trivially, $\varphi(t) = \varphi(0)$ for all time t.

We have studied a simple model, similar to the Winfree model [70], of synchronisation with and without presence of time delay. We have gone in detail with the two-oscillator cases. We retained Winfree's assumptions of identical or nearly identical dynamics, and each oscillator is coupled to all the others, but not to themeselves, *i.e.* $\mathrm{J}_{ii} = 0$ for all i. We only assume that the phases of all oscillators are monotonically increasing over time t. Our main result is that, to leading order, a time delay causes synchronisation and systems without time delay should never synchronise. The analytical solution reveals the importance of the assumption on monotonically increasing function θ_i. Our analysis on the numerics also shows consistency with the analytics; however the standard Euler scheme disagrees due to its self-implemented time delay feature.

In hindsight it may seem obvious that our time delay models will always synchronise. We have made some strong assumptions, such as setting all initial frequencies to be the same, *i.e.* $\omega_i = \omega$; assuming all the oscillators are identical or nearly identical in dynamics; each pair of the oscillators is coupled by the coupling strength which are equal and symmetrical. On the other hand, we might well have imagined that the system would contain two, or more, alternating synchronisation states or other various hybrid states such as the oscillators being frequency-locked.

Chapter 3

N-oscillator Model

We have discovered that without the presence of time delay, our model of the two-oscillator systems should never synchronise and with the presence of time delay, our model of two-oscillator systems will eventually be synchronised. Now we try to extend our analysis to a large ensemble of oscillators with size N.

3.1 Non-Time Delay systems and Mean-Field Theory

For N-oscillator non-time delay systems, the equation of motion is

$$\dot{\theta}_i = \omega_i + \sum_{j=1}^{N} \mathrm{J}_{ij}\sigma(\theta_j) \ . \tag{3.1}$$

To cope with this kind of large ensembles of oscillators, we can implement the coupling strength J_{ij} on a lattice so that each $[i, j]$ entry of the lattice corresponding to the coupling strength between the i^{th} and j^{th} oscillator.

For convenience, we set $\omega_i = \omega$ for all i and the amplitudes of the coupling are symmetric and the same among all oscillators, i.e. $\mathrm{J}_{ij} = \mathrm{J}_{ji} = \frac{\mathrm{J}}{N-1}$ for all pairs of oscillators but $\mathrm{J}_{ii} = 0$. We now define the corresponding value of $\bar{\theta}$, the average of N

oscillators, and φ_i, the difference between the i^{th} oscillator and $\bar{\theta}$, such that

$$\bar{\theta} = \frac{1}{N}\sum_{i=1}^{N}\theta_i \ , \tag{3.2}$$

$$\varphi_i = \theta_i - \bar{\theta} \ . \tag{3.3}$$

From our definition of synchronisation, see Definition 1.1, this means that our system will result in synchrony if and only if all values of $\varphi_i(t)$ converge to 0 as $t \to \infty$. Therefore, using Eq. (3.3) and by expanding σ for small values of φ_i gives

$$\sigma(\theta_i) = \sigma(\bar{\theta} + \varphi_i) = \sigma(\bar{\theta}) + \varphi_i\sigma'(\bar{\theta}) + \mathcal{O}(\varphi_i)^2 \ . \tag{3.4}$$

Using this expression of σ, up to first order in φ_i, we can express our equation of motion, in terms of $\bar{\theta}$ and φ_i, as

$$\begin{aligned}
\dot{\theta}_i &= \omega + \frac{\mathrm{J}}{N-1}\left(\sigma(\theta_1) + \cdots + \sigma(\theta_N) - \sigma(\theta_i)\right) \\
&= \omega + \frac{\mathrm{J}}{N-1}\left[(N-1)\sigma(\bar{\theta}) + \left(\sum_{j=1}^{N}\varphi_j\sigma'(\bar{\theta})\right) - \varphi_i\sigma'(\bar{\theta})\right] \\
&= \omega + \mathrm{J}\sigma(\bar{\theta}) - \frac{\varphi_i}{N-1}\mathrm{J}\sigma'(\bar{\theta})
\end{aligned}$$

since $\sum_{j=1}^{N}\varphi_j = 0$. We now find the expressions of $\dot{\bar{\theta}}$ and $\dot{\varphi}_i$ as

$$\begin{aligned}
\dot{\bar{\theta}} &= \frac{1}{N}\sum_{i=1}^{N}\dot{\theta}_i = \omega + \mathrm{J}\sigma(\bar{\theta}) \\
\dot{\varphi}_i &= \dot{\theta}_i - \dot{\bar{\theta}} = -\frac{\varphi_i}{N-1}\mathrm{J}\sigma'(\bar{\theta}) \ .
\end{aligned}$$

As $\theta_i(t)$ is strictly positive and monotonically increasing, therefore so does $\bar{\theta}$, then we can define φ' where

$$\varphi_i' = \frac{\dot{\varphi}_i}{\dot{\bar{\theta}}} = \frac{-\varphi_i}{N-1}\frac{\mathrm{J}\sigma'(\bar{\theta})}{\omega + \mathrm{J}\sigma(\bar{\theta})} = \frac{-\varphi_i}{N-1}\frac{\mathrm{d}}{\mathrm{d}\bar{\theta}}\left[\ln(\omega + \mathrm{J}\sigma(\bar{\theta})) + C_i\right] \tag{3.5}$$

with C_i an integration constant. Therefore, by using separation of variables, we can

obtain the linearised solution for our N-oscillator system as

$$\varphi_i(\bar{\theta}) = \varphi_i(0)\frac{[\omega + \mathrm{J}\sigma(\bar{\theta}(0))]^{\frac{1}{N-1}}}{[\omega + \mathrm{J}\sigma(\bar{\theta})]^{\frac{1}{N-1}}} \tag{3.6}$$

From this linearised solution (3.6), we can see that the system will never be synchronised as $\sigma(\bar{\theta})$ is a periodic function and $\bar{\theta}$ is a monotonically increasing in time t. Then φ_i itself is periodic with same period as σ. We can also note that if we set $N = 2$, i.e. a two-oscillator system, then we recover our linearised solution (2.15), of the two-oscillator non-time delay system.

3.2 Time Delay systems and Mean-Field Theory

For N-oscillator time delay systems, the equation of motion is defined as

$$\dot{\theta}_i = \omega_i + \sum_{j=1}^{N} \mathrm{J}\sigma(\theta_j(t-\delta t)) \tag{3.7}$$

where δt is the time delay, which is small but finite. Similar to the non-time delay system, we have the values of $\bar{\theta}$ and φ_i defined as in (3.2) and (3.3) correspondingly. Since time delay does not enter the derivation of $\dot{\bar{\theta}}$ and $\dot{\varphi}_i$ expressions, in order to implement the time delay system, we would only need to have $t \to t - \delta t$ in the expression of φ_i' (3.5), therefore we have

$$\begin{aligned}
\varphi_i' = \frac{\dot{\varphi}_i(t)}{\dot{\bar{\theta}}(t)} &= \frac{-\varphi_i(t-\delta t)\mathrm{J}\sigma'(\bar{\theta}(t-\delta t))}{(N-1)(\omega + \mathrm{J}\sigma(\bar{\theta}(t-\delta t)))} \\
&\approx \frac{-(\varphi_i(t) - \delta t\dot{\varphi}_i(t))\mathrm{J}[\sigma'(\bar{\theta}(t)) - \delta t\sigma''(\bar{\theta}(t))\dot{\bar{\theta}}(t)]}{(N-1)(\omega + \mathrm{J}[\sigma(\bar{\theta}(t)) - \delta t\sigma'(\bar{\theta}(t))\dot{\bar{\theta}}(t)])} + \mathcal{O}(\delta t)^2 \\
&= \frac{-\mathrm{J}}{N-1}\frac{\varphi_i\sigma' - \delta t(\varphi_i\sigma''\dot{\bar{\theta}} + \dot{\varphi}_i\sigma') + \mathcal{O}(\delta t)^2}{\omega + \mathrm{J}(\sigma - \delta t\sigma'\dot{\bar{\theta}}) + \mathcal{O}(\delta t)^2} \\
&\approx -\frac{\varphi_i}{N-1}\frac{\mathrm{J}(\sigma' - \delta t(\sigma''\dot{\bar{\theta}} - \frac{J\sigma'^2}{N-1}))}{\omega + \mathrm{J}(\sigma - \delta t\sigma'\dot{\bar{\theta}})} \ .
\end{aligned} \tag{3.8}$$

If we let $T(\bar{\theta}) = \omega + \mathrm{J}(\sigma - \delta t\sigma'\dot{\bar{\theta}})$, *i.e.* $T(\bar{\theta}) = \dot{\bar{\theta}}(t)$ up to first order in δt, and consider the derivative of $T(\bar{\theta})$ with respect to $\bar{\theta}$, this gives

$$\frac{\mathrm{d}}{\mathrm{d}\bar{\theta}}T(\bar{\theta}) = \mathrm{J}\left[\sigma'(\bar{\theta}) - \delta t\left(\sigma''(\bar{\theta})\dot{\bar{\theta}} + \sigma'\frac{\mathrm{d}}{\mathrm{d}\bar{\theta}}T\right)\right]$$

which yields,

$$\frac{\mathrm{d}}{\mathrm{d}\bar{\theta}}T(\bar{\theta}) = \mathrm{J}[\sigma'(\bar{\theta}) - \delta t(\sigma''\dot{\bar{\theta}} + \mathrm{J}\sigma'^2)] + \mathcal{O}(\delta t)^2 \ .$$

By using the expressions of T and $\frac{\mathrm{d}}{\mathrm{d}\bar{\theta}}T(\bar{\theta})$, we can simplify (3.8) into

$$\varphi_i' = -\frac{\varphi_i}{N-1}\frac{T' + \delta t\mathrm{J}^2\sigma'^2 + \delta t\mathrm{J}^2\frac{\sigma'^2}{N-1}}{T} = -\frac{\varphi_i}{N-1}\left(\frac{T'}{T} + \frac{N}{N-1}\delta t\mathrm{J}^2\frac{\sigma'^2}{T}\right)$$

giving a differential equation in T and φ_i, namely

$$\varphi_i' T + \frac{\varphi_i}{N-1} T' = -\frac{N}{(N-1)^2} \varphi_i \delta t \mathrm{J}^2 \sigma'^2 \ . \tag{3.9}$$

By inspection, we try a solution of $\tilde{\varphi}_i$ such that $\tilde{\varphi}_i = T^{\frac{1}{N-1}} \varphi_i$, yields

$$\begin{aligned} \tilde{\varphi}_i' &= \frac{1}{N-1} T^{\frac{1}{N-1}-1} T' \varphi_i + T^{\frac{1}{N-1}} \varphi_i' = T^{\frac{1}{N-1}-1} \left(\frac{1}{N-1} T' \varphi_i + T \varphi_i' \right) \\ &= -\varphi_i T^{\frac{1}{N-1}-1} \frac{N}{(N-1)^2} \delta t \mathrm{J}^2 \sigma'^2 = -\frac{\tilde{\varphi}_i}{T} \left(\frac{N}{(N-1)^2} \delta t \mathrm{J}^2 \sigma'^2 \right) \ . \end{aligned}$$

Therefore, the differential equation (3.9) can be solved by using this particular function $\tilde{\varphi}_i$ and by separation of variable, this gives the solution

$$\tilde{\varphi}_i(\bar{\theta}) = \tilde{\varphi}_i(0) \exp \left(-\frac{N}{(N-1)^2} \delta t \mathrm{J}^2 \int_0^{\bar{\theta}} \frac{\sigma'^2(\bar{\theta}')}{T(\bar{\theta}')} \mathrm{d}\bar{\theta}' \right) \tag{3.10}$$

where the solution of φ_i is given by

$$\varphi_i(t) = \varphi_i(0) \frac{[T(\bar{\theta}(0))]^{\frac{1}{N-1}}}{[T(\bar{\theta}(t))]^{\frac{1}{N-1}}} \exp \left(-\frac{N}{(N-1)^2} \delta t \mathrm{J}^2 \int_0^{\bar{\theta}(t)} \frac{\sigma'^2(\bar{\theta}')}{T(\bar{\theta}')} \mathrm{d}\bar{\theta}' \right) \ . \tag{3.11}$$

Since $T(\bar{\theta}(t)) = \dot{\bar{\theta}}(t)$ to first order in δt, hence if we set $N = 2$, *i.e.* a two-oscillator system, we then recover our linearised solution (2.41), of the two-oscillator time delay system; if we have $N = 2$ and we turn off the time delay, we then recover the linearised solution (2.15) of two-oscillator non-time delay models. From the linearised solution (3.11) above, we can conclude that for our system, all oscillators will be synchronised after some time and the larger value of the time delay, the quicker the system will synchronise. From here onwards, we are only interested in the time delay systems as the non-time delay systems can be obtained by setting $\delta t = 0$ in the time delay systems.

3.3 General case with Arbitrary J_{ij} for N-oscillator Time Delay Model

In order to analyse more rigorously on how our system will behave if we have arbitrary couplings J_{ij}, we turn ourselves to eigenvalues and eigenvectors of the coupling matrix $\boldsymbol{J}$, where each $[i, j]$ entry, J_{ij}, of $\boldsymbol{J}$ corresponding to the coupling strength between the i^{th} and j^{th} oscillator. In this section, we still retain the fact that all the initial frequencies are the same, *i.e.* $\omega_i = \omega$. Using linear algebra, we can write the equation of motion of our N-oscillator time delay model as

$$\dot{\theta}_i = \omega + \sum_{j=1}^{N} \mathrm{J}_{ij}\sigma(\theta_j(t-\delta t)) \quad \Rightarrow \quad \left|\dot{\theta}\right\rangle = \omega\,|1\rangle + \boldsymbol{J}\,|\sigma(\theta(t-\delta t))\rangle \tag{3.12}$$

where $|\sigma(\theta(t))\rangle = (\sigma(\theta_1(t)), \sigma(\theta_2(t)), \cdots, \sigma(\theta_N(t)))^T$. We define the mean field quantity $|\varphi\rangle$ such that

$$|\varphi\rangle = |\theta\rangle - \bar{\theta}\,|1\rangle \tag{3.13}$$

for which $\bar{\theta}$ satisfies the equation of motion

$$\dot{\bar{\theta}} = \omega + \tilde{\mathrm{J}}\sigma(\bar{\theta})\ . \tag{3.14}$$

Similar to previous sections, synchronisation means that all values of $\varphi_i(t)$ converge to 0 as $t \to \infty$.

Property 1 For synchronisation, we require $\sum_{j=1}^{N} \mathrm{J}_{ij} = \tilde{\mathrm{J}}$ which is independent of i.

To see Property 1 should always hold for synchronisation, suppose $\tilde{\mathrm{J}}$ is dependent of i, *i.e.* $\tilde{\mathrm{J}}_i = \sum_{j=1}^{N} \mathrm{J}_{ij}$, the sums over the columns of $\boldsymbol{J}$ are different. Then in the synchronised state, which means $\theta_j = \bar{\theta}$ for every value of j, two different oscillators i and k will have the equations of motion $\dot{\theta}_i = \omega + \tilde{\mathrm{J}}_i\sigma(\bar{\theta})$ and $\dot{\theta}_k = \omega + \tilde{\mathrm{J}}_k\sigma(\bar{\theta})$ respectively. Since $i \neq k$ and therefore $\tilde{\mathrm{J}}_i \neq \tilde{\mathrm{J}}_k$, this suggests that the system is *not* synchronised, which contradicts to our assumption that all the oscillators are in the synchronised state. Hence synchrony is achievable if and only if $\sum_{j=1}^{N} \mathrm{J}_{ij} = \tilde{\mathrm{J}}$.

3.3.1 Remarks on the arbitrary adjacency matrix $\boldsymbol{J}$

Since we have learnt that synchronisation can only be accomplished by having the row sums of matrix $\boldsymbol{J}$ independent of row, then given that $\sum_{j=1}^{N} \mathrm{J}_{ij} = \tilde{\mathrm{J}}$ we can write

$$\boldsymbol{J}\,|1\rangle = \tilde{\mathrm{J}}\,|1\rangle \tag{3.15}$$

where $|1\rangle$ denotes a column vector with all entries equal to 1 with corresponding eigenvalue $\tilde{\mathrm{J}}$ [1]. Now we consider the function f_λ where

$$f_\lambda = \langle e|\varphi\rangle \tag{3.16}$$

such that $\langle e|$ is an eigenvector of $\boldsymbol{J}$ with eigenvalue λ, *i.e.* $\langle e|\,\boldsymbol{J} = \lambda\,\langle e|$ with $\lambda \neq \tilde{\mathrm{J}}$. By differentiating and by use of Eq. (3.13), we get $\dot{f}_\lambda = \langle e|\dot{\varphi}\rangle = \left\langle e|\dot{\theta}\right\rangle - \langle e|\dot{\bar{\theta}}|1\rangle$. If we consider $\left\langle e|\dot{\theta}\right\rangle$ and $\langle e|\dot{\bar{\theta}}|1\rangle$ separately then

$$\begin{aligned}
\left\langle e|\dot{\theta}\right\rangle &= \langle e|\left(\omega\,|1\rangle + \boldsymbol{J}\,|\sigma(\theta)\rangle\right) = \langle e|\omega|1\rangle + \langle e|\boldsymbol{J}|\sigma(\theta)\rangle \\
&= \omega\,\langle e|1\rangle + \lambda\,\langle e|\sigma(\theta)\rangle \\
\langle e|\dot{\bar{\theta}}|1\rangle &= \langle e|\Big(\omega + \tilde{\mathrm{J}}\sigma(\bar{\theta})\Big)|1\rangle = \omega\,\langle e|1\rangle + \langle e|\tilde{\mathrm{J}}\sigma(\bar{\theta})|1\rangle \\
&= \omega\,\langle e|1\rangle + \langle e|\sigma(\bar{\theta})\tilde{\mathrm{J}}|1\rangle = \omega\,\langle e|1\rangle + \langle e|\sigma(\bar{\theta})\boldsymbol{J}|1\rangle \\
&= \omega\,\langle e|1\rangle + \langle e|\boldsymbol{J}\sigma(\bar{\theta})|1\rangle \\
&= \omega\,\langle e|1\rangle + \lambda\sigma(\bar{\theta})\,\langle e|1\rangle \ .
\end{aligned} \tag{3.17}$$

However, $\langle e|\dot{\bar{\theta}}|1\rangle$ can also be written as

$$\langle e|\dot{\bar{\theta}}|1\rangle = \Big(\omega + \tilde{\mathrm{J}}\sigma(\bar{\theta})\Big)\,\langle e|1\rangle = \omega\,\langle e|1\rangle + \tilde{\mathrm{J}}\sigma(\bar{\theta})\,\langle e|1\rangle \ . \tag{3.18}$$

By comparing Eq. (3.17) and Eq. (3.18), if and only if $\langle e|$ is the corresponding left-hand eigenvector of $|1\rangle$ then $\lambda = \tilde{\mathrm{J}}$. However, this is not true in our case as $\lambda \neq \tilde{\mathrm{J}}$; since for

[1] Due to this independence, we can always rescale or set the constant $\tilde{\mathrm{J}}$ to be 1.

any non-degenerate matrix $\boldsymbol{M}$, we have $\langle e|\,\boldsymbol{M} = \mu\,\langle e|$ and $\boldsymbol{M}\,|1\rangle = \nu\,|1\rangle$, for which μ and ν are distinct eigenvalues. Then $\mu\,\langle e|1\rangle = \langle e|\boldsymbol{M}|1\rangle = \nu\,\langle e|1\rangle$ [2] implies that $\langle e|1\rangle = 0$. Hence the derivative of f_λ is simplified down to

$$\dot{f}_\lambda = \lambda\,\big\langle e|\sigma(\bar{\theta})\big\rangle \ .$$

Therefore, our system can be rewriten into a new function f_λ by means of the eigenvectors of the adjacency matrix $\boldsymbol{J}$,

$$f_\lambda = \langle e|\varphi\rangle \quad \Rightarrow \quad \dot{f}_\lambda = \lambda\,\big\langle e|\sigma(\bar{\theta})\big\rangle \ . \tag{3.19}$$

This property is convenient in further development since time delay does not enter the derivation.

3.3.2 Linearised solution in first orders of δt and φ

In the light of the above, we have a matrix $\boldsymbol{J}$, an $N \times N$ matrix with entries equal to J_{ij}. Since we require $\sum_{j=1}^{N} J_{ij}$ to be constant, say $\tilde{J}$, to have synchronisation; similar to the Markov matrices, our matrix $\boldsymbol{J}$ has an eigenvalue $\tilde{J}$ and for this particular eigenvalue, we know that the corresponding right-hand eigenvector $|1\rangle$ is a column vector with all entries equal to 1. We denote the corresponding left-hand eigenvector of $\boldsymbol{J}$, with eigenvalue $\tilde{J}$, as $\langle 1|$. We also denote the other eigenvalues by λ_i, and its corresponding left-hand and right-hand eigenvectors as $\langle e_i|$ and $|e_i\rangle$ respectively. For our system, we have mean field quantity $|\varphi\rangle$ defined as in Eq. (3.13), and $\bar{\theta}$ defined [3] as

$$\bar{\theta} = \frac{1}{q}\,\langle 1|\theta\rangle \tag{3.20}$$

---

[2] If $\boldsymbol{M}$ is Hermitian then the scalar product $\langle e|1\rangle = 0$ always.

[3] This definition does not contradict with previous definitions of $\bar{\theta}$ as for our matrix $\boldsymbol{J}$, the property $\langle 1|\,\boldsymbol{J} = \langle 1|\,\tilde{J}$, then Eq. (3.21) is the same as Eq. (3.14) since $\langle 1|$ is a row vector with all entries equal to 1.

which implies

$$\dot{\bar{\theta}} = \frac{1}{q}\left\langle 1|\dot{\theta}\right\rangle = \frac{1}{q}\left\langle 1|(\omega\,|1\rangle + \boldsymbol{J}\,|\sigma(\theta)\rangle)\right\rangle = \omega + \frac{1}{q}\langle 1|\boldsymbol{J}|\sigma(\theta(t-\delta t))\rangle \tag{3.21}$$

where q is the scalar product $\langle 1|1\rangle$. It is quite straight forward to see that, for our system as defined above, the projection of $|\varphi\rangle$, and its derivatives, onto the left-hand eigenvector $\langle 1|$ always vanishes, since $\langle 1|\varphi\rangle = \langle 1|\theta\rangle - \bar{\theta}\,\langle 1|1\rangle = \langle 1|\theta\rangle - q\bar{\theta} = 0$. Now, if we define a new variable φ' such that

$$|\varphi'\rangle = \frac{|\dot{\varphi}\rangle}{\dot{\bar{\theta}}}\ .$$

If we have $|\varphi'\rangle$ projected onto any left-hand eigenvectors $\langle e_i|$, *i.e.* all eigenvectors except the left-hand eigenvector with eigenvalue $\tilde{\mathrm{J}}$, and apply the property we had from Eq. (3.19) yields

$$\langle e_i|\varphi'\rangle = \frac{\lambda_i\,\langle e_i|\sigma(\theta(t-\delta t))\rangle}{\omega + \frac{1}{q}\tilde{\mathrm{J}}\,\langle 1|\sigma(\theta(t-\delta t))\rangle}\ . \tag{3.22}$$

Now if we look into expanding the vector $|\sigma(\theta(t-\delta t))\rangle$ in small values of δt and φ_i, we have

$$\begin{aligned}
|\sigma(\theta(t-\delta t))\rangle =& \sigma(\bar{\theta}(t-\delta t))\,|1\rangle + \sigma'(\bar{\theta}(t-\delta t))\,|\varphi(t-\delta t)\rangle + \mathcal{O}(\varphi_i^2)\\
=& \sigma(\bar{\theta}(t))\,|1\rangle - \delta t\dot{\bar{\theta}}(t)\sigma'(\bar{\theta}(t))\,|1\rangle\\
&+ \sigma'(\bar{\theta}(t))\,|\varphi(t)\rangle - \delta t\dot{\bar{\theta}}(t)\sigma''(\bar{\theta}(t))\,|\varphi(t)\rangle\\
&- \delta t\sigma'(\bar{\theta}(t))\,|\dot{\varphi}(t)\rangle + \mathcal{O}(\delta t^2)\ .
\end{aligned}$$

Again, for simplicity, we will denote $\theta_i = \theta_i(t)$ for non-time delay θ variables, and we shall explicitly use $\theta_i(t-\delta t)$ for time delay θ variables; similarly for all other time dependent variables. Now, if we look into the projections of this expansion onto $\langle e_i|$ and $\langle 1|$, where $\langle e_i|1\rangle$ and $\langle 1|\varphi\rangle$, and its derivatives, all vanish, we have

$$\langle 1|\sigma(\theta(t-\delta t))\rangle = q\left[\sigma(\bar{\theta}) - \delta t\dot{\bar{\theta}}\sigma'(\bar{\theta})\right]$$

and

$$\begin{aligned}\langle e_i|\sigma(\theta(t-\delta t))\rangle &= \langle e_i|\varphi\rangle\,\sigma'(\bar{\theta}) - \delta t\left[\sigma''(\bar{\theta})\dot{\bar{\theta}}\,\langle e_i|\varphi\rangle + \sigma'(\bar{\theta})\,\langle e_i|\dot{\varphi}\rangle\right]\\ &= \langle e_i|\varphi\rangle\,\sigma'(\bar{\theta}) - \delta t\left[\sigma''(\bar{\theta})\dot{\bar{\theta}}\,\langle e_i|\varphi\rangle + \lambda_i\sigma'^2(\bar{\theta})\,\langle e_i|\varphi\rangle\right]\end{aligned}$$

since $\langle e_i|\dot{\varphi}\rangle = \left\langle e_i|\dot{\theta}\right\rangle - \dot{\bar{\theta}}\,\langle e_i|1\rangle = \lambda_i\,\langle e_i|\sigma(\theta(t-\delta t))\rangle = \lambda_i\sigma'(\bar{\theta})\,\langle e_i|\varphi\rangle + \mathcal{O}(\delta t)$. Therefore, Eq. (3.22) becomes

$$\langle e_i|\varphi'\rangle = \frac{\lambda_i\,\langle e_i|\varphi\rangle\left[\sigma'(\bar{\theta}) - \delta t[\sigma''(\bar{\theta})\dot{\bar{\theta}} + \lambda_i\sigma'^2(\bar{\theta})]\right]}{\omega + \tilde{\mathrm{J}}\left[\sigma(\bar{\theta}) - \delta t\dot{\bar{\theta}}\sigma'(\bar{\theta})\right]}\ . \tag{3.23}$$

If we now let $T(\bar{\theta}) = \omega + \tilde{\mathrm{J}}\left[\sigma(\bar{\theta}) - \delta t\dot{\bar{\theta}}\sigma'(\bar{\theta})\right]$, this will imply

$$T'(\bar{\theta}) = \tilde{\mathrm{J}}\left(\sigma'(\bar{\theta}) - \delta t[\sigma''(\bar{\theta})\dot{\bar{\theta}} + \sigma'(\bar{\theta})T']\right) = \tilde{\mathrm{J}}\left(\sigma'(\bar{\theta}) - \delta t[\sigma''(\bar{\theta})\dot{\bar{\theta}} + \tilde{\mathrm{J}}\sigma'^2(\bar{\theta})]\right) + \mathcal{O}(\delta t^2)\ .$$

We can rewrite Eq. (3.23) using this expression of $T = T(\bar{\theta})$ and $T' = T'(\bar{\theta})$,

$$\langle e_i|\varphi'\rangle = \langle e_i|\varphi\rangle\,\frac{1}{T}\frac{\lambda_i}{\tilde{\mathrm{J}}}\left(\tilde{\mathrm{J}}\left(\sigma'(\bar{\theta}) - \delta t[\sigma''(\bar{\theta})\dot{\bar{\theta}} + \tilde{\mathrm{J}}\sigma'^2(\bar{\theta})]\right) + \delta t\sigma'^2(\bar{\theta})(\tilde{\mathrm{J}}^2 - \lambda_i\tilde{\mathrm{J}})\right)$$

and hence,

$$\langle e_i|\varphi'\rangle = \langle e_i|\varphi\rangle\,\frac{\lambda_i}{\tilde{\mathrm{J}}}\left[\frac{T'}{T} + \frac{\delta t\sigma'^2(\bar{\theta})(\tilde{\mathrm{J}}^2 - \lambda_i\tilde{\mathrm{J}})}{T}\right]$$

and by rearranging this equation, we obtain a differential equation in $\langle e_i|\varphi\rangle$ using linearisation approximation

$$\langle e_i|\varphi'\rangle\,T - \frac{\lambda_i}{\tilde{\mathrm{J}}}\,\langle e_i|\varphi\rangle\,T' = \delta t\sigma'^2(\bar{\theta})\left[\lambda_i(\tilde{\mathrm{J}} - \lambda_i)\right]\langle e_i|\varphi\rangle\ .$$

If we now let $|\tilde{\varphi}\rangle = T^{-\frac{\lambda_i}{\tilde{\mathrm{J}}}}\,|\varphi\rangle$ and we differentiate with respect to $\bar{\theta}$, we get

$$\begin{aligned}\langle e_i|\tilde{\varphi}'\rangle &= -\frac{\lambda_i}{\tilde{\mathrm{J}}}T^{-\frac{\lambda_i}{\tilde{\mathrm{J}}}-1}T'\,\langle e_i|\varphi\rangle + T^{-\frac{\lambda_i}{\tilde{\mathrm{J}}}}\,\langle e_i|\varphi'\rangle = T^{-\frac{\lambda_i}{\tilde{\mathrm{J}}}-1}\left(-\frac{\lambda_i}{\tilde{\mathrm{J}}}\,\langle e_i|\varphi\rangle\,T' + \langle e_i|\varphi'\rangle\,T\right)\\ &= \frac{T^{-\frac{\lambda_i}{\tilde{\mathrm{J}}}}}{T}\left(\delta t\sigma'^2(\bar{\theta})\left[\lambda_i(\tilde{\mathrm{J}} - \lambda_i)\right]\langle e_i|\varphi\rangle\right) = \frac{1}{T}\delta t\sigma'^2(\bar{\theta})\left[\lambda_i(\tilde{\mathrm{J}} - \lambda_i)\right]\langle e_i|\tilde{\varphi}\rangle\ ,\end{aligned}$$

gives the solution of the form

$$\langle e_i|\tilde{\varphi}\rangle = A_i \exp\left(\lambda_i(\tilde{\mathrm{J}} - \lambda_i)\delta t \int_0^{\bar{\theta}} \frac{\sigma'^2(\bar{\theta}')}{T(\bar{\theta}')}\mathrm{d}\bar{\theta}'\right)$$

where A_i is given by initial condition. Therefore, our general solution in first orders of δt and φ is

$$\langle e_i|\varphi\rangle = \frac{A_i T^{\frac{\lambda_i}{\tilde{\mathrm{J}}}}}{T_0^{\frac{\lambda_i}{\tilde{\mathrm{J}}}}} \exp\left(\lambda_i(\tilde{\mathrm{J}} - \lambda_i)\delta t \int_0^{\bar{\theta}} \frac{\sigma'^2(\bar{\theta}')}{T(\bar{\theta}')}\mathrm{d}\bar{\theta}'\right). \tag{3.24}$$

For non-time delay systems, *i.e.* when $\delta t = 0$, we have an oscillating solution as $T = T(\bar{\theta})$ is periodic and bounded and consequently the non-time delay systems will not synchronise.

3.3.3 Numerics for N-oscillator Time Delay Model

The key in the linearisation method above is to relate the eigenvalues, and the corresponding eigenvectors, of the associated arbitrary adjacency matrix $\boldsymbol{J}$ in order to approximate the behaviour of our system. In order to obtain the eigenvalues λ_i, where $\lambda_i \neq \tilde{\mathrm{J}}$ we have chosen the method introduced by Press *et al.* [53], where we first reduce our matrix $\boldsymbol{J}$ into (upper) Hessenberg Form, say $\bar{\boldsymbol{J}}$, then apply QR transformation on $\bar{\boldsymbol{J}}$. The hqr function [53] will then output the corresponding eigenvalues, of $\bar{\boldsymbol{J}}$ and therefore, $\boldsymbol{J}$, see Section 11.5 and 11.6 of [53]. In order to obtain the associated eigenvectors, we implemented numerically the method Press *et al.* outlined in Section 11.7 of [53]. A reference of our implementation can be found in Appendix B.1.

According to Eq. (3.24), for coupling matrices $\boldsymbol{J}$ which have negative eigen-products, $E(\lambda_i) = \lambda_i(\tilde{\mathrm{J}} - \lambda_i) < 0$, we expect to synchronisation once the transient behaviour has died off. Numerics of $N = 3$ and $N = 4$ cases can be found in Figure 3.1 - 3.4 with RK4 with interpolation and our linearised solution using qsimp routine. The coupling matrix $\boldsymbol{J}$ for these systems has the form $\mathrm{J}_{ij} = \frac{1}{N-1}$ and $\mathrm{J}_{ii} = 0$, therefore $\sum_j \mathrm{J}_{ij} = 1$. However if we compare the trajectories of full system and the linearised solution, see Figure 3.5 and Figure 3.6, the trajectories of the linearised solution is perfectly symmetric while the full system has some asymmetric transient behaviour. This might seem to be a second order

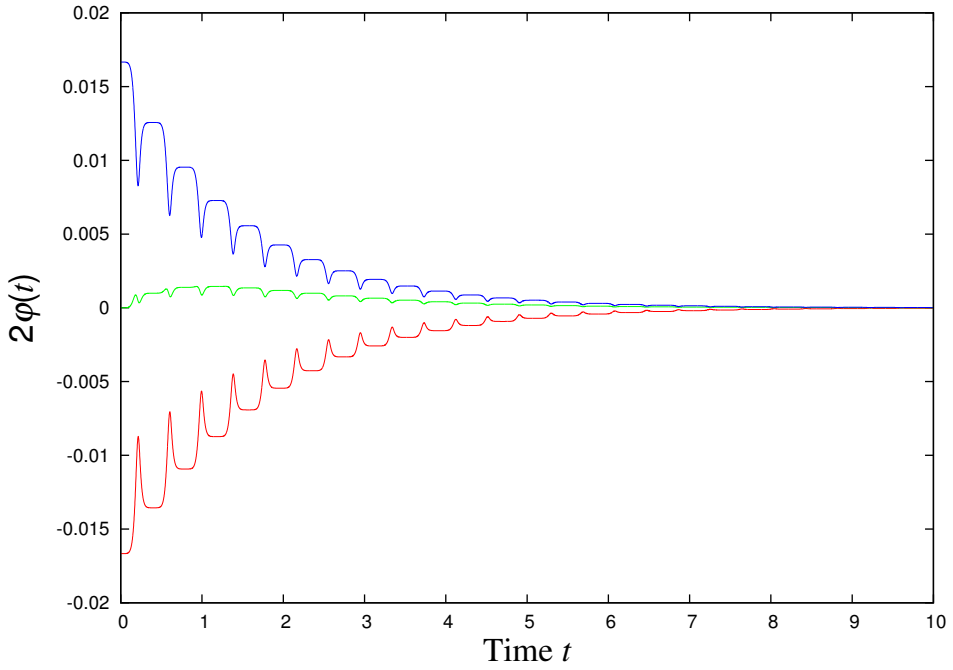

Figure 3.1: Trajectories of full system with $N = 3$ by using RK4 method with interpolation approximation. Parameters used: $\Delta t = 1\times10^{-6}$, $\xi = 1.01$, $\zeta = 0.1$ and $\delta t = 0.01$.

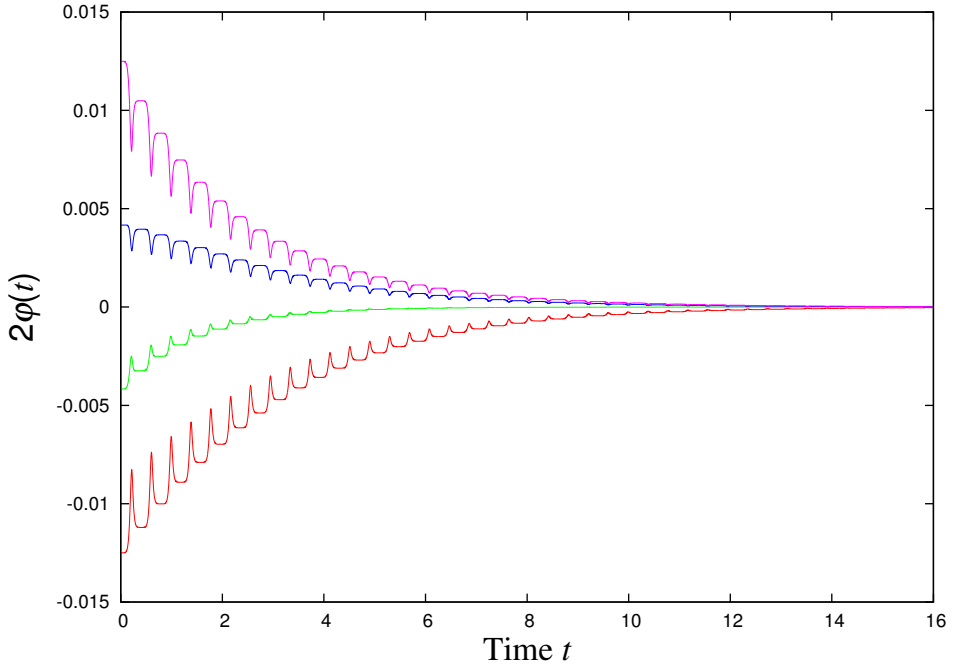

Figure 3.2: Trajectories of full system with $N = 4$ by using RK4 method with interpolation approximation. Parameters used: $\Delta t = 1\times10^{-6}$, $\xi = 1.01$, $\zeta = 0.1$ and $\delta t = 0.01$.

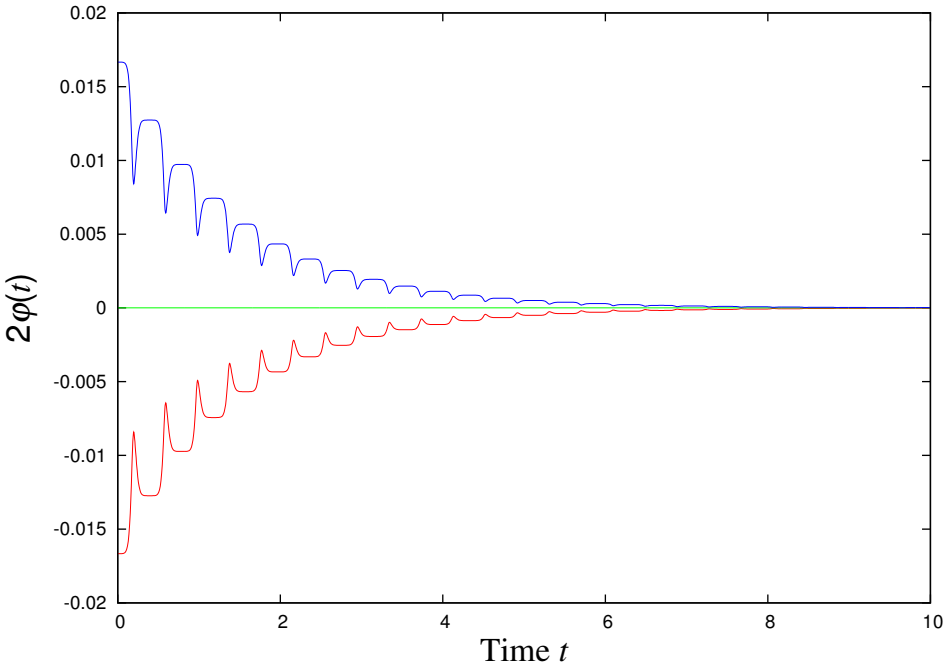

Figure 3.3: Trajectories of linearised solution with $N = 3$ by using qsimp routine. Parameters used: $\Delta t = 1 \times 10^{-6}$, $\xi = 1.01$, $\zeta = 0.1$ and $\delta t = 0.01$.

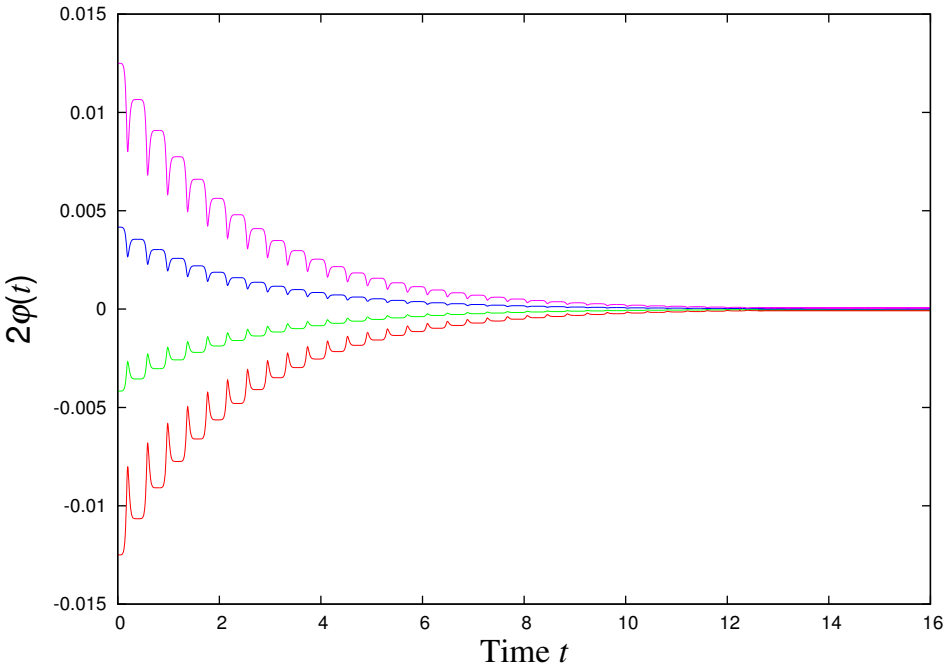

Figure 3.4: Trajectories of linearised solution with $N = 4$ by using qsimp routine. Parameters used: $\Delta t = 1 \times 10^{-6}$, $\xi = 1.01$, $\zeta = 0.1$ and $\delta t = 0.01$.

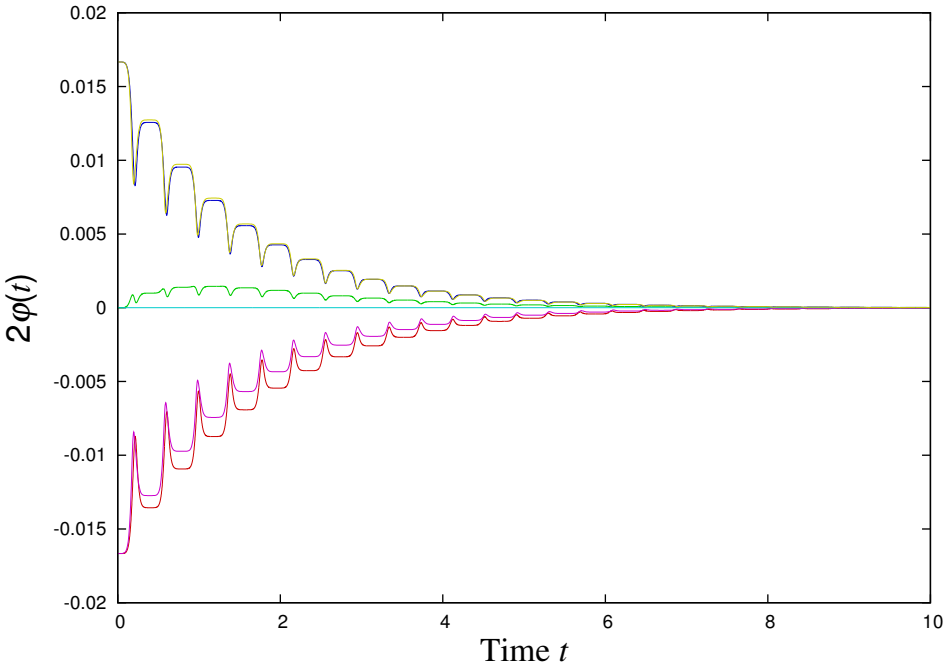

Figure 3.5: Trajectories comparisons between full system and linearised solution with $N = 3$, where the linearised solution is perfectly symmetric while the full system has asymmetric transient behaviour. Parameters used: $\Delta t = 1 \times 10^{-6}$, $\xi = 1.01$, $\zeta = 0.1$ and $\delta t = 0.01$.

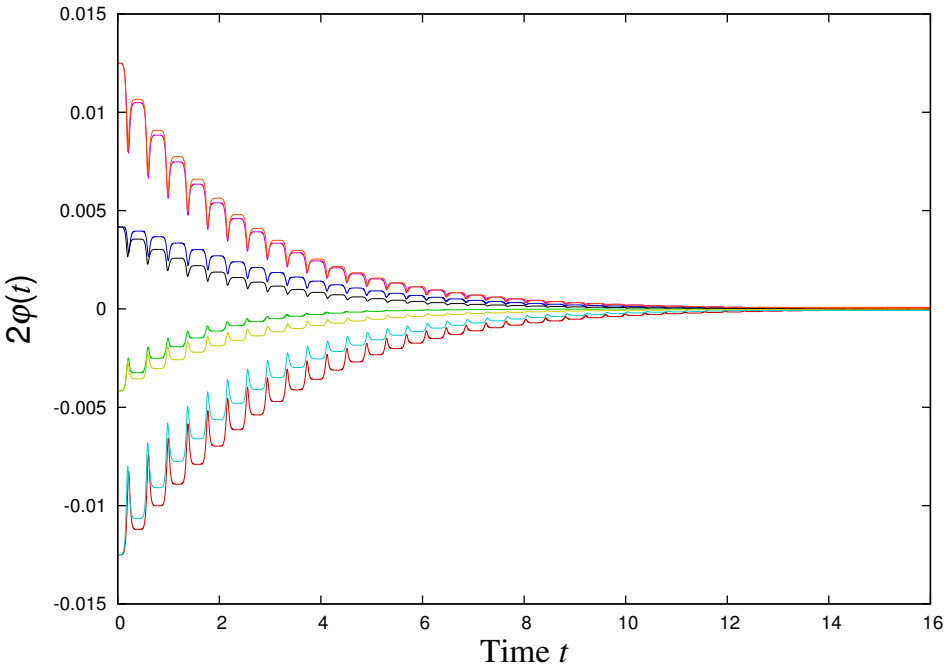

Figure 3.6: Trajectories comparisons between full system and linearised solution with $N = 4$, where the linearised solution is perfectly symmetric while the full system has asymmetric transient behaviour. Parameters used: $\Delta t = 1 \times 10^{-6}$, $\xi = 1.01$, $\zeta = 0.1$ and $\delta t = 0.01$.

effect coming from φ, which is being considered in Section 3.3.4, where the linearised solution is not capable to capture.

3.3.4 Linearised solution in first order of δt and second order of φ

It seems that the linearisation suggests synchronisation is only achievable while the eigen-product $E(\lambda_i)$, where $E(\lambda_i) = \lambda_i(\tilde{\mathrm{J}} - \lambda_i)$ with $\lambda_i \neq \tilde{\mathrm{J}}$, is negative. Interestingly while we were investigating different forms of $\boldsymbol{J}$, it occurs to us that the linearisation fails to predict somewhat synchronisation-like behaviours for some particular $\boldsymbol{J}$. For example, taking a 2-oscillator model with coupling matrix $\boldsymbol{J}$

$$\boldsymbol{J} = \begin{pmatrix} 1 & 0 \\ \frac{1}{2} & \frac{1}{2} \end{pmatrix} \tag{3.25}$$

where the two eigenvalues are 1 and $\frac{1}{2}$ correspondingly. Our eigen-product is then $E(\frac{1}{2}) = \frac{1}{4}$ and therefore our linearisation suggests that the system will not synchronise, instead it diverges, see Figure 3.7. However the numerics of the full system using RK4 displays somewhat synchronisation-like behaviour, see Figure 3.8.

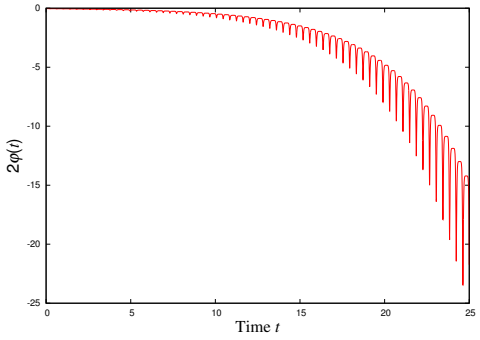

Figure 3.7: Trajectories of linearised solution by using qsimp routine, where linearised solution suggests unstable behaviour of the system.

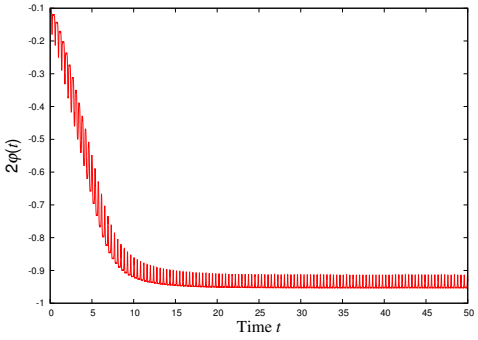

Figure 3.8: Trajectories of full system by using RK4 method with interpolation approximation. As compared to the numerics of the linearised solution, RK4 seems to suggest some sort of entrainment even for negative values of eigen-product $E(\lambda_i)$.

Possible answer for this phenomenon is that, although according to linearisation the system is unstable, *i.e.* $E(\lambda_i) = \lambda_i(\tilde{\mathrm{J}} - \lambda_i) > 0$, linearisation does not apply when $\langle e_i|\varphi\rangle$ gets too big. Therefore we suspect that this is due to the second order behaviour of φ

which our linearisation does not capture. Hence, instead of looking into expanding the vector $|\sigma(\theta(t-\delta t))\rangle$ up to the first order in φ, we expand the vector $|\sigma(\theta(t-\delta t))\rangle$ up to the second order in φ. The expansion of $|\sigma(\theta(t-\delta t))\rangle$ is then

$$\begin{aligned}|\sigma(\theta(t-\delta t))\rangle &= \sigma(\bar{\theta}(t-\delta t))\,|1\rangle + \sigma'(\bar{\theta}(t-\delta t))\,|\varphi(t-\delta t)\rangle \\ &\quad + \frac{1}{2}\sigma''(\theta(t-\delta t))\,\left|\varphi^2(t-\delta t)\right\rangle + \mathcal{O}(\varphi_i^3) \\ &= \sigma(\bar{\theta})\,|1\rangle - \delta t\dot{\bar{\theta}}\sigma'(\bar{\theta})\,|1\rangle + \sigma'(\bar{\theta})\,|\varphi\rangle - \delta t\dot{\bar{\theta}}\sigma''(\bar{\theta})\,|\varphi\rangle - \delta t\sigma'(\bar{\theta})\,|\dot{\varphi}\rangle \\ &\quad + \frac{1}{2}\sigma''(\bar{\theta})\,\left|\varphi^2\right\rangle - \frac{1}{2}\delta t\dot{\bar{\theta}}\sigma'''(\bar{\theta})\,\left|\varphi^2\right\rangle - \delta t\sigma''(\bar{\theta})\,|\varphi\dot{\varphi}\rangle + \mathcal{O}(\delta t^2)\ .\end{aligned}$$

Again, if we look into the projections of this expansion onto $\langle e_i|$ and $\langle 1|$, where scalar products $\langle e_i|1\rangle$ and $\langle 1|\varphi\rangle$ vanish, we have

$$\begin{aligned}\langle 1|\sigma(\theta(t-\delta t))\rangle &= q\sigma(\bar{\theta}) + \frac{1}{2}\sigma''(\bar{\theta})\,\langle 1|\varphi^2\rangle \\ &\quad - \delta t\left[q\dot{\bar{\theta}}\sigma'(\bar{\theta}) + \sigma''(\bar{\theta})\,\langle 1|\varphi\dot{\varphi}\rangle + \frac{1}{2}\dot{\bar{\theta}}\sigma'''(\bar{\theta})\,\langle 1|\varphi^2\rangle\right]\end{aligned}$$

and

$$\begin{aligned}\langle e_i|\sigma(\theta(t-\delta t))\rangle &= \sigma'(\bar{\theta})\,\langle e_i|\varphi\rangle + \frac{1}{2}\sigma''(\bar{\theta})\,\langle e_i|\varphi^2\rangle \\ &\quad - \delta t\Big[\sigma'(\bar{\theta})\,\langle e_i|\dot{\varphi}\rangle + \dot{\bar{\theta}}\sigma''(\bar{\theta})\,\langle e_i|\varphi\rangle + \sigma''(\bar{\theta})\,\langle e_i|\varphi\dot{\varphi}\rangle + \frac{1}{2}\dot{\bar{\theta}}\sigma'''(\bar{\theta})\,\langle e_i|\varphi^2\rangle\Big]\ .\end{aligned}$$

Hence, by neglecting small quantities such as $\mathcal{O}(\delta t\varphi\dot{\varphi})$ and $\mathcal{O}(\delta t\varphi^2)$, we obtain

$$\begin{aligned}\langle e_i|\varphi'\rangle &= \frac{\lambda_i\,\langle e_i|\sigma(\theta(t-\delta t))\rangle}{\omega + \frac{1}{q}\mathrm{J}\,\langle 1|\sigma(\theta(t-\delta t))\rangle} \\ &= \frac{\lambda_i\left[\sigma'(\bar{\theta})\,\langle e_i|\varphi\rangle + \frac{1}{2}\sigma''(\bar{\theta})\,\langle e_i|\varphi^2\rangle\right] - \lambda_i\delta t\left[\sigma'(\bar{\theta})\,\langle e_i|\dot{\varphi}\rangle + \dot{\bar{\theta}}\sigma''(\bar{\theta})\,\langle e_i|\varphi\rangle\right]}{\omega + \frac{1}{q}\tilde{\mathrm{J}}\left(q\sigma(\bar{\theta}) + \frac{1}{2}\sigma''(\bar{\theta})\,\langle 1|\varphi^2\rangle - \delta t\left[q\dot{\bar{\theta}}\sigma'(\bar{\theta})\right]\right)}\ .\end{aligned}$$

In order to solve this analytically, we will require $\langle 1|\varphi^2\rangle = 0$, which equivalently means φ^2 are negligible, and $\langle e_i|\varphi^2\rangle = \mu_i^2\,\langle e_i|\varphi\rangle^2$ [4], which means that we hunt for a value μ_i for

[4] We demand that μ_i to be constant in time t.

each λ_i which minimises $\langle e_i|\varphi\rangle$. In addition, we use $\langle e_i|\dot{\varphi}\rangle = \left\langle e_i|\dot{\theta}\right\rangle - \langle e_i|\dot{\bar{\theta}}|1\rangle = \left\langle e_i|\dot{\theta}\right\rangle = \lambda_i \langle e_i|\varphi\rangle \sigma'(\bar{\theta}) + \mathcal{O}(\delta t)$, our expression of $\langle e_i|\varphi'\rangle$ therefore becomes

$$\langle e_i|\varphi'\rangle = \frac{\lambda_i \left[\sigma'(\bar{\theta}) \langle e_i|\varphi\rangle + \frac{1}{2}\sigma''(\bar{\theta})\mu_i^2 \langle e_i|\varphi\rangle^2\right] - \lambda_i \delta t \left[\lambda_i \sigma'^2(\bar{\theta}) \langle e_i|\varphi\rangle + \dot{\bar{\theta}}\sigma''(\bar{\theta}) \langle e_i|\varphi\rangle\right]}{\omega + \tilde{\mathrm{J}}\left[\sigma(\bar{\theta}) - \delta t \dot{\bar{\theta}}\sigma'(\bar{\theta})\right]} \tag{3.26}$$

by dividing both sides of the equation by $\langle e_i|\varphi\rangle^2$ and rearrange, we have

$$\frac{\langle e_i|\varphi'\rangle}{\langle e_i|\varphi\rangle^2} = \frac{\lambda_i}{\langle e_i|\varphi\rangle} \frac{\sigma'(\bar{\theta}) - \delta t \left[\lambda_i \sigma'^2(\bar{\theta}) + \dot{\bar{\theta}}\sigma''(\bar{\theta})\right]}{\omega + \tilde{\mathrm{J}}\left[\sigma(\bar{\theta}) - \delta t \dot{\bar{\theta}}\sigma'(\bar{\theta})\right]} + \frac{\frac{1}{2}\lambda_i \mu_i^2 \sigma''(\bar{\theta})}{\omega + \tilde{\mathrm{J}}\left[\sigma(\bar{\theta}) - \delta t \dot{\bar{\theta}}\sigma'(\bar{\theta})\right]} \ .$$

Now, if we let $\Omega = \frac{1}{\langle e_i|\varphi\rangle}$ and therefore, $\frac{\mathrm{d}\Omega}{\mathrm{d}\bar{\theta}} = \frac{-1}{\langle e_i|\varphi\rangle^2} \langle e_i|\varphi'\rangle$ which gives a first order differential equation in Ω

$$\frac{\mathrm{d}\Omega}{\mathrm{d}\bar{\theta}} + \lambda_i \Omega \frac{\sigma'(\bar{\theta}) - \delta t \left[\lambda_i \sigma'^2(\bar{\theta}) + \dot{\bar{\theta}}\sigma''(\bar{\theta})\right]}{\omega + \tilde{\mathrm{J}}\left[\sigma(\bar{\theta}) - \delta t \dot{\bar{\theta}}\sigma'(\bar{\theta})\right]} = \frac{-\frac{1}{2}\lambda_i \mu_i^2 \sigma''(\bar{\theta})}{\omega + \tilde{\mathrm{J}}\left[\sigma(\bar{\theta}) - \delta t \dot{\bar{\theta}}\sigma'(\bar{\theta})\right]} \ .$$

If we now write this equation in the form of

$$\frac{\mathrm{d}\Omega}{\mathrm{d}\bar{\theta}} + \lambda_i \Omega h_i \left(\sigma(\bar{\theta}), \sigma'(\bar{\theta}), \sigma''(\bar{\theta}), \dot{\bar{\theta}}; \delta t, \lambda_i, \omega, \tilde{\mathrm{J}}, t\right) = \frac{-\frac{1}{2}\lambda_i \mu_i^2 \sigma''(\bar{\theta})}{\omega + \tilde{\mathrm{J}}\left[\sigma(\bar{\theta}) - \delta t \dot{\bar{\theta}}\sigma'(\bar{\theta})\right]} \tag{3.27}$$

then by similar approach we have before, *i.e.* let $T(\bar{\theta}) = \omega + \tilde{\mathrm{J}}[\sigma(\bar{\theta}) - \delta t \dot{\bar{\theta}}\sigma'(\bar{\theta})]$, with $T(\bar{\theta}) = \dot{\bar{\theta}}$ up to first order in δt, which yields [5]

$$\begin{aligned} \frac{\mathrm{d}}{\mathrm{d}\bar{\theta}} T(\bar{\theta}) = T'(\bar{\theta}) &= \tilde{\mathrm{J}}\left(\sigma'(\bar{\theta}) - \delta t[\sigma'(\bar{\theta})T' + \dot{\bar{\theta}}\sigma''(\bar{\theta})]\right) \\ &= \tilde{\mathrm{J}}\left(\sigma'(\bar{\theta}) - \delta t[\tilde{\mathrm{J}}\sigma'^2(\bar{\theta}) + \dot{\bar{\theta}}\sigma''(\bar{\theta})] + \mathcal{O}(\delta t^2)\right) \ . \end{aligned}$$

[5] In the following it is useful to assume that T has only one sign, even when, strictly, this does not follow from $T(\bar{\theta}) = \dot{\bar{\theta}} + \mathcal{O}(\delta t^2)$. In fact, we could have done much of the following on the basis of $\dot{\bar{\theta}}$ and introduced its expansion without claiming anything about its sign.

By use of this expression of $T'(\bar{\theta})$, we can write our function h_i as

$$\begin{aligned} h_i &= \frac{1}{T}\frac{\lambda_i}{\tilde{\mathrm{J}}}\left[\tilde{\mathrm{J}}\left(\sigma'(\bar{\theta}) - \delta t[\tilde{\mathrm{J}}\sigma'^2(\bar{\theta}) + \dot{\bar{\theta}}\sigma''(\bar{\theta})] + \delta t(\tilde{\mathrm{J}}^2 - \lambda_i\tilde{\mathrm{J}})\sigma'^2(\bar{\theta})\right)\right] \\ &= \frac{\lambda_i}{\tilde{\mathrm{J}}}\left[\frac{T'(\bar{\theta})}{T(\bar{\theta})} + (\tilde{\mathrm{J}}^2 - \lambda_i\tilde{\mathrm{J}})\delta t\frac{\sigma'^2(\bar{\theta})}{T(\bar{\theta})}\right] \end{aligned}$$

we obtain our integrating factor as

$$\begin{aligned} \exp\left(\int h_i \mathrm{d}\bar{\theta}\right) &= \exp\left(\frac{\lambda_i}{\tilde{\mathrm{J}}}\int\left[\frac{T'(\bar{\theta})}{T(\bar{\theta})} + (\tilde{\mathrm{J}}^2 - \lambda_i\tilde{\mathrm{J}})\delta t\frac{\sigma'^2(\bar{\theta})}{T(\bar{\theta})}\right]\mathrm{d}\bar{\theta}\right) \\ &= \exp\left(\frac{\lambda_i}{\tilde{\mathrm{J}}}\ln(T)\right)\exp\left(\lambda_i(\tilde{\mathrm{J}} - \lambda_i)\delta t\int\frac{\sigma'^2(\bar{\theta})}{T(\bar{\theta})}\mathrm{d}\bar{\theta}\right) \\ &= T^{\frac{\lambda_i}{\tilde{\mathrm{J}}}}\exp\left(\lambda_i(\tilde{\mathrm{J}} - \lambda_i)\delta t\int\frac{\sigma'^2(\bar{\theta})}{T(\bar{\theta})}\mathrm{d}\bar{\theta}\right). \end{aligned}$$

Hence, we can solve Eq. (3.27) by use of this integrating factor

$$\int_{\bar{\theta}_0}^{\bar{\theta}}\left(\Omega\exp\left(\int_{\bar{\theta}_0}^{\bar{\theta}''} h_i\mathrm{d}\bar{\theta}'\right)\right)'\mathrm{d}\bar{\theta}'' = \int_{\bar{\theta}_0}^{\bar{\theta}(t)}\left(-\frac{1}{2}\lambda_i\mu_i^2\sigma''(\bar{\theta}'')\frac{1}{T(\bar{\theta}'')}\exp\left(\int_{\bar{\theta}_0}^{\bar{\theta}''} h_i\mathrm{d}\bar{\theta}'\right)\right)\mathrm{d}\bar{\theta}'',$$

and therefore, the solution to Eq. (3.27) is

$$\frac{\langle e_i|\varphi_0\rangle}{\langle e_i|\varphi(t)\rangle}\frac{T^{\frac{\lambda_i}{\tilde{\mathrm{J}}}}}{T_0^{\frac{\lambda_i}{\tilde{\mathrm{J}}}}}e^{\left(\lambda_i(\tilde{\mathrm{J}}-\lambda_i)\delta t\int_{\bar{\theta}_0}^{\bar{\theta}}\frac{\sigma'^2(\bar{\theta}')}{T(\bar{\theta}')}\mathrm{d}\bar{\theta}'\right)} = \int_{\bar{\theta}_0}^{\bar{\theta}(t)} -\frac{1}{2}\lambda_i\mu_i^2\sigma''(\bar{\theta}'')T^{\frac{\lambda_i}{\tilde{\mathrm{J}}}-1}e^{\left(\lambda_i(\tilde{\mathrm{J}}-\lambda_i)\delta t\int_{\bar{\theta}_0}^{\bar{\theta}''}\frac{\sigma'^2(\bar{\theta}')}{T(\bar{\theta}')}\mathrm{d}\bar{\theta}'\right)}\mathrm{d}\bar{\theta}''$$

which yields a solution to our system [6]

$$\langle e_i|\varphi(t)\rangle = \frac{\langle e_i|\varphi_0\rangle\, T^{\frac{\lambda_i}{\tilde{\mathrm{J}}}}}{T_0^{\frac{\lambda_i}{\tilde{\mathrm{J}}}}}\frac{e^{\left(\lambda_i(\tilde{\mathrm{J}}-\lambda_i)\delta t\int_{\bar{\theta}_0}^{\bar{\theta}}\frac{\sigma'^2(\bar{\theta}')}{T(\bar{\theta}')}\mathrm{d}\bar{\theta}'\right)}}{\int_{\bar{\theta}_0}^{\bar{\theta}(t)} -\frac{1}{2}\lambda_i\mu_i^2\sigma''(\bar{\theta}'')T^{\frac{\lambda_i}{\tilde{\mathrm{J}}}-1}e^{\left(\lambda_i(\tilde{\mathrm{J}}-\lambda_i)\delta t\int_{\bar{\theta}_0}^{\bar{\theta}''}\frac{\sigma'^2(\bar{\theta}')}{T(\bar{\theta}')}\mathrm{d}\bar{\theta}'\right)}\mathrm{d}\bar{\theta}''} \tag{3.28}$$

where $|\varphi_0\rangle = (\varphi_1(0), \varphi_2(0), \cdots, \varphi_N(0))$, $T_0 = T(0)$, and $\bar{\theta}_0 = \bar{\theta}(0)$. At first sight, one might wonder whether this is an algebraic decay in $\bar{\theta}$, brought about by the denominator. The reason why we are not seeing synchronisation in the numerics of the linearised solution would then be explained by the algebraic decay being very slow. However we

[6] Clearly, now that T is taken to some arbitrary power, we should have a statement about the sign of T, which we have made above.

can rewrite Eq. (3.28) as

$$\langle e_i|\varphi(t)\rangle = -2T^{\frac{\lambda_i}{\tilde{\jmath}}}\left(\int_{\bar{\theta}_0}^{\bar{\theta}(t)}\lambda_i\mu_i^2\sigma''(\bar{\theta}'')T^{\frac{\lambda_i}{\tilde{\jmath}}-1}\exp\left(-\lambda_i(\tilde{\jmath}-\lambda_i)\delta t\int_{\bar{\theta}''(t)}^{\bar{\theta}(t)}\frac{\sigma'^2(\bar{\theta}')}{T(\bar{\theta}')}\mathrm{d}\bar{\theta}'\right)\mathrm{d}\bar{\theta}''\right)^{-1}. \tag{3.29}$$

We would like to investigate whether this result coincide with our numerics, such that this kind of system will eventually have synchronisation-like behaviour; therefore we would like to evaluate the right hand side of Eq. (3.29). Note that the inner integrand in the exponential will behave like $A(\bar{\theta}-\bar{\theta}'')$, where $A=\frac{1}{\xi}\int_0^{\xi}\frac{\sigma^2(\bar{\theta}')}{T(\bar{\theta}')}\mathrm{d}\bar{\theta}'$ and ξ is the periodicity of σ, then

$$\langle e_i|\varphi(t)\rangle \cong -2T^{\frac{\lambda_i}{\tilde{\jmath}}}\left(\int_{\bar{\theta}_0}^{\bar{\theta}(t)}\lambda_i\mu_i^2\sigma''(\bar{\theta}'')T^{\frac{\lambda_i}{\tilde{\jmath}}-1}\exp\Big(-\tilde{A}_i(\bar{\theta}-\bar{\theta}'')\Big)\mathrm{d}\bar{\theta}''\right)^{-1}$$

where $\tilde{A}_i=\lambda_i(\tilde{\jmath}-\lambda_i)\delta t A$. Observing that the sign of $\tilde{A}_i$ is solely depending on the sign of the eigen-product $E(\lambda_i)$. If $\tilde{A}_i<0$ then the integral increases as we increase t, since all expressions in the integrand are either constant or periodic and bounded, we recover the behaviour of our linearised solution in Section 3.3.2; the system will synchronise, *i.e.* $\langle e_i|\varphi\rangle$ converges to 0, if the eigen-product is negative. If now we consider the case that $\tilde{A}_i>0$, by change of integration limits such that $\tilde{A}_i(\bar{\theta}-\bar{\theta}'')=1$, then the exponential acts as an effective cut-off of our integration

$$\begin{aligned}\langle e_i|\varphi(t)\rangle &\cong -2T^{\frac{\lambda_i}{\tilde{\jmath}}}\left(\int_{\bar{\theta}(t)-\frac{1}{\tilde{A}_i}}^{\bar{\theta}(t)}\lambda_i\mu_i^2\sigma''(\bar{\theta}'')T^{\frac{\lambda_i}{\tilde{\jmath}}-1}\mathrm{d}\bar{\theta}''\right)^{-1}\cong -2T^{\frac{\lambda_i}{\tilde{\jmath}}}\left(\frac{1}{C_i\tilde{A}_i}\right)^{-1}\\ &= -2T^{\frac{\lambda_i}{\tilde{\jmath}}}C_iA_i\lambda_i(\tilde{\jmath}-\lambda_i)\delta t\ .\end{aligned}$$

Since $T(\bar{\theta})$ is periodic and bounded, the system indeed does not synchronise. Rather, it displays a form of entrainment, with the projection having an amplitude proportional to the time delay. This explains why the systems we looked at numerically "almost" synchronised: the phase difference was very small, but that's just because δt is very small. The phase difference is thus proportional to δt.

We have learnt that our N-oscillator time delay model will eventually be synchronised

if the eigen-product $E(\lambda_i)$ is negative otherwise the system will end up be entrained to an amplitude proportional to the time delay δt. Comparing Eq. (3.23) and Eq. (3.26), the term

$$\frac{\frac{1}{2}\lambda_i \mu_i^2 \sigma''(\bar{\theta}) \langle e_i|\varphi\rangle^2}{\omega + \tilde{\mathrm{J}}\left[\sigma(\bar{\theta}) - \delta t \dot{\bar{\theta}} \sigma'(\bar{\theta})\right]} \tag{3.30}$$

in the second order approximation is responsible for this entrainment phenomenon. In hindsight, by realising the fact that any pair of oscillators θ_i and θ_j will never *know* that each other are too far apart as θ_i is bounded by the periodicity of σ, therefore our linearisation in first orders of φ and δt bound to fail on predicting this entrainment behaviour.

One may think that this second order approximation is also responsible for the asymmetric transient behaviour of the full system as mentioned in Section 3.3.3. For the coupling matrices $\boldsymbol{J}$ used in Section 3.3.3, one of the eigenvalues is $\tilde{\mathrm{J}} = 1$ and the rest of the eigenvalues are equal with $\lambda_i = -\frac{\tilde{\mathrm{J}}}{N-1} = -\frac{1}{N-1}$, which means that all the eigen-products are negative. Therefore, no explicit approximations can be made for Eq. (3.29) and the problem remains unsolved. The reasoning of the assymmetric transient behaviour occur in the numerics of the full system is probably more challenging as the transient behaviour will die off in finite time.

In regards to linear stability, in technical terms we say a system is linearly stable or unstable by referring stability to a particular structure of ordinary differential equation, for example an ordinary differential equation of the form $\dot{\varphi} = -H(t)\varphi$ with $H(t)$ a non-periodic function of t, then $\varphi \to 0$ when $t \to \infty$. In fact, we have taken linear approximation to obtain Eq. (3.23) which is similar, but not quite, to this particular form of ordinary differential equation. As a result, one has to take great care that whether linearisation applies for this particular form of equation as our $H(t)$ is not that simple and it may not be straight forward to show that $\varphi \to 0$ when $t \to \infty$.

3.4 General case with Arbitrary J_{ij} with different eigen-frequencies for N-oscillator Model

We have a better understanding on how our systems behave under certain constraints, we continue to investigate the effects of our systems with different initial (eigen-)frequencies as introduced in the Winfree model and the Kuramoto model.

3.4.1 General case with different eigen-frequencies for 2-oscillator model

Before we proceed ahead for an N-oscillator model, in order to get a better understanding of the behaviour in the simplest model, we first consider a 2-oscillator model with different, but fixed, eigen-frequencies ω_1 and ω_2:

$$\begin{aligned}\dot{\theta}_1 &= \omega_1 + \mathrm{J}\sigma(\theta_2(t-\delta t))\\ \dot{\theta}_2 &= \omega_2 + \mathrm{J}\sigma(\theta_1(t-\delta t))\ .\end{aligned}$$

We can always generalise the above equations into

$$\dot{\theta}_1 = \omega + \epsilon + \mathrm{J}\sigma(\theta_2(t-\delta t)) \tag{3.31}$$

$$\dot{\theta}_2 = \omega - \epsilon + \mathrm{J}\sigma(\theta_1(t-\delta t)) \tag{3.32}$$

with average eigen-frequency ω and the deviation ϵ; where $\omega = \frac{1}{2}(\omega_1 + \omega_2)$ and $\epsilon = \frac{1}{2}(\omega_1 - \omega_2)$. Note that this pair of equations of motion only different to the 2-oscillator time delay model with same initial eigen-frequency, (2.35) and (2.36), up to a constant ϵ. Therefore if we define $\theta_1 = \bar{\theta} + \varphi$ and $\theta_2 = \bar{\theta} - \varphi$, then $\dot{\bar{\theta}} = \frac{1}{2}(\dot{\theta}_1 + \dot{\theta}_2)$ and the approximation of $\dot{\bar{\theta}}$ stay unaffected as ϵ averages out, while $\dot{\varphi} = \frac{1}{2}(\dot{\theta}_1 - \dot{\theta}_2)$ will be shifted by ϵ in comparison to the 2-oscillator time delay model with same initial eigen-frequency.

If we then expand in first order of small δt and φ of our function σ will give

$$\dot{\bar{\theta}} = \frac{1}{2}(\dot{\theta}_1 + \dot{\theta}_2) = \omega + \mathrm{J}\left(\sigma(\bar{\theta}) - \delta t\dot{\bar{\theta}}\sigma'(\bar{\theta})\right) \tag{3.33}$$

$$\dot{\varphi} = \frac{1}{2}(\dot{\theta}_1 - \dot{\theta}_2) = \epsilon + \mathrm{J}\left(-\varphi\sigma'(\bar{\theta}) + \delta t(\varphi\dot{\bar{\theta}}\sigma''(\bar{\theta}) + \dot{\varphi}\sigma'(\bar{\theta}))\right) . \tag{3.34}$$

We now rearrange and simplify the expression of $\dot{\varphi}$

$$\begin{aligned}
\dot{\varphi} &= \left[\epsilon + \mathrm{J}\left(-\varphi\sigma'(\bar{\theta}) + \delta t\varphi\dot{\bar{\theta}}\sigma''(\bar{\theta})\right)\right]\left[1 + \mathrm{J}\delta t\sigma'(\bar{\theta}) + \mathcal{O}(\delta t^2)\right] \\
&= \left[\epsilon - \mathrm{J}\varphi\left(\sigma'(\bar{\theta}) - \delta t\dot{\bar{\theta}}\sigma''(\bar{\theta})\right)\right] + \epsilon\mathrm{J}\delta t\sigma'(\bar{\theta}) - \mathrm{J}^2\delta t\varphi\sigma'^2(\bar{\theta}) + \mathcal{O}(\delta t^2) \\
&\cong \epsilon[1 + \mathrm{J}\delta t\sigma'(\bar{\theta})] - \varphi\left(\mathrm{J}\sigma'(\bar{\theta}) - \mathrm{J}\delta t\dot{\bar{\theta}}\sigma''(\bar{\theta}) + \mathrm{J}^2\delta t\sigma'^2(\bar{\theta})\right) .
\end{aligned}$$

Using the expression of $\frac{\mathrm{d}}{\mathrm{d}\bar{\theta}}(\dot{\bar{\theta}})$ (2.39) and let $T = \dot{\bar{\theta}} = \omega + \mathrm{J}\sigma(\bar{\theta}) - \mathrm{J}\delta t\dot{\bar{\theta}}\sigma'(\bar{\theta})$,

$$\begin{aligned}
\varphi' = \frac{\mathrm{d}\varphi}{\mathrm{d}\bar{\theta}} &= \frac{\epsilon[1 + \mathrm{J}\delta t\sigma'(\bar{\theta})] - \varphi\left(\mathrm{J}\sigma'(\bar{\theta}) - \mathrm{J}\delta t\dot{\bar{\theta}}\sigma''(\bar{\theta}) + \mathrm{J}^2\delta t\sigma'^2(\bar{\theta})\right)}{T} \\
&= \frac{\epsilon[1 + \mathrm{J}\delta t\sigma'(\bar{\theta})]}{T} - \frac{\varphi\left(\mathrm{J}\sigma'(\bar{\theta}) - \mathrm{J}\delta t\dot{\bar{\theta}}\sigma''(\bar{\theta}) - \mathrm{J}^2\delta t\sigma'^2(\bar{\theta}) + 2\mathrm{J}^2\delta t\sigma'^2(\bar{\theta})\right)}{T} \\
&= \frac{\epsilon[1 + \mathrm{J}\delta t\sigma'(\bar{\theta})]}{T} - \varphi\left(\frac{\mathrm{d}}{\mathrm{d}\bar{\theta}}\ln(T) + \frac{2\mathrm{J}^2\delta t\sigma'^2(\bar{\theta})}{T}\right) .
\end{aligned}$$

By writing $g(\bar{\theta}) = \left(\frac{\mathrm{d}}{\mathrm{d}\bar{\theta}}\ln(T) + \frac{2\mathrm{J}^2\delta t\sigma'^2(\bar{\theta})}{T}\right)$, we can rewrite the above equation as

$$\varphi' = -\varphi g(\bar{\theta}) + \frac{\epsilon[1 + \mathrm{J}\delta t\sigma'(\bar{\theta})]}{T} . \tag{3.35}$$

From Section 2.4, we know the solution to $\varphi' + \varphi g(\bar{\theta}) = 0$ is

$$\varphi(t) = \varphi_0\frac{\dot{\bar{\theta}}(0)}{\dot{\bar{\theta}}(t)}\exp\left(-2\mathrm{J}^2\delta t\int_{\bar{\theta}(0)}^{\bar{\theta}(t)}\frac{\sigma'^2(\bar{\theta}')}{T}\mathrm{d}\bar{\theta}'\right) . \tag{3.36}$$

Therefore, in order to solve the ODE we have, we multiply the above equation by $\exp\left(\int_{\bar{\theta}(0)}^{\bar{\theta}(t)} g(\bar{\theta}')\mathrm{d}\bar{\theta}'\right)$; and therefore

$$\frac{\mathrm{d}}{\mathrm{d}\bar{\theta}}\left(\varphi e^{\int_{\bar{\theta}(0)}^{\bar{\theta}(t)} g(\bar{\theta}')\mathrm{d}\bar{\theta}'} + C\right) = \frac{\epsilon[1 + \mathrm{J}\delta t\sigma'(\bar{\theta})]}{T}e^{\int_{\bar{\theta}(0)}^{\bar{\theta}(t)} g(\bar{\theta}')\mathrm{d}\bar{\theta}'}$$

where C is an integration constant. The solution is then

$$\begin{aligned}\varphi &= -Ce^{-\int_{\bar{\theta}(0)}^{\bar{\theta}(t)} g(\bar{\theta}')\mathrm{d}\bar{\theta}'} + e^{-\int_{\bar{\theta}(0)}^{\bar{\theta}(t)} g(\bar{\theta}')\mathrm{d}\bar{\theta}'} \int_{\bar{\theta}(0)}^{\bar{\theta}(t)} \frac{\epsilon[1+\mathrm{J}\delta t\sigma'(\bar{\theta}'')]}{T(\bar{\theta}'')} e^{\int_{\bar{\theta}(0)}^{\bar{\theta}''(t)} g(\bar{\theta}')\mathrm{d}\bar{\theta}'}\mathrm{d}\bar{\theta}'' \\ &= -Ce^{-\int_{\bar{\theta}(0)}^{\bar{\theta}(t)} g(\bar{\theta}')\mathrm{d}\bar{\theta}'} + \epsilon \int_{\bar{\theta}(0)}^{\bar{\theta}(t)} \frac{[1+\mathrm{J}\delta t\sigma'(\bar{\theta}'')]}{T(\bar{\theta}'')} e^{-\int_{\bar{\theta}''(t)}^{\bar{\theta}(t)} g(\bar{\theta}')\mathrm{d}\bar{\theta}'}\mathrm{d}\bar{\theta}'' \ . \end{aligned} \tag{3.37}$$

The first term of Eq. (3.37) will converge to 0 as $t \to \infty$ therefore the dynamics of φ is linearly approximated by the second term. By taking approximation for the inner integrand of the second term [7], the inner integral then becomes $e^{(-K(\bar{\theta}-\bar{\theta}''))}$, where $K = \frac{1}{\xi}\int_0^{\xi} g(\bar{\theta}')\mathrm{d}\bar{\theta}'$. Since this exponential will suppress any $\bar{\theta}(t) < \bar{\theta}''(t)$ asymptotically as $t \to \infty$, we need only consider the outer integral limit from $\bar{\theta}'' = \bar{\theta} - \frac{1}{K}$, therefore the solution becomes

$$\varphi(t) = -Ce^{-\int_{\bar{\theta}(0)}^{\bar{\theta}(t)} g(\bar{\theta}')\mathrm{d}\bar{\theta}'} + \epsilon \int_{\bar{\theta}(t)-\frac{1}{K}}^{\bar{\theta}(t)} \frac{[1+\mathrm{J}\delta t\sigma'(\bar{\theta}'')]}{T(\bar{\theta}'')}\mathrm{d}\bar{\theta}'' \cong \frac{\epsilon}{KL} \tag{3.38}$$

where $\frac{1}{L} = \frac{1}{\xi}\int_0^{\xi} \frac{[1+\mathrm{J}\delta t\sigma'(\bar{\theta}'')]}{T(\bar{\theta}'')}\mathrm{d}\bar{\theta}''$. Therefore, $\varphi \cong \frac{\epsilon}{KL}$ asymptotically as $t \to \infty$. The numerics agrees quite well (in absolute terms) with this approximation, see Figure 3.9, despite a consistent percentage error of roughly 12.7% between the numerics of the full system (column 2) and the linear approximation (column 3), see Table 3.1. This consistent percentage error is possibly an fallout of not taking the effect of second order behaviour of $\varphi(t)$ into consideration in our analysis. However, if we average the phase differences once the transient behaviour died off, we have a very good agreement, in the margin of 3-5%, between the linear approximation (column 3) (3.38) and our numerical averages (column 4). If we look at the trajectories of the full system, see Figure 3.9 inset, we can notice that there are sloping in the phase difference. These slopings are caused by θ_1 travelling faster than θ_2 from the effect of ϵ.

One may then ask what is the maximum sustainable value of ϵ a system like this can result in entrainment. In order to give a reasonable explanation, we look into the asymptotic behaviour, *i.e.* for large values of t, over one characteristic period. Similar to

[7] See Section 3.3.4 for similar but more detailed explanation.

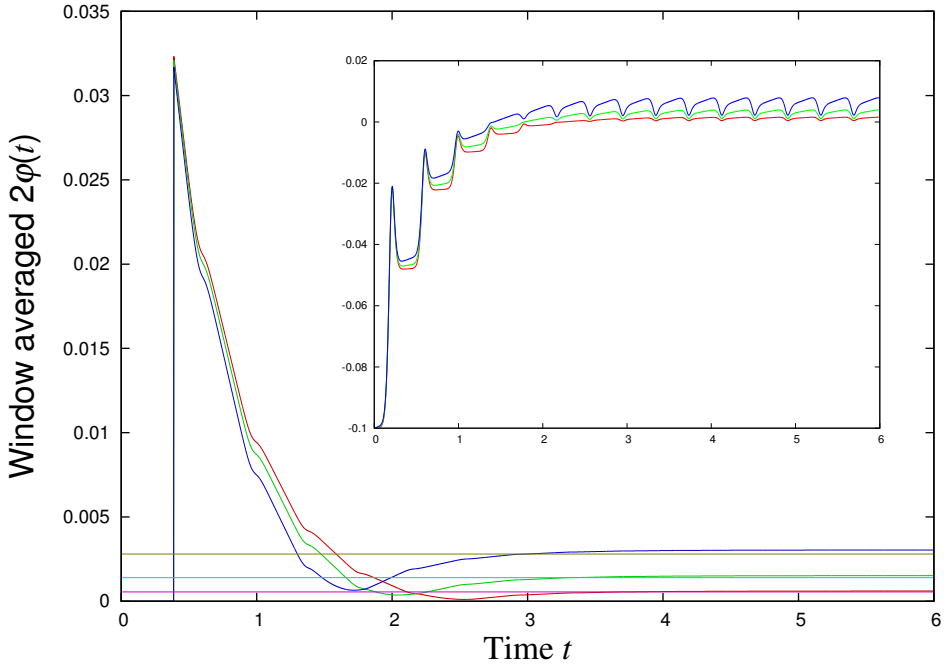

Figure 3.9: Window averaged trajectories of full system (RK4) and linearisation approximation of the asymptotic values from Table 3.1 with parameters $\Delta t = 1 \times 10^{-6}$, $\xi = 1.01$, $\zeta = 0.1$ and $\delta t = 0.01$. Inset: trajectories of φ with $\epsilon = 0.001$ (red), 0.0025 (green) and 0.005 (blue) between time 0 to 6.

ϵ	$\varphi(t)$	$\frac{\epsilon}{KL}$	Numerical averages
0.00050	3.0386×10^{-4}	2.6529×10^{-4}	2.7569×10^{-4}
0.00075	4.5579×10^{-4}	3.9794×10^{-4}	4.1559×10^{-4}
0.00100	6.0773×10^{-4}	5.3059×10^{-4}	5.5401×10^{-4}
0.00250	1.5194×10^{-3}	1.3265×10^{-3}	1.3978×10^{-3}
0.00500	3.0395×10^{-3}	2.6529×10^{-3}	2.7993×10^{-3}
0.00750	4.5609×10^{-3}	3.9794×10^{-3}	4.1418×10^{-3}
0.01000	6.0843×10^{-3}	5.3059×10^{-3}	5.5693×10^{-3}

Table 3.1: Table of numerics outputs of asymptotic values of φ, linearisation approximation of $\frac{\epsilon}{KL}$, and numerical averages after transient behaviour died off. Parameters used: $\Delta t = 1 \times 10^{-6}$, $\xi = 1.01$, $\zeta = 0.1$, $\delta t = 0.01$ and $2\varphi_0 = 0.1$.

Section 2.7, we define the quantities ψ and S such that

$$\psi = \int_0^{\xi} \frac{\mathrm{d}\bar{\theta}'}{T(\bar{\theta}')} , \qquad S = \int_0^{\xi} \frac{\sigma'^2(\bar{\theta}')\mathrm{d}\bar{\theta}'}{T(\bar{\theta}')} \tag{3.39}$$

where $T(\bar{\theta}) = \dot{\bar{\theta}} = \omega + \mathrm{J}\sigma(\bar{\theta}) - \mathrm{J}\delta t\dot{\bar{\theta}}\sigma'(\bar{\theta})$ to linear order in δt. If we assume $\lim_{t\to\infty} \frac{1}{t}\int_0^t \varphi(t')\mathrm{d}t' = \tilde{\varphi}$, where $\tilde{\varphi}$ is the asymptotic phase difference, then by Eq. (2.56) (linearised solution with $\epsilon = 0$) and Eq. (3.38) (linearsed solution with $\epsilon \neq 0$), after one characteristic period ψ, we have $\tilde{\varphi}e^{-\frac{\psi}{\tau}}$ and $\tilde{\varphi}$ correspondingly. τ is defined as the characteristic synchronisation time where $\tau = \frac{\psi}{2\mathrm{J}^2\delta t S}$. If we then equate the contribution of desynchronisation, effectively the entrainment strength, per period of σ, to the contribution of synchronisation per cycle yields

$$\epsilon\psi = \tilde{\varphi}\left(1 - e^{-\frac{\psi}{\tau}}\right) \tag{3.40}$$

$$\tilde{\varphi} = \frac{\epsilon\psi}{\frac{\psi}{\tau} - \frac{1}{2}\left(\frac{\psi}{\tau}\right)^2 + \cdots} \approx \epsilon\tau \ . \tag{3.41}$$

It is intuitive to check whether this holds for large values of t in comparison to Eq. (3.38), *i.e.* $\tau \approx \frac{1}{KL}$. Since our $g(\bar{\theta})$ has the form $g(\bar{\theta}) = \left(\frac{\mathrm{d}}{\mathrm{d}\bar{\theta}}\ln(T) + \frac{2\mathrm{J}^2\delta t\sigma'^2(\bar{\theta})}{T}\right)$ and therefore

$$\frac{1}{KL} = \frac{\frac{1}{\xi}\left[\psi + \mathrm{J}\delta t\int_0^{\xi}\frac{\sigma'(\bar{\theta}'')}{T(\bar{\theta}'')}\mathrm{d}\bar{\theta}''\right]}{\frac{1}{\xi}\left[\ln\left(\frac{T(\xi)}{T(0)}\right) + 2\mathrm{J}^2\delta t S\right]} \approx \frac{\psi}{2\mathrm{J}^2\delta t S} = \tau \ .$$

The ratio $\frac{T(\xi)}{T(0)} = 1$ since T is periodic with period ξ. In particular, we require $\tilde{\varphi} < \frac{\xi}{2}$, and consequently $\epsilon < \frac{\xi}{2\tau}$ to have the system remains entrained asymptotically. However this condition is necessary but not sufficient. In fact we require $\epsilon \ll \frac{\xi}{2\tau}$ in order to keep the system entrained. The necessary condition $\tilde{\varphi} < \frac{\xi}{2}$ arises due to the fact that our linearised solution (2.41) assumes synchronisation strength is linear, somewhat in the form of $\dot{\varphi} = -\frac{\varphi}{\tau}$, according to the displacement in θ_i. Keeping in mind that our linearsation only valid for small values of φ and δt, therefore linearisation breaks down for $\varphi \geq \frac{\xi}{2}$ [8].

[8] As indicated in Section 2.5.3, for any $(\theta_2(0) - \theta_1(0)) \in \left(n\xi - \frac{\xi}{2}, n\xi\right)$ then the system should syn-

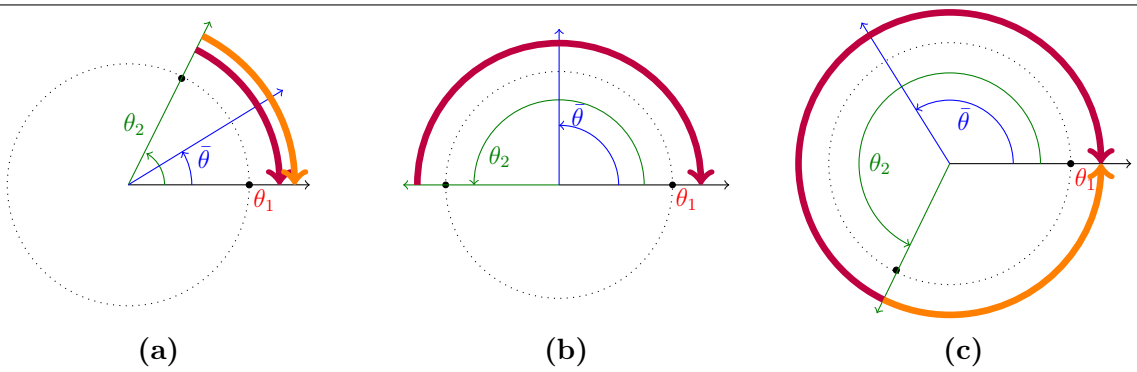

(a) **(b)** **(c)**

Figure 3.10: Graphical illustration of synchronisation behaviour, *i.e.* $E(\lambda_i)$ is negative, of our linearised solution (thick red) in comparison to our full system (thick orange). Figure 3.10a: if $2\varphi_0 = \theta_2(0) - \theta_1(0)$ is small then both linearisation and full system will synchronise to zero phase difference. Figure 3.10b: if $2\varphi_0 = \frac{\xi}{2}$, linearised solution shows convergence but analytically the system will be stuck at the unstable fixed point. Figure 3.10c: linearised solution continues to predict convergence to 0 proportional to the displacement but the full system should synchronise to 1.

Subsequently we could take a step further to have time dependent $\epsilon = \epsilon(t)$, the logic in the derivation above holds however our $\tilde{\varphi}$ will then also be time dependent, *i.e.* $\tilde{\varphi} = \tilde{\varphi}(t)$. This comes naturally as we expect oscillatory behaviour if the system remains in entrainment. The contribution of desynchronisation is then $\int_0^{\psi} \epsilon(t)\mathrm{d}t$ while the contribution of synchronisation is $\tilde{\varphi}\left(1 - e^{-\frac{\psi}{\tau}}\right) \approx \frac{\tilde{\varphi}}{\tau}\psi = \frac{\tilde{\varphi}}{\tau}\int_0^{\psi} \mathrm{d}t$ per period of σ. If we now consider the rate of the varying $\tilde{\varphi}$ in terms of the rivalry between desynchronisation and synchronisation, this gives

$$\epsilon - \frac{\tilde{\varphi}}{\tau} = \dot{\tilde{\varphi}} \tag{3.42}$$

which has a general solution of the form, with integration constant C,

$$\tilde{\varphi}(t) = -Ce^{-\frac{t}{\tau}} + \int_0^t e^{-\frac{t-t'}{\tau}}\epsilon(t')\mathrm{d}t' \approx \int_0^t e^{-\frac{t-t'}{\tau}}\epsilon(t')\mathrm{d}t' \tag{3.43}$$

as the first term is negligible if t is large. In the cases that we have $t = \psi$ and ϵ is constant in time, then we recover the approximation by Eq. (3.41). If we now consider

chronise to $n\xi$ because of the unstable fixed point at $n\xi - \frac{\xi}{2}$ but our linearisation (2.41) suggested that the phase difference always converges to 0 in the presence of time delay.

$\epsilon(t) = a\sin\left(\frac{t}{b}\right)$, after some calculus Eq. (3.43) yields

$$\tilde{\varphi} = \frac{a\tau}{\left(\frac{\tau}{b}\right)^2+1}\left[\sin\left(\frac{t}{b}\right) - \frac{\tau}{b}\cos\left(\frac{t}{b}\right) + \mathcal{O}(e^{-\frac{t}{\tau}})\right] \in \left[-\frac{a\tau\left(1+\frac{\tau}{b}\right)}{\left(\frac{\tau}{b}\right)^2+1}, \frac{a\tau\left(1+\frac{\tau}{b}\right)}{\left(\frac{\tau}{b}\right)^2+1}\right] \quad . \quad (3.44)$$

This gives a description of the system when the transient behaviour has died off, that is; when the first term of Eq. (3.37) is approximately zero. The system will be oscillating but encapsulated within a periodic function, see Figure 3.11.

If the value of $b \gg \tau$, adequately means that the effect of sine function is diluted by factor b, this gives the necessary, but not sufficient, condition that $a < \frac{\xi}{2\tau}$. If the value of b is significantly large, then due to the fact that $\lim_{x\to\infty}\left(x\sin\left(\frac{1}{x}\right)\right) = 1$ then we are effectively implementing $\epsilon(t) = a$, see Figure 3.12.

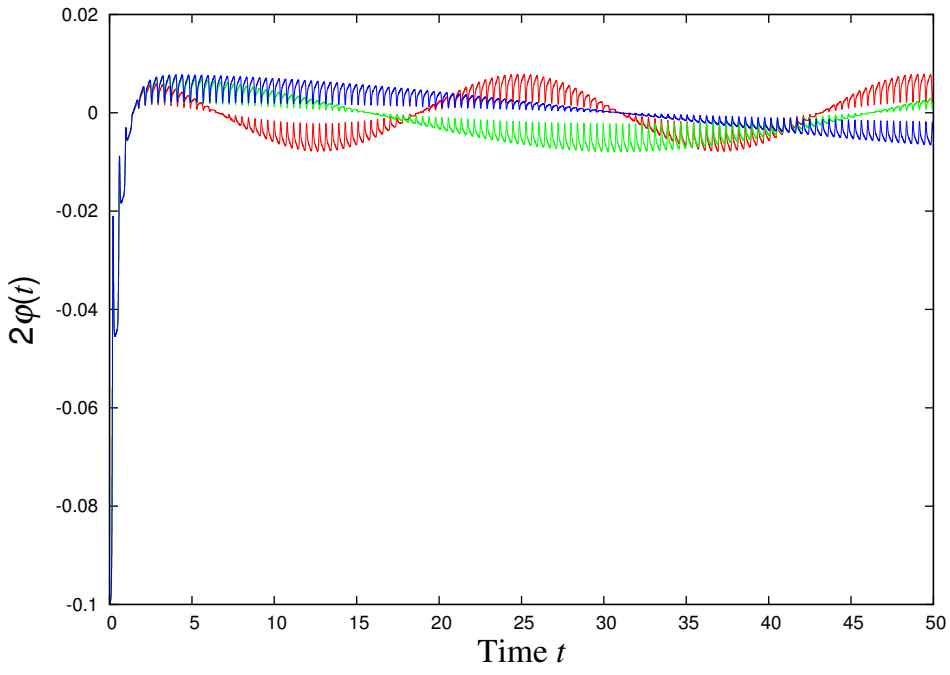

Figure 3.11: Trajectories of full system (RK4) with $a = 0.005$ and different values of b: $b = 10$ (red), $b = 25$ (green) and $b = 50$ (blue). Parameters used: $\Delta t = 1 \times 10^{-6}$, $\xi = 1.01$, $\zeta = 0.1$ and $\delta t = 0.01$.

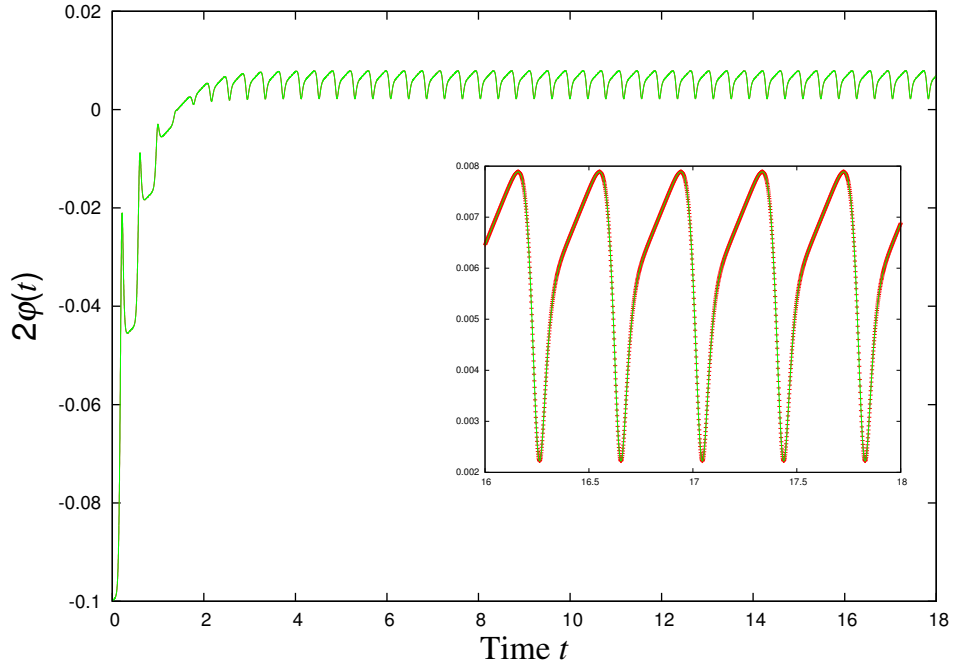

Figure 3.12: Trajectories of full system (RK4) with $\epsilon = 0.005$ (red) and $\epsilon(t) = 0.005 \sin\left(\frac{t}{1000000}\right)$ (green). Parameters used: $\Delta t = 1 \times 10^{-6}$, $\xi = 1.01$, $\zeta = 0.1$ and $\delta t = 0.01$. Inset: trajectories between time 16 and 18.

3.4.2 General case with different eigen-frequencies for N-oscillator model

If we now extend our analysis into N-oscillator time delay system with different, but fixed, initial eigen-frequencies, our equations of motion for our system are

$$\dot{\theta}_i = \omega_i + \sum_{j=1}^{N} J_{ij}\sigma(\theta_j(t-\delta t)) \ . \tag{3.45}$$

In the light of the 2-oscillator case, we can express our $\omega_i = \omega + \epsilon_i$; with average eigen-frequency ω and the deviations ϵ_i and therefore we can write the equations of motion in vector form

$$\dot{\theta}_i = \omega + \epsilon_i + \sum_{j}^{N} J_{ij}\sigma(\theta_j(t-\delta t)) \quad \Rightarrow \quad \left|\dot{\theta}\right\rangle = \omega\,|1\rangle + |\epsilon\rangle + \boldsymbol{J}\,|\sigma(\theta)\rangle \ . \tag{3.46}$$

Similarly, we define $|\varphi\rangle = |\theta\rangle - \bar{\theta}\,|1\rangle$ and $\bar{\theta} = \frac{1}{q}\left\langle 1|\dot{\theta}\right\rangle$, where $q = \langle 1|1\rangle$. We then define $|\varphi'\rangle = \frac{|\dot{\varphi}\rangle}{\dot{\bar{\theta}}}$, and since $\langle e_i|1\rangle = 0$ (see Section 3.3.2), we have

$$\begin{aligned}\langle e_i|\varphi'\rangle = \frac{\langle e_i|\varphi'\rangle}{\dot{\bar{\theta}}} &= \frac{\langle e_i|\epsilon\rangle + \langle e_i|\boldsymbol{J}|\sigma(\theta(t-\delta t))\rangle}{\frac{1}{q}\left(q\omega + \langle 1|\epsilon\rangle + \langle 1|\boldsymbol{J}|\sigma(\theta(t-\delta t))\rangle\right)} \\ &= \frac{\langle e_i|\epsilon\rangle + \lambda_i\,\langle e_i|\sigma(\theta(t-\delta t))\rangle}{\omega + \frac{1}{q}\,\langle 1|\epsilon\rangle + \frac{\tilde{\mathrm{J}}}{q}\,\langle 1|\sigma(\theta(t-\delta t))\rangle}\end{aligned} \tag{3.47}$$

where $\langle e_i|$ are the corresponding left-hand side eigenvectors of eigenvalues λ_i; and $\langle 1|$ is the left-hand side eigenvector of eigenvalue $\tilde{\mathrm{J}}$ where $\tilde{\mathrm{J}} = \tilde{\mathrm{J}}_i = \sum_j \mathrm{J}_{ij}$. Comparing Eq. (3.47) to Eq. (3.33) and (3.34), the term $\langle e_i|\epsilon\rangle$ is expected as it corresponds to the projection of $\langle e_i|$ onto the deviations $|\epsilon\rangle$. However there is an extra term, namely the $\langle 1|\epsilon\rangle$ term, in the $\dot{\bar{\theta}}$ expression, where it does not exist in Eq. (3.33), this is just because the scalar product $\langle 1|\epsilon\rangle$ vanishes [9] in Eq. (3.33). Combining the results from Section 3.3.2 and Section 3.4.1, this directly yields

$$\langle e_i|\varphi'\rangle = \langle e_i|\varphi\rangle\, g_i(\bar{\theta}) + \langle e_i|\epsilon\rangle\,\frac{\left[1-\lambda_i\delta t\sigma'(\bar{\theta})\right]}{T} \tag{3.48}$$

where $g_i(\bar{\theta}) = \frac{\lambda_i}{\tilde{\mathrm{J}}}\left[\frac{T'}{T} + \frac{\delta t\left(-\tilde{\mathrm{J}}\lambda_i\sigma'^2(\bar{\theta}) + \tilde{\mathrm{J}}^2\sigma'^2(\bar{\theta})\right)}{T}\right]$ and $T(\bar{\theta}) = \dot{\bar{\theta}} = \omega + \frac{1}{q}\,\langle 1|\epsilon\rangle + \tilde{\mathrm{J}}\left[\sigma(\bar{\theta}) - \delta t\dot{\bar{\theta}}\sigma'\bar{\theta})\right]$. The factor $\frac{\left[1-\lambda_i\delta t\sigma'(\bar{\theta})\right]}{T}$ comes from rearranging the expansion in the linearisation of $\langle e_i|\varphi\rangle$, see Appendix A for the full derivation. Eq. (3.48) coincides with Eq. (3.35) since the other eigenvalue of the matrix $\left(\begin{smallmatrix}0 & \mathrm{J}\\ \mathrm{J} & 0\end{smallmatrix}\right)$ is $-\mathrm{J}$. We solve our equation by using the integrating factor $\exp\left(-\int_{\bar{\theta}(0)}^{\bar{\theta}(t)} g_i(\bar{\theta}')\mathrm{d}\bar{\theta}'\right)$, which gives

$$\langle e_i|\varphi\rangle = -C_i e^{\int_{\bar{\theta}(0)}^{\bar{\theta}(t)} g_i(\bar{\theta}')\mathrm{d}\bar{\theta}'} + \int_{\bar{\theta}(0)}^{\bar{\theta}(t)} \langle e_i|\epsilon\rangle\,\frac{\left[1-\lambda_i\delta t\sigma'(\bar{\theta}'')\right]}{T(\bar{\theta}'')} e^{\int_{\bar{\theta}''(t)}^{\bar{\theta}(t)} g_i(\bar{\theta}')\mathrm{d}\bar{\theta}'}\mathrm{d}\bar{\theta}'' \tag{3.49}$$

where C_i is the integration constant. Again, since our $g(\bar{\theta})$ has the form

$$g_i(\bar{\theta}) = \frac{\lambda_i}{\tilde{\mathrm{J}}}\left[\frac{T'}{T} + \frac{\delta t\left(-\tilde{\mathrm{J}}\lambda_i\sigma'^2(\bar{\theta}) + \tilde{\mathrm{J}}^2\sigma'^2(\bar{\theta})\right)}{T}\right] = \frac{\mathrm{d}}{\mathrm{d}\bar{\theta}}\ln T^{\frac{\lambda_i}{\tilde{\mathrm{J}}}} + \frac{\lambda_i(\tilde{\mathrm{J}}-\lambda_i)\delta t\sigma'^2}{T} \tag{3.50}$$

[9] Indeed, our matrix in Section 3.3.2 is $\boldsymbol{J} = \left(\begin{smallmatrix}0 & \mathrm{J}\\ \mathrm{J} & 0\end{smallmatrix}\right)$ and therefore the eigenvector $\langle 1|$ is $(1\ 1)$ with associated eigenvalue J. For $|\epsilon\rangle = (\epsilon, -\epsilon)$ and then $\langle 1|\epsilon\rangle$ vanishes.

then our linearised solution suggests that whether the system will result in effective entrainment [10] will be solely depended on the sign of the eigen-product $E(\lambda_i)$. If the eigen-product is negative, then we can consequently simplify Eq. (3.49) to obtain the asymptotic behaviour of such system, *i.e.* the system will effectively entrained to a certain amplitude $\langle e_i|\varphi\rangle \cong \frac{\langle e_i|\epsilon\rangle}{K_i L_i}$ with $K_i = \frac{1}{\xi}\int_0^{\xi} g_i(\bar{\theta}')\mathrm{d}\bar{\theta}'$ and $\frac{1}{L_i} = \frac{1}{\xi}\int_0^{\xi} \frac{[1+\lambda_i\delta\sigma'(\bar{\theta}'')]}{T(\bar{\theta}'')}\mathrm{d}\bar{\theta}''$ as proposed in the two-oscillator model. However as suggested by our findings in Section 3.3.4, this linearised solution (3.49) will not capture the entrainment behaviour, instead it suggests unstable behaviour as long as the eigen-product is positive, disregard the effect of ϵ. In order to capture the entrainment behaviour for positive values of eigen-products, we will need to include the second order approximation of φ (3.30) then Eq. (3.48) becomes

$$\langle e_i|\varphi'\rangle = \frac{\langle e_i|\epsilon\rangle\left[1-\lambda_i\delta t\sigma'(\bar{\theta})\right]}{T} + \langle e_i|\varphi\rangle\, g_i(\bar{\theta}) + \langle e_i|\varphi\rangle^2\,\frac{\frac{1}{2}\lambda_i\mu_i^2\sigma''(\bar{\theta})}{T}\,. \tag{3.51}$$

For ordinary differential equation in the form of Eq. (3.51), neither a Berloulli's equation nor Abel equation of the first kind, is very difficult to solve. However as we know that the system should still remain in entrainment as both second order approximation of φ (entrainment) and effect of ϵ (effective entrainment) produce entrainement effects, the overall effect should still be periodic, despite there may have some rivalrous, or even additive, development between these quantities. We expect $\langle e_i|\varphi\rangle$ to be linear in t plus a periodic function, so one may consider the (Fourier sum) ansatz $\langle e_i|\varphi\rangle = \bar{\theta} + \sum_j A_j \sin\left(\frac{j\pi\bar{\theta}}{\xi}\right)$ to solve Eq. (3.51) however an explicit solution is yet to be found.

One may think that the system should behave the same if we have ϵ_i to be time dependent, $\epsilon_i = \epsilon_i(t)$, however the solution (3.49) is not true for all functions $\epsilon_i(t)$ due to the fact that $\frac{\mathrm{d}}{\mathrm{d}\theta}\langle 1|\epsilon(t)\rangle$ only vanishes if and only if $\langle 1|\epsilon(t)\rangle$ is constant. Generally this is not the case unless we compose $\epsilon(t)$ in a way that by knowing $\langle 1|$, *i.e.* the structure of the coupling matrix, and we weigh the corresponding $\epsilon(t)$ so that the scalar product $\langle 1|\epsilon(t)\rangle$ vanishes. However it will be unrealistic to put constraints on our initial eigen-frequencies.

[10] If the eigen-product is negative then this entrainment phenomenon is produced by the effect of ϵ and therefore we regard this as the effective entrainment as compared to the entrainment captured by the second order approximation of φ.

If we take this into account, then an extra term should be contemplated in the expression of $g_i(\bar{\theta})$, namely the term [11]

$$-\frac{\lambda_i}{\tilde{\mathfrak{J}}}\frac{1}{T}\frac{1}{q}\frac{\mathrm{d}}{\mathrm{d}\bar{\theta}}\langle 1|\epsilon(t)\rangle \ . \tag{3.52}$$

We are able to determine this term because we have bijection between $\bar{\theta}$ and t. However it will be very difficult to characterise or interpret the effect of this term unless $\epsilon_i(t)$ is periodic and bounded. This is because as long as $\epsilon_i(t)$ is periodic and bounded then it is sufficient to show that for negative values of eigen-products, the system will remain in effective entrainment asymptotically [12].

[11] See Section 3.5 for the derivation: to replace η by $\epsilon(t)$ as no properties of Gaussian white noise η has been used .

[12] If the eigen-product is negative, *e.g.* $E_i(\lambda_i) < 0$ and $\epsilon_i(t)$ is periodic and bounded then the contribution of Eq. (3.52), *i.e.* $e^{\left(\int_{\bar{\theta}(0)}^{\bar{\theta}(t)} -\frac{\lambda_i}{\tilde{\mathfrak{J}}}\frac{1}{T}\frac{\mathrm{d}}{\mathrm{d}\bar{\theta}'}\langle 1|\epsilon(t)\rangle \mathrm{d}\bar{\theta}'\right)}$ which is also periodic, will be suppressed by $e^{\int_{\bar{\theta}(0)}^{\bar{\theta}(t)} \frac{E_i(\lambda)\delta t\sigma'^2}{T}\mathrm{d}\bar{\theta}'}$ in the first term of our linearised solution (3.49) while adding additional oscillation to the integrand in the second term, which can then be absorbed into, and therefore approximated by, the function K_i, asymptotically as $t \to \infty$.

3.5 General case with Arbitrary J_{ij} with Gaussian White Noise for N-oscillator Model

We have considered N-oscillator time delay model with different initial eigen-frequencies and explicitly for time dependent initial eigen-frequencies, due to the difficulty posted by the extra effect from Eq. (3.52) in the time dependent case, we suspect that if we consider $\epsilon_i(t)$ as white noises then taking the ensemble averages can facilitate an explicit solution. Therefore in the following section we look into noisy systems whether synchronisation can be obtained or under what condition these N-oscillator models can be synchronised or entrained (with a certain deviation). For simplification, we consider all oscillators has the same initial eigen-frequency. Our equation of motion with white noise added is then

$$\dot{\theta}_i = \omega + \sum_{j=1}^{N} J_{ij}\sigma(\theta_j(t-\delta t)) + \eta_i \quad \Rightarrow \quad \left|\dot{\theta}\right\rangle = \omega\,|1\rangle + \boldsymbol{J}\,|\sigma(\theta(t-\delta t))\rangle + |\eta\rangle \ . \tag{3.53}$$

with $|\eta\rangle = (\eta_1(t), \eta_2(t), \cdots, \eta_N(t))$, where white noise $\eta_i(t)$ is a random Gaussian process with properties

$$\mathbb{E}\left[\eta(t)\right] = 0 \ , \tag{3.54}$$

$$\mathbb{E}\left[\eta(t)\eta(t')\right] = 2\Gamma^2\delta(t-t') < \infty \ . \tag{3.55}$$

In terms of derivation, we do not require any properties of the white noise to obtain the expression of $\langle e_i|\varphi'\rangle$, therefore by comparing Eq. (3.46) and (3.53), which directly gives

$$\langle e_i|\varphi'\rangle = \frac{\langle e_i|\eta\rangle + \lambda_i\,\langle e_i|\sigma(\theta(t-\delta t))\rangle}{\omega + \frac{1}{q}\,\langle 1|\eta\rangle + \frac{\tilde{J}}{q}\,\langle 1|\sigma(\theta(t-\delta t))\rangle}$$

and similarly for our linear approximation of first orders in φ and δt

$$\langle e_i|\varphi'\rangle = \frac{\langle e_i|\eta\rangle\left[1-\lambda_i\delta t\sigma'(\bar{\theta})\right] + \lambda_i\,\langle e_i|\varphi\rangle\left[\sigma'(\bar{\theta}) - \delta t\left(\dot{\bar{\theta}}\sigma''(\bar{\theta}) + \lambda_i\sigma'^2(\bar{\theta})\right)\right]}{\omega + \frac{1}{q}\,\langle 1|\eta\rangle + \tilde{J}\left[\sigma(\bar{\theta}) - \delta t\dot{\bar{\theta}}\sigma'(\bar{\theta})\right]} \ .$$

If we now let $T(\theta) = \omega + \frac{1}{q}\langle 1|\eta\rangle + \tilde{\jmath}\left[\sigma(\bar{\theta}) - \delta t\dot{\bar{\theta}}\sigma'(\bar{\theta})\right]$, then

$$\begin{aligned} T' = \frac{\mathrm{d}}{\mathrm{d}\bar{\theta}}T &= \frac{1}{q}\frac{\mathrm{d}}{\mathrm{d}\bar{\theta}}\langle 1|\eta\rangle + \tilde{\jmath}\left[\sigma'(\bar{\theta}) - \delta t\left(\dot{\bar{\theta}}\sigma''(\bar{\theta}) + \sigma'(\bar{\theta})T'(\bar{\theta})\right)\right] \\ &= \frac{1}{q}\frac{\mathrm{d}}{\mathrm{d}\bar{\theta}}\langle 1|\eta\rangle + \tilde{\jmath}\left[\sigma'(\bar{\theta}) - \delta t\left(\dot{\bar{\theta}}\sigma''(\bar{\theta}) + \tilde{\jmath}\sigma'^2(\bar{\theta})\right)\right] + \mathcal{O}(\delta t^2)\ . \end{aligned}$$

Using this expression of T and T', $\langle e_i|\varphi'\rangle$ can be written as

$$\begin{aligned} \langle e_i|\varphi'\rangle = \frac{\lambda_i}{\tilde{\jmath}}\langle e_i|\varphi\rangle\frac{1}{T(\bar{\theta})}\left[\frac{\mathrm{d}}{\mathrm{d}\bar{\theta}}T(\bar{\theta}) + \tilde{\jmath}^2\delta\sigma'^2(\bar{\theta}) - \lambda_i\tilde{\jmath}\delta t\sigma'^2(\bar{\theta}) - \frac{1}{q}\frac{\mathrm{d}}{\mathrm{d}\bar{\theta}}\langle 1|\eta\rangle\right] \\ + \frac{\langle e_i|\eta\rangle\left[1 - \lambda_i\delta t\sigma'(\bar{\theta})\right]}{T(\bar{\theta})}\ . \end{aligned}$$

Let $\tilde{g}_i(\bar{\theta}) = g_i(\bar{\theta}) - \frac{\lambda_i}{\tilde{\jmath}}\frac{1}{T(\bar{\theta})}\frac{1}{q}\frac{\mathrm{d}}{\mathrm{d}\bar{\theta}}\langle 1|\eta\rangle$, where $g_i(\bar{\theta})$ as defined in Eq. (3.50), and by using the integrating factor $\exp\left(-\int_{\bar{\theta}(0)}^{\bar{\theta}(t)}\tilde{g}_i(\bar{\theta}')\mathrm{d}\bar{\theta}'\right)$ yields the general solution

$$\langle e_i|\varphi\rangle = -C_i e^{\int_{\bar{\theta}(0)}^{\bar{\theta}(t)}\tilde{g}_i(\bar{\theta}')\mathrm{d}\bar{\theta}'} + \int_{\bar{\theta}(0)}^{\bar{\theta}(t)}\frac{\langle e_i|\eta\rangle\left[1 - \lambda_i\delta t\sigma'(\bar{\theta}'')\right]}{T(\bar{\theta}'')}e^{\int_{\bar{\theta}''(t)}^{\bar{\theta}(t)}\tilde{g}_i(\bar{\theta}')\mathrm{d}\bar{\theta}'}\mathrm{d}\bar{\theta}''\ . \tag{3.56}$$

If we now calculate the expectation of the first term in Eq. (3.56) with $\bar{\theta}_0 = \bar{\theta}(0)$,

$$\begin{aligned} \mathbb{E}\left[-C_i e^{\int_{\bar{\theta}_0}^{\bar{\theta}(t)}\tilde{g}_i(\bar{\theta}')\mathrm{d}\bar{\theta}'}\right] &= -C_i e^{\int_{\bar{\theta}_0}^{\bar{\theta}(t)}g_i(\bar{\theta}')\mathrm{d}\bar{\theta}'}\mathbb{E}\left[e^{-\frac{\lambda_i}{\tilde{\jmath}}\int_{\bar{\theta}_0}^{\bar{\theta}(t)}\frac{1}{T(\bar{\theta})}\frac{1}{q}\frac{\mathrm{d}}{\mathrm{d}\bar{\theta}}\langle 1|\eta\rangle\mathrm{d}\bar{\theta}'}\right] \\ &= -C_i e^{\int_{\bar{\theta}_0}^{\bar{\theta}(t)}g_i(\bar{\theta}')\mathrm{d}\bar{\theta}'}\mathbb{E}\left[e^{-\frac{\lambda_i}{\tilde{\jmath}}\frac{1}{q}\int_0^t\frac{1}{T(t')}\frac{\mathrm{d}}{\mathrm{d}t}\langle 1|\eta\rangle\mathrm{d}t'}\right] \\ &= \tilde{C}_i\mathbb{E}\left[\exp\left\{-\frac{\lambda_i}{\tilde{\jmath}}\frac{1}{q}\left(\frac{\langle 1|\eta\rangle}{T(t')}\Big|_0^t - \int_0^t\langle 1|\eta\rangle\frac{\mathrm{d}}{\mathrm{d}t}\left(\frac{1}{T(t')}\right)\mathrm{d}t'\right)\right\}\right]\ . \end{aligned} \tag{3.57}$$

If we put our noise in stochastic calculus terms, our stochastic differential equation is a scalar Wiener process with zero drift and the diffusion coefficient is Γ^2, *i.e.* $\mathrm{d}X_t = \sqrt{2\Gamma^2}\mathrm{d}W_t$. Therefore the corresponding Fokker-Planck equation is $\frac{\partial p}{\partial t} = \Gamma^2\frac{\partial^2 p}{\partial X_t^2}$ which has the solution $p(X_t, t) = \frac{1}{\sqrt{4\pi\Gamma^2 t}}e^{-\frac{X_t^2}{4\Gamma^2 t}}$ with initial condition $p(X_t, 0) = \delta(X_t)$. Then by using this probability density function $p(X_t, t)$, we can compute $\mathbb{E}\left[e^{X_t}\right] = e^{\Gamma^2 t}$. If we now use Feynman path integral, with properties of white noises (3.54) and (3.55), to

determine

$$\mathbb{E}\left[e^{-\int_0^t \eta(t')y(t')\mathrm{d}t'}\right] = \frac{1}{C}\oint e^{-\frac{1}{4\Gamma^2}\int_0^t \eta^2(t')\mathrm{d}t'} e^{\int_0^t \eta(t')y(t')\mathrm{d}t'}\mathrm{D}\eta$$
$$= \frac{1}{C}\oint e^{-\frac{1}{4\Gamma^2}\int_0^t \left(\eta(t')+2\Gamma^2 y(t')\right)^2\mathrm{d}t'}\mathrm{D}\eta \cdot e^{\Gamma^2\int_0^t y^2(t')\mathrm{d}t'} = e^{\Gamma^2\int_0^t y^2(t')\mathrm{d}t'} \quad (3.58)$$

where C is the normalisation constant. Therefore the expectation on the right hand side of Eq. (3.57), by inspection, is somewhat periodic and bounded, of the form $e^{\Gamma^2 Y(t)}$ with appropriately defined $Y(t)$. Hence, if the eigen-product $E(\lambda_i)$ is negative, then the term $e^{E(\lambda_i)\delta t\int_{\bar{\theta}_0}^{\bar{\theta}(t)}\frac{\sigma'^2}{T}\mathrm{d}\bar{\theta}'}$ in $g_i(\bar{\theta})$ will suppress all terms and therefore the expectation of contribution of the first term in Eq. (3.56) is 0 as $t\to\infty$. The second term of Eq. (3.56) is much harder to deal with. However, to some extend, the integrand has the form of $X_t e^{X_t}$, of which we can determine the expectation $\mathbb{E}\left[X_t e^{X_t}\right] = 2\Gamma^2 t e^{\Gamma^2 t}$ by use of Eq. (3.58) with $y(t)$ constant in time. Yet, we are not able to deduce an explicit approximation for Eq. (3.56) but the asymptotic behaviour seems to be related with the diffusion coefficient. In order to find a suitable measure, we look into the desynchronisation strength versus the synchronisation strength as discussed in Section 3.4.1 and Section 3.4.2. We define the quantity d such that, in Riemann sum representation, $d = \sum_{i=0}^{N}\epsilon_i\Delta t$ with $N = \frac{\psi}{\Delta t}$ is the effect of ϵ_i for time ψ, the time for σ to travel through one period. If ϵ_i is Gaussian white noise, then $d = \sum_{i=0}^{N} R\eta_i\Delta t$ where R is the rescaling factor. By property (3.54) we have $\bar{d} = \mathbb{E}[d] = 0$, and by property (3.55)

$$\mathrm{Var}[d] = \mathbb{E}\left[d^2\right] = \mathbb{E}\left[\sum_{i=0}^{N} R\eta_i\Delta t\right]\mathbb{E}\left[\sum_{j=0}^{N} R\eta_j\Delta t\right] = R^2\Delta t^2\mathbb{E}\left[\sum_{i=0}^{N}\eta_i\right]\mathbb{E}\left[\sum_{j=0}^{N}\eta_j\right]$$
$$= R^2\Delta t^2 2\Gamma^2\sum_{i,j}\delta_{ij} = 2\Gamma^2 R^2\Delta t^2\frac{\psi}{\Delta t} = 2\Gamma^2\psi R^2\Delta t$$

since Gaussian white noise is uncorrelated. For standard Gaussian, the second moment is $2\Gamma^2 t$ therefore the rescaling factor is $\frac{1}{\sqrt{\Delta t}}$. If we consider the variance as the average value of the quantity $(d^2-\bar{d})^2$, by dimensional analysis , the desynchronisation strength must be

the standard deviation [13]. On the same page, note that one may write the right hand side of Eq. (3.40) in the form of $\hat{\varphi}(\psi) = \int_0^{t=\psi} \frac{\tilde{\varphi}}{\tau} e^{-\frac{t}{\tau}} \mathrm{d}t$. By defining $\mathbb{E}\left[\hat{\varphi}^n(\psi)\right] = \frac{1}{\psi}\int_0^{\psi} \hat{\varphi}^n(t)\mathrm{d}t$, *i.e.* the moments of $\hat{\varphi}$, then

$$\begin{aligned}
\mathbb{E}\left[\hat{\varphi}(\psi)\right] &= \frac{1}{\psi}\int_0^{\psi} \hat{\varphi}(t)\mathrm{d}t = \frac{1}{\psi}\int_0^{\psi}\int_0^{t} \frac{\tilde{\varphi}}{\tau} e^{-\frac{t'}{\tau}} \mathrm{d}t'\mathrm{d}t \\
&= \tilde{\varphi} + \frac{\tilde{\varphi}}{\psi/\tau}\left(e^{-\frac{\psi}{\tau}} - 1\right) \cong 0 + \mathcal{O}\left(\frac{\psi}{\tau}\right)^2 , \\
\mathrm{Var}\left[\hat{\varphi}(\psi)\right] &= \mathbb{E}\left[\hat{\varphi}^2(\psi)\right] - \left(\mathbb{E}\left[\hat{\varphi}(\psi)\right]\right)^2 \\
&= \frac{\tilde{\varphi}^2}{2\psi/\tau}\left(1 - e^{-\frac{2\psi}{\tau}}\right) - \frac{\tilde{\varphi}^2}{(\psi/\tau)^2}\left(1 - e^{-\frac{\psi}{\tau}}\right)^2 \cong \frac{\tilde{\varphi}^2}{12}\frac{\psi^2}{\tau^2} + \mathcal{O}\left(\frac{\psi}{\tau}\right)^3 .
\end{aligned}$$

Hence Eq. (3.40) in noisy systems becomes $\sqrt{2\Gamma^2\psi} = \tilde{\varphi}\frac{\psi}{\tau\sqrt{12}}$ and therefore we obtain the necessary condition for noisy system on the standard deviation such that

$$\sqrt{2\Gamma^2} < \frac{\xi\sqrt{\psi}}{2\sqrt{12}\tau} . \tag{3.59}$$

If we now consider the rate of the varying $\tilde{\varphi}$ in terms of the rivalry between desynchronisation and synchronisation, Eq. (3.42) is then

$$\mathrm{d}\tilde{\varphi}_t = -\frac{\tilde{\varphi}_t}{\tau}\mathrm{d}t + \mathrm{d}W_t \tag{3.60}$$

a stochastic differentital equation which has drift towards zero at an exponential rate $\frac{1}{\tau}$. We seek a change of variable in the form of $z_t = \tilde{\varphi}_t e^{\frac{t}{\tau}}$ then z_t statisfies the stochastic differential equation $\mathrm{d}z_t = e^{\frac{t}{\tau}}\mathrm{d}W_t$ which gives the solution of $\tilde{\varphi}_t$ as

$$\tilde{\varphi}_t = \tilde{\varphi}_0 e^{-\frac{t}{\tau}} + \int_0^t e^{-\frac{t-u}{\tau}}\mathrm{d}W_u .$$

[13] One may think that, by use of dimensional analysis, we can approximate the desynchronisation strength by the standard deviation, *i.e.* $\sqrt{2\Gamma^2\psi} = \tilde{\varphi}\left(1 - e^{-\frac{\psi}{\tau}}\right) \cong \frac{\tilde{\varphi}\psi}{\tau}$, then $\sqrt{2\Gamma^2} < \frac{\xi\sqrt{\psi}}{2\tau}$ is only a (very) rough estimate as compared to Eq. (3.59).

Then $\mathbb{E}[\tilde{\varphi}_t] = \tilde{\varphi}_0 e^{-\frac{t}{\tau}} \cong 0$ as $t \to \infty$. We can also compute the variance, by use of Itô's isometry,

$$\mathrm{Var}[\tilde{\varphi}_t] = \int_0^t e^{-\frac{2(t-u)}{\tau}} 2\Gamma^2 du = \Gamma^2\tau\left(1 - e^{-\frac{2t}{\tau}}\right) \cong \Gamma^2\tau$$

as $t \to \infty$. Consequently our system with noise, asymptotically, will hover around zero with variance of order $\Gamma^2\tau$, given that our initial phase difference φ and time delay δt are small.

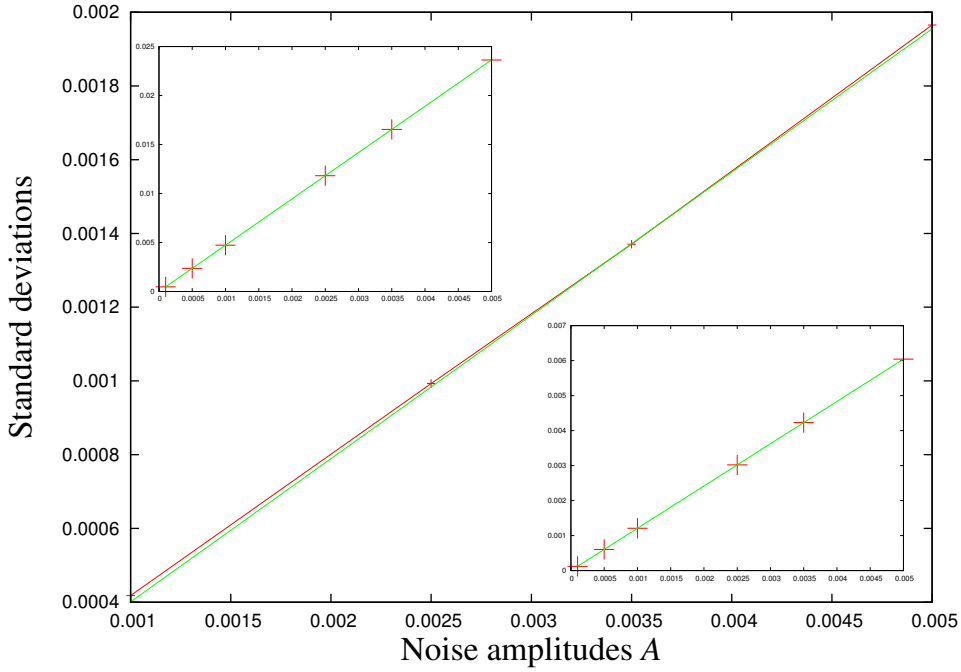

Figure 3.13: Numerical comparisons of different random number generators. Main: Our implementation of Guassian noise outputs, slope = 0.3884. Left inset: ran1 outputs, slope = 0.3488. Right inset: gasdev outputs, slope = 1.3643.

If we now look into the numerical implementation of our system, for any random number generator, say ran(i) which will return the i^{th} random number between 0 and 1. In order to have the mean at zero, we will need to shift ran(i) by $-\frac{1}{2}$. If we have, say, $H_d = \sum_{i=0}^{\frac{t}{\Delta t}} \eta_i \Delta t$ a Riemann sum of the cumulative effect of the noise terms, $\eta_i = \frac{A}{\sqrt{\Delta t}}\mathrm{ran}(i)$ where A defines the noise amplitude, then

$$\mathbb{E}\left[H_d^2\right] = \sum_{i,j} \Delta t^2 \mathbb{E}[\eta_i \eta_j] = \sum_{i,j} \frac{A^2}{\Delta t}\delta_{ij} \int_{-\frac{1}{2}}^{\frac{1}{2}} x^2 \mathrm{d}x = \frac{A^2}{12} t \ .$$

Comparing this to $\mathbb{E}\left[H_c^2\right]$, where $\lim_{\Delta t\to\infty} H_d = \int_0^t \eta(t')\mathrm{d}t' = H_c$,

$$\mathbb{E}[H_c^2] = \mathbb{E}\left[\int_0^t \eta(t_1)\mathrm{d}t_1 \int_0^t \eta(t_2)\mathrm{d}t_2\right] = 2\Gamma^2 t \ .$$

then the relationship $2\Gamma^2 = \frac{A^2}{12}$ should hold. Therefore another, numerical, interpretation of the necessary condition (3.59) is then

$$A < \frac{\xi\sqrt{\psi}}{2\tau} \ . \tag{3.61}$$

One should note that the condition that $2\Gamma^2 = \frac{A^2}{12}$ will generally depend on the random number generator you use. However A should be proportional to $\sqrt{2\Gamma^2}$. Figure 3.13 and insets show the relationships between A and $\sqrt{2\Gamma^2}\sqrt{12}$ for random generators ran1 [53], gasdev by Press *et al.* [53] and our implementation of Gaussian noise. A reference of our implementation can be found in Appendix B.2. We can see that our naïve implementation has a good approximation on the proportionality while ran1 and gasdev have perfect fits.

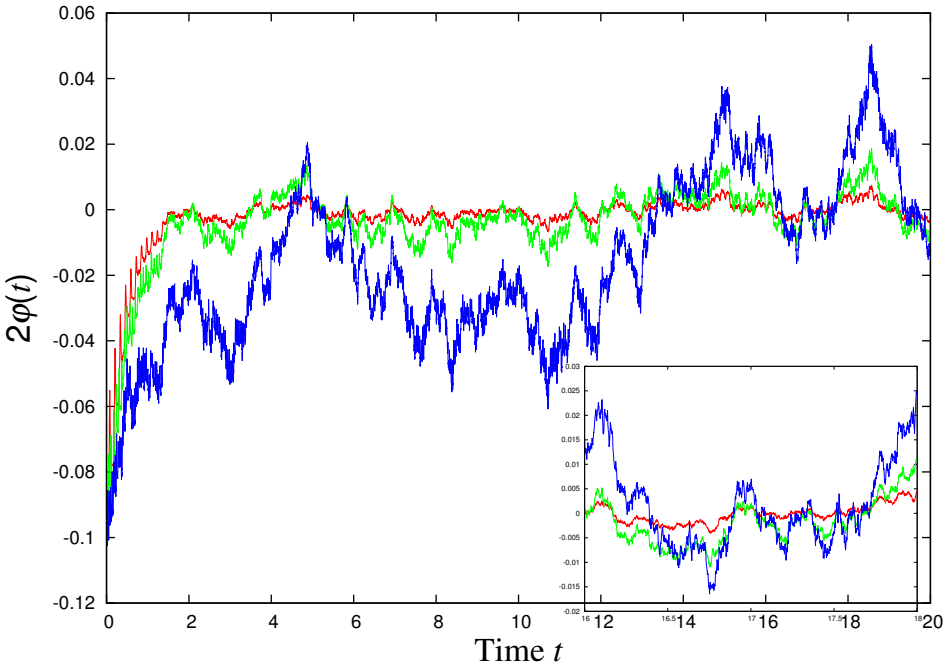

Figure 3.14: Trajectories of noisy systems by RK4 with different noise amplitudes A: $A = 0.01$ (red), $A = 0.025$ (green) and $A = 0.05$ (blue). Inset: trajectories between time 16 and 18. Parameters used: $\delta t = 0.01$, $\xi = 1.01$, $\omega = 2.0$ and $\zeta = 0.1$.

A series of trajectories of noisy system with $N = 2$ can be found in Figure 3.14. If the noise amplitude is relatively large, then the asymptotic behaviour, or in some cases

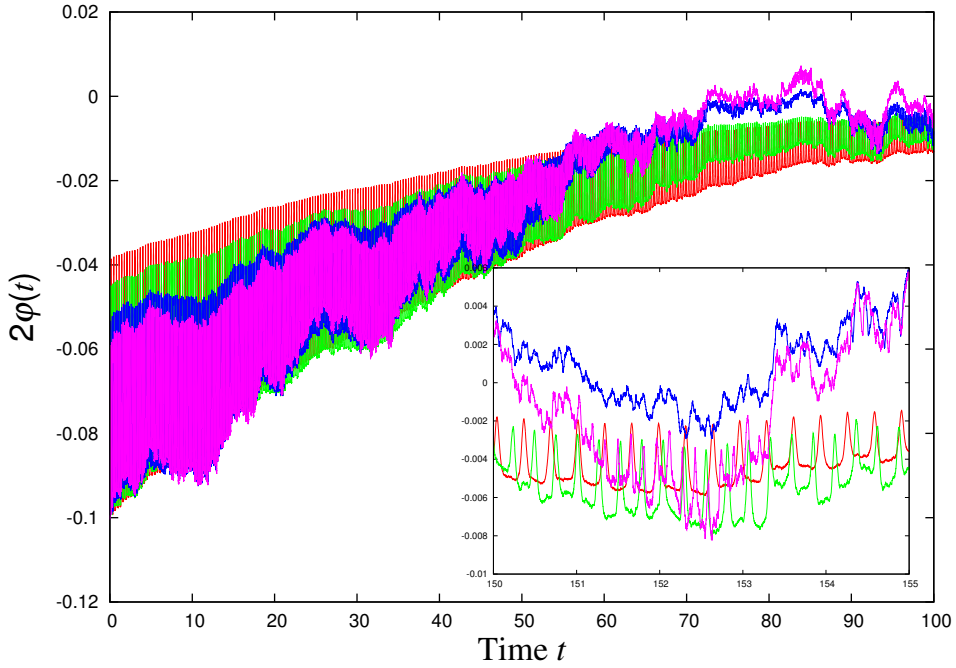

Figure 3.15: Trajectories of noisy systems by RK4 with different noise amplitudes A: $A = 0.001$ (red), $A = 0.0025$ (green), $A = 0.005$ (blue) and $A = 0.0075$ (purple). Inset: trajectories between time 16 and 18, we can see that noise start to dominate in cases of $A = 0.005$ and $A = 0.0075$. Parameters used: $\delta t = 0.0001$, $\xi = 1.01$, $\omega = 2.0$ and $\zeta = 0.1$.

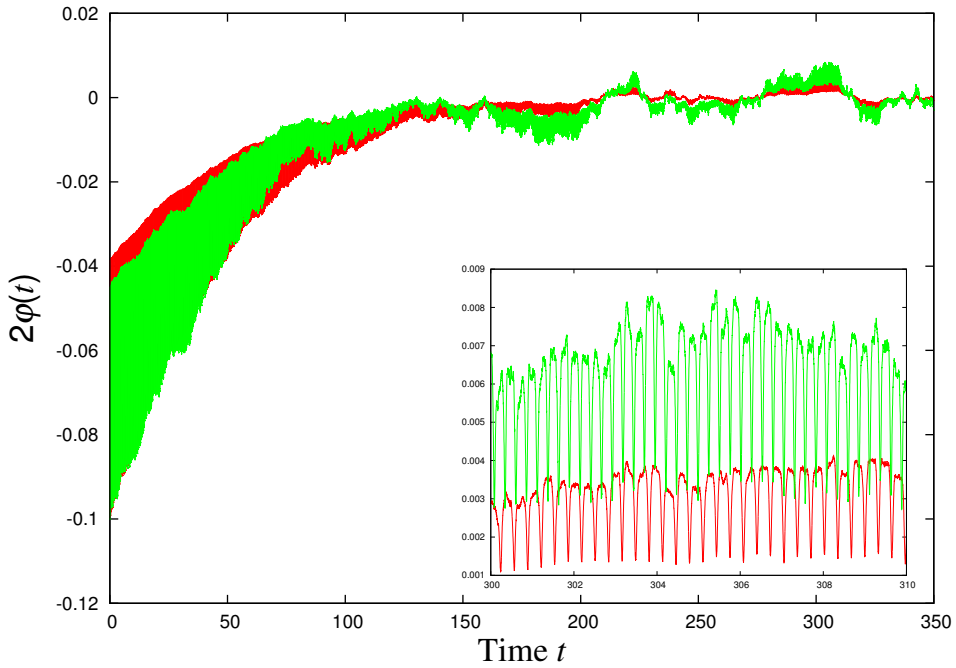

Figure 3.16: Trajectories of noisy systems by RK4 with noise amplitudes $A = 0.001$ (red) and $A = 0.0025$ (green). Oscillations are still encapsulated within noise amplitudes after long time. Inset: trajectories between time 300 and 310. Parameters used: $\delta t = 0.0001$, $\xi = 1.01$, $\omega = 2.0$ and $\zeta = 0.1$.

Noise Amplitude A	Expected Std. Dev. A	Numerical Std. Dev.
0.0010	0.00082757	0.00077960
0.0025	0.00206894	0.00198046
0.0050	0.00413789	0.00380735
0.0075	0.00620683	0.00564561

Table 3.2: Table of numerical outputs of expected standard deviation and the numerical outputs of standard deviations.

that even the transient behaviour, of the system are affected due to large noise amplitude and the behaviour will be purely governed by the noise and therefore chaotic. If this is the case, then one may wonder if the necessary condition (3.61) is ever true, *i.e.* whether we will see some sort of effective entrainment encapsulated between noise amplitudes, as compared to the time dependent $\epsilon(t) = a \sin\left(\frac{t}{b}\right)$ case that effective entrainment being encapsulated in sine waves. We should remind ourselves that the necessary condition (3.61) is only valid for small values of time delay δt (see Section 2.7), therefore large values of τ, compared to ψ (3.39). If we decrease the value of δt, effectively decreasing the necessary condition by same order as τ is inversely proportional to δt, we can see oscillations which are encapsulated within noise amplitudes, see Figure 3.15. However for relatively large values of noise amplitudes A, some point in time the noise will dominate the behaviour (Figure 3.15 inset) while systems with small values of A continues the same behaviour through time (Figure 3.16). If we now look at the expected standard deviation, which is calculated based on the slope factor m of the random number generator (in our case ran1) *i.e.* S.D. $= \frac{A}{m\sqrt{12}}$, and the standard deviations from the numerics, we observed that the percentage errors increases as the noise amplitude A increases (from 4% with $A = 0.001$ to 9% with $A = 0.0075$), see Table 3.2. Despite the fact that there will be numerical errors, for $\delta t = 0.0001$, $\tau \approx 54.83$ (time taken to reduce the initial phase difference by a factor of $\frac{1}{e}$ without noise) and with noise coming into play it will be hard to determine when the transient behaviour has totally died off. Notwithstanding the latter concern, we can see reasonable behaviour of our noisy system, therefore the necessary condition (3.61) indeed holds but only if δt is small compared to ψ and small noise amplitude A.

Chapter 4

Conclusion

We have studied a simple model, which is rooted in Winfree's mean-field model for spontaneous synchronisation [70], with N coupled oscillators with equations of motion

$$\dot{\theta}_i(t) = \omega + \epsilon_i(t) + \sum_{j=1}^{N} \mathrm{J}_{ij}\sigma(\theta_j(t-\delta t)) \ . \tag{4.1}$$

For synchronised state to exist indefinitely, then the constraint $\sum_j \mathrm{J}_{ij} = \tilde{\mathrm{J}}$ needs to be fulfilled. In the cases when $\epsilon_i(t) = 0$, for which we have studied extensively, one might think time delay is insignificant, however it turns out that time delay δt plays a crucial role in synchronisation. We extended our analysis to arbitrary coupling matrices $\boldsymbol{J}$ where $\boldsymbol{J}$ has each $[i,j]$-entry to be the corresponding coupling strength between the i^{th} and j^{th} oscillators. We denote the eigenvalues as λ_i with associated left $\langle e_i|$ and right $|e_i\rangle$ eigenvectors; in the case that the eigenvalue has value $\tilde{\mathrm{J}}$, due to the Markov property of $\boldsymbol{J}$, the right eigenvector, denoted as $|1\rangle$, is a column vector with entries equal to 1. Assume the eigenvectors of $\boldsymbol{J}$ are normalised, so that $\langle e_i|e_j\rangle = 0$ for $i \neq j$, and span the basis of $\boldsymbol{J}$. We define an appropriate parameterisation of the system $|\varphi\rangle = |\theta\rangle - \bar{\theta}\,|1\rangle$, which is the deviation of $|\theta\rangle$ from the asympototic synchronised state $\bar{\theta}$ where $\bar{\theta}$ is defined by the scalar product $\langle 1|\theta\rangle$. Then the linearised solution of Eq. (4.1) with $\epsilon(t) = 0$ is

$$\langle e_i|\varphi(t)\rangle = C_i \left(\frac{T(\bar{\theta}(t))}{T_0}\right)^{\frac{\lambda_i}{\tilde{\mathrm{J}}}} e^{\lambda_i(\tilde{\mathrm{J}}-\lambda_i)\int_{\bar{\theta}_0}^{\bar{\theta}(t)} \frac{\sigma'^2(\bar{\theta}')}{T(\bar{\theta}')}\mathrm{d}\bar{\theta}'} \tag{4.2}$$

with $T_0 = T(\bar{\theta}(0))$, $\bar{\theta}_0 = \bar{\theta}(0)$ and $T(\bar{\theta}) = \dot{\bar{\theta}}$ to first order in δt. The linearised approximation (4.2) suggests that the time evolution of $\langle e_i|\varphi\rangle$ will either converge to zero (synchronisation) or diverge (instability), depending on the sign of the eigen-product $E(\lambda_i) = \lambda_i(\tilde{\mathfrak{J}} - \lambda_i)$ because $T(\bar{\theta})$ is periodic. If $E(\lambda_i) < 0$, the characteristic synchronisation time can be approximated, to leading order, as

$$\tau_i \approx \frac{\psi}{-\lambda_i(\tilde{\mathfrak{J}} - \lambda_i)\delta t S} \tag{4.3}$$

where $\psi = \int_0^{\xi} \frac{\mathrm{d}\bar{\theta}'}{T(\bar{\theta}')}$ and $S = \int_0^{\xi} \frac{\sigma'^2(\bar{\theta}')}{T(\bar{\theta}')}\mathrm{d}\bar{\theta}'$. However, numerical integration of the full system by RK4 scheme [53] suggests something contrasting. For positive values of eigen-products, the numerics of the full system shows that the system will result in entrainment while linearised solution (4.2) proposed that the system diverges. We have showed that this entrainment behaviour correspond to the second order effect of φ, where the system will be entrained to a certain phase difference proportional to the time delay.

In the cases of ϵ is constant, we found that the system will result in effective entrainment, where entrainment is caused by the effect of ϵ, to an amplitude proportional to ϵ. The numerical averages, excluding the transient behaviour, of the full system match very well with the linearised approximation. We use our numerics of the linearised solution to obtain the linear approximation of $\frac{\epsilon}{K_i L_i}$ and compare this approximation to the numerics of the full system. We have obtained an explicit approximation of the full system for eigen-products being negative, and we have argued that for negative eigen-products then with ϵ constant the full system will always result in effective entrainment. For positive values of eigen-products, the linearised solution is not capable to capture the entrainment behaviour unless we include the second order approximation of φ. Since both the second order behaviour and the effect of ϵ are periodic, we expect $\langle e_i|\varphi\rangle$ to be linear in time plus a periodic function, but we were not able to obtain an explicit solution.

If we now make $\epsilon(t)$ to be time dependent, this poses extra difficulty on the linearised solution as we are not able to characterise or interpret the extra , namely the $\frac{\mathrm{d}}{\mathrm{d}\theta}\langle 1|\epsilon(t)\rangle$, term produced when we differentiate the expression of $T(\bar{\theta})$ with respect to $\bar{\theta}$. However,

it is sufficient to argue that if $\epsilon(t)$ is periodic and bounded, then the full system will result in oscillations encapsulated within a periodic function. We have considered the case that $\epsilon(t) = a\sin\left(\frac{t}{b}\right)$ and we found that for significantly large values of b, we are effectively implementing $\epsilon(t) = a$. We have also compared the desynchronisation strength to the synchronisation strength which generally has the form

$$\int_0^{\psi} \epsilon(t')\mathrm{d}t' = \int_0^{\psi} \frac{\tilde{\varphi}}{\tau} e^{-\frac{t}{\tau}} \mathrm{d}t' \ . \tag{4.4}$$

We could simplify Eq. (4.4) according to the structure of $\epsilon(t)$, hence we were able to find necessary, but not sufficient, conditions such that the system can remain in effective entrainment.

Lastly, we considered $\epsilon(t)$ as white noise in Eq. (4.1), hoping that we can deduce an explicit (linear) approximation to the full system by taking ensemble averages. But the difficulty, again, lies in the $\langle 1|\epsilon(t)\rangle$ term of the $T(\bar{\theta})$ expression. Noting that $T(\bar{\theta}) = \dot{\bar{\theta}}$ to first order in δt, and by our very definition $\bar{\theta} = \langle 1|\theta\rangle$, this implies $\dot{\bar{\theta}} = \left\langle 1|\dot{\theta}\right\rangle$. If we try to get our ordinary differential equation in the form of $\varphi' = -H(t(\bar{\theta}))\varphi$ then the term $\frac{\mathrm{d}}{\mathrm{d}\bar{\theta}}\langle 1|\epsilon(t)\rangle$ is unavoidable; otherwise $\langle 1|\epsilon(t)\rangle$ is constant, which is generally unattainable. In hindsight, we may want to consider working with $\langle e_i|\dot{\varphi}\rangle$ instead of $\langle e_i|\varphi'\rangle$. However we made some progress when we considered the desynchronisation strength in terms of standard deviation of the white noise as opposed to the standard deviation of the solution of Eq. (4.4) in stochastic form with asymptotic phase difference $\tilde{\varphi}$, where $\tilde{\varphi} = \lim_{t\to\infty} \frac{1}{t}\int_0^t \varphi(t')\mathrm{d}t'$. The first and second moments of the solution of Eq. (4.4) give a good description of what is happening in the full system. A necessary condition of having oscillation encapsulated in noise amplitude was also derived.

References

[1] Acebrón, J., L. Bonilla, C. Vicente, F. Ritort, and R. Spigler, 2005, *The Kuramoto model: A simple paradigm for synchronization phenomena*, Rev. Mod. Phys. **77**(1), 137–185.

[2] Alstrøm, P., B. Christiansen, and M. T. Levinsen, 1988, *Nonchaotic transition from quasiperiodicity to complete phase locking*, Phys. Rev. Lett. **61**(15), 1679–1682.

[3] Appleton, E., and B. van der Pol, 1922, *XVI. On a type of oscillation-hysteresis in a simple triode generator*, Philos. Mag. Series 6 **43**(253), 177–193.

[4] Appleton, E. V., 1922, in *PCPS-P. Camb. Philol. S.* (Cambridge University Press, Cambridge, England, UK), pp. 420–422.

[5] Arenas, A., A. Díaz-Guilera, J. Kurths, Y. Moreno, and C. Zhou, 2008, *Synchronization in complex networks*, Phys. Rep. **469**(3), 93–153.

[6] Ariaratnam, J., and S. Strogatz, 2001, *Phase diagram for the Winfree model of coupled nonlinear oscillators*, Phys. Rev. Lett. **86**(19), 4278–4281.

[7] Atay, F. M., 2010, *Complex time-delay systems: Theory and applications* (Springer-Verlag Berlin Heidelberg, Germany).

[8] Barahona, M., and L. M. Pecora, 2002, *Synchronization in small-world systems*, Phys. Rev. Lett. **89**(5), 054101–1–4.

[9] Basnarkov, L., and V. Urumov, 2007, *Phase transitions in the Kuramoto model*, Phys. Rev. E **76**(5), 057201.

[10] Basnarkov, L., and V. Urumov, 2009, *Critical exponents of the transition from incoherence to partial oscillation death in the Winfree model*, J. Stat. Mech. **2009**(10), P10014.

[11] Bélair, J., 1986, *Periodic pulsatile stimulation of a nonlinear oscillator*, J. Math. Biol. **24**(2), 217–232.

[12] Boccaletti, S., V. Latora, Y. Moreno, M. Chavez, and D.-U. Hwang, 2006, *Complex networks: Structure and dynamics*, Phys. Rep. **424**(4), 175–308.

[13] Cheang, S., and G. Pruessner, 2011, *The Edwards–Wilkinson equation with drift and Neumann boundary conditions*, J. Phys. A: Math. Theor. **44**(6), 065003.

[14] Choe, C.-U., T. Dahms, P. Hövel, and E. Schöll, 2010, *Controlling synchrony by delay coupling in networks: From in-phase to splay and cluster states*, Phys. Rev. E **81**(2), 025205.

[15] Dahms, T., J. Lehnert, and E. Schöll, 2012, *Cluster and group synchronization in delay-coupled networks*, Phys. Rev. E **86**(1), 016202.

[16] Daprati, E., S. Wriessnegger, and F. Lacquaniti, 2007, *Kinematic cues and recognition of self-generated actions*, Exp. Brain Res. **177**(1), 31–44.

[17] De Mairan, J., 1729, *Observation botanique*, Hist. Acad. R. Sci. Paris , 35–36.

[18] Dhamala, M., V. K. Jirsa, and M. Ding, 2004, *Enhancement of neural synchrony by time delay*, Phys. Rev. Lett. **92**(7), 074104.

[19] Englert, A., S. Heiligenthal, W. Kinzel, and I. Kanter, 2011, *Synchronization of chaotic networks with time-delayed couplings: An analytic study*, Phys. Rev. E **83**(4), 046222.

[20] Flunkert, V., 2011, *Delay-coupled complex systems* (Springer-Verlag Berlin Heidelberg, Germany).

[21] Flunkert, V., O. D'Huys, J. Danckaert, I. Fischer, and E. Schöll, 2009, *Bubbling in delay-coupled lasers*, Phys. Rev. E **79**(6), 065201.

[22] Flunkert, V., S. Yanchuk, T. Dahms, and E. Schöll, 2010, *Synchronizing distant nodes: a universal classification of networks*, Phys. Rev. Lett. **105**(25), 254101.

[23] Glass, L., and M. C. Mackey, 1988, *From clocks to chaos: The rhythms of life* (Princeton University Press, Princeton, NJ, USA).

[24] Heiligenthal, S., T. Dahms, S. Yanchuk, T. Jüngling, V. Flunkert, I. Kanter, E. Schöll, and W. Kinzel, 2011, *Strong and weak chaos in nonlinear networks with time-delayed couplings*, Phys. Rev. Lett. **107**(23), 234102.

[25] Huang, L., Q. Chen, Y.-C. Lai, and L. M. Pecora, 2009, *Generic behavior of master-stability functions in coupled nonlinear dynamical systems*, Phys. Rev. E **80**(3), 036204.

[26] Huygens, C., 1986, *H. Oscillatorium - The Pendulum Clock (Translated by RJ Blackwell)*, Iowa State University Press, Ames, Iowa, USA .

[27] Huygens, C., and J. Vollgraff, 1967, *Oeuvres complètes de Christiaan Huygens: Travaux mathématiques, 1645-1651*, Volume 11 (M. Nijhoff).

[28] Hwang, D.-U., M. Chavez, A. Amann, and S. Boccaletti, 2005, *Synchronization in complex networks with age ordering*, Phys. Rev. Lett. **94**(13), 138701.

[29] Jalife, J., 1984, *Mutual entrainment and electrical coupling as mechanisms for synchronous firing of rabbit sino-atrial pace-maker cells.*, J. Physiol. **356**(1), 221–243.

[30] Jarett, L., 1984, *Psychosocial and biological influences on menstruation: synchrony, cycle length, and regularity*, Psychoneuroendocrino. **9**(1), 21–28.

[31] Just, W., E. Reibold, K. Kacperski, P. Fronczak, J. A. Hołyst, and H. Benner, 2000, *Influence of stable Floquet exponents on time-delayed feedback control*, Phys. Rev. E **61**(5), 5045–5056.

[32] Kaempfer, E., S. Delboe, H. Gibben, and W. Ramsden, 1906, *The history of Japan, together with a description of the Kingdom of Siam, 1690-92* (Macmillan).

[33] Keener, J. P., F. Hoppensteadt, and J. Rinzel, 1981, *Integrate-and-fire models of nerve membrane response to oscillatory input*, SIAM J. Appl. Math. **41**(3), 503–517.

[34] Kim, S., S. Park, and C. Ryu, 1997, *Multistability in coupled oscillator systems with time delay*, Phys. Rev. Lett. **79**(15), 2911–2914.

[35] Kinzel, W., A. Englert, G. Reents, M. Zigzag, and I. Kanter, 2009, *Synchronization of networks of chaotic units with time-delayed couplings*, Phys. Rev. E **79**(5), 056207.

[36] Knight, B. W., 1972, *Dynamics of encoding in a population of neurons*, J. Gen. Physiol. **59**(6), 734–766.

[37] Kuramoto, Y., 1975, in *International symposium on mathematical problems in theoretical physics* (Springer, Berlin, Germany), pp. 420–422.

[38] Kuramoto, Y., 2003, *Chemical oscillations, waves, and turbulence* (Dover Publications, New York, USA).

[39] Kuramoto, Y., and T. Tsuzuki, 1974, *Reductive perturbation approach to chemical instabilities*, Progr. Theoret. Phys. **52**, 1399.

[40] Lehnert, J., T. Dahms, P. Hövel, and E. Schöll, 2011, *Loss of synchronization in complex neuronal networks with delay*, Europhys. Lett. **96**(6), 60013.

[41] Lichtner, M., M. Wolfrum, and S. Yanchuk, 2011, *The spectrum of delay differential equations with large delay*, SIAM J. Math. Anal. **43**(2), 788–802.

[42] Michaels, D., E. Matyas, and J. Jalife, 1987, *Mechanisms of sinoatrial pacemaker synchronization: a new hypothesis*, Circ. Res. **61**(5), 704–714.

[43] Mirollo, R. E., and S. H. Strogatz, 1990, *Synchronization of pulse-coupled biological oscillators*, SIAM J. Appl. Math. **50**(6), 1645–1662.

[44] Néda, Z., E. Ravasz, T. Vicsek, Y. Brechet, and A.-L. Barabási, 2000, *Physics of the rhythmic applause*, Phys. Rev. E **61**(6), 6987–6992.

[45] Niebur, E., H. G. Schuster, and D. M. Kammen, 1991, *Collective frequencies and metastability in networks of limit-cycle oscillators with time delay*, Phys. Rev. Lett. **67**(20), 2753–2756.

[46] Pazó, D., 2005, *Thermodynamic limit of the first-order phase transition in the Kuramoto model*, Phys. Rev. E **72**(4), 046211.

[47] Pecora, L. M., and M. Barahona, 2005, *Synchronization of oscillators in complex networks*, Chaos and Complexity Letters **1**(1), 61–91.

[48] Pecora, L. M., and T. L. Carroll, 1990, *Synchronization in chaotic systems*, Phys. Rev. Lett. **64**(8), 821–824.

[49] Pecora, L. M., and T. L. Carroll, 1998, *Master stability functions for synchronized coupled systems*, Phys. Rev. Lett. **80**(10), 2109–2112.

[50] Peskin, C. S., 1975, *Mathematical aspects of heart physiology* (Courant Institute of Mathematical Sciences, New York University, New York, USA).

[51] Pikovsky, A., M. Rosenblum, and J. Kurths, 2003, *Synchronization: A universal concept in nonlinear sciences* (Cambridge University Press, Cambridge, England, UK).

[52] Popovych, O. V., C. Hauptmann, and P. A. Tass, 2005, *Effective desynchronization by nonlinear delayed feedback*, Phys. Rev. Lett. **94**(16), 164102.

[53] Press, W., B. Flannery, S. Teukolsky, and W. Vetterling, 1992, *Numerical recipes in C* (Cambridge University Press, Cambridge, England, UK).

[54] Pruessner, G., S. Cheang, and H. Jensen, 2012, *Doppler synchronization of pulsating phases by time delay*, http://arxiv.org/abs/1212.2746.

[55] Pyragas, K., 1998, *Synchronization of coupled time-delay systems: Analytical estimations*, Phys. Rev. E **58**(3), 3067–3071.

[56] Rayleigh, J. W. S., 1896, *The Theory of Sound* (Macmillan).

[57] Russell, M., G. Switz, and K. Thompson, 1980, *Olfactory influences on the human menstrual cycle*, Pharmacol. Biochem. Be. **13**(5), 737–738.

[58] Sakaguchi, H., 1988, *Cooperative phenomena in coupled oscillator systems under external fields*, Prog. Theor. Phys. **79**(1), 39–46.

[59] Sakaguchi, H., and Y. Kuramoto, 1986, *A soluble active rotater model showing phase transitions via mutual entertainment*, Prog. Theor. Phys. **76**(3), 576–581.

[60] Sevdalis, V., and P. Keller, 2009, *Self-recognition in the Perception of Actions Performed in Synchrony with Music*, Ann. N.Y. Acad. Sci. **1169**(1), 499–502.

[61] Sherman, A., and J. Rinzel, 1991, *Model for synchronization of pancreatic beta-cells by gap junction coupling*, Biophys. J. **59**(3), 547–559.

[62] Sherman, A., J. Rinzel, and J. Keizer, 1988, *Emergence of organized bursting in clusters of pancreatic beta-cells by channel sharing*, Biophys. J. **54**(3), 411–425.

[63] Smith, H., 1935, *Synchronous flashing of fireflies*, Science **82**(2120), 151–152.

[64] Strogatz, S., 2000, *From Kuramoto to Crawford: exploring the onset of synchronization in populations of coupled oscillators*, Physica D **143**(1-4), 1–20.

[65] Strogatz, S. H., 2003, *Sync: The emerging science of spontaneous order* (Penguin, London, England, UK).

[66] Strogatz, S. H., R. E. Mirollo, and P. C. Matthews, 1992, *Coupled nonlinear oscillators below the synchronization threshold: relaxation by generalized Landau damping*, Phys. Rev. Lett. **68**(18), 2730–2733.

[67] Sun, J., E. M. Bollt, and T. Nishikawa, 2009, *Master stability functions for coupled nearly identical dynamical systems*, Europhys. Lett. **85**(6), 60011.

[68] Van Der Pol, B., 1927, *VII. Forced oscillations in a circuit with non-linear resistance. (Reception with reactive triode)*, Philos. Mag. Series 7 **3**(13), 65–80.

[69] Van Vreeswijk, C., L. Abbott, and G. B. Ermentrout, 1994, *When inhibition not excitation synchronizes neural firing*, J. Comput. Neurosci. **1**(4), 313–321.

[70] Winfree, A., 1967, *Biological rhythms and the behavior of populations of coupled oscillators*, J. Theor. Biol. **16**, 15–42.

[71] Winfree, A. T., 2001, *The geometry of biological time*, Volume 12 (Springer-Verlag, Berlin, Germany).

[72] Wolfrum, M., S. Yanchuk, P. Hövel, and E. Schöll, 2010, in *The European Physical Journal Special Topics* (Springer, Berlin, Germany), pp. 91–103.

[73] Yanchuk, S., and P. Perlikowski, 2009, *Delay and periodicity*, Phys. Rev. E **79**(4), 046221.

[74] Yanchuk, S., M. Wolfrum, P. Hövel, and E. Schöll, 2006, *Control of unstable steady states by long delay feedback*, Phys. Rev. E **74**(2), 026201.

[75] Yeung, M. S., and S. H. Strogatz, 1999, *Time delay in the Kuramoto model of coupled oscillators*, Phys. Rev. Lett. **82**(3), 648–651.

Appendix A

Derivation of Ordinary Differential Equation of linearised $\langle e_i|\varphi\rangle$ in first of φ and δt

We take the system of equations of motion in the form of Eq. (3.46)

$$\dot{\theta}_i = \omega + \epsilon_i + \sum_j^n \mathrm{J}_{ij}\sigma(\theta_j(t-\delta t)) \Rightarrow \left|\dot{\theta}\right\rangle = \omega\,|1\rangle + |\epsilon\rangle + \boldsymbol{J}\,|\sigma(\theta)\rangle$$

then one can obtain Eq. (3.47)

$$\langle e_i|\varphi'\rangle = \frac{\langle e_i|\epsilon\rangle + \lambda_i\,\langle e_i|\sigma(\theta(t-\delta t))\rangle}{\omega + \frac{1}{q}\,\langle 1|\epsilon\rangle + \frac{\tilde{\mathrm{I}}}{q}\,\langle 1|\sigma(\theta(t-\delta t))\rangle}$$

where $|\varphi\rangle = |\theta\rangle - \bar{\theta}\,|1\rangle$ and $\bar{\theta} = \frac{1}{q}\left\langle 1|\dot{\theta}\right\rangle$ with $q = \langle 1|1\rangle$. By expanding $|\sigma(\theta(t-\delta t))\rangle$,

$$|\sigma(\theta(t-\delta t))\rangle = \sigma(\bar{\theta})\,|1\rangle - \delta t\dot{\bar{\theta}}\sigma'(\bar{\theta})\,|1\rangle + \sigma'(\bar{\theta})\,|\varphi\rangle - \delta t\dot{\varphi}\sigma''(\bar{\theta})\,|\varphi\rangle - \delta t\sigma'(\bar{\theta})\,|\dot{\varphi}\rangle$$

Now, we consider the projections of the left-hand side eigenvectors,

$$\begin{aligned}
\langle 1|\sigma(\theta(t-\delta t))\rangle &= q\left[\sigma(\bar{\theta})-\delta t\dot{\bar{\theta}}\sigma(\bar{\theta})\right]\\
\langle e_i|\sigma(\theta(t-\delta t))\rangle &= \langle e_i|\varphi\rangle\,\sigma'(\bar{\theta})-\delta t\left[\langle e_i|\varphi\rangle\,\dot{\bar{\theta}}\sigma''(\bar{\theta})+\langle e_i|\dot{\varphi}\rangle\,\sigma'(\bar{\theta})\right]\\
&= \langle e_i|\varphi\rangle\,\sigma'(\bar{\theta})-\langle e_i|\varphi\rangle\,\delta t\left[\dot{\bar{\theta}}\sigma''(\bar{\theta})+\frac{\langle e_i|\epsilon\rangle}{\langle e_i|\varphi\rangle}\sigma'(\bar{\theta})+\lambda_i\sigma'^2(\bar{\theta})\right]
\end{aligned}$$

where here $\langle e_i|\dot{\varphi}\rangle = \langle e_i|\epsilon\rangle + \lambda_i\sigma'(\bar{\theta})\,\langle e_i|\varphi\rangle + \mathcal{O}(\delta t)$. Therefore, our expression of $\langle e_i|\varphi'\rangle$ becomes

$$\begin{aligned}
\langle e_i|\varphi'\rangle &= \frac{\langle e_i|\epsilon\rangle+\lambda_i\,\langle e_i|\varphi\rangle\left[\sigma'(\bar{\theta})-\delta t\left(\dot{\bar{\theta}}\sigma''(\bar{\theta})+\frac{\langle e_i|\epsilon\rangle}{\langle e_i|\varphi\rangle}\sigma'(\bar{\theta})+\lambda_i\sigma'^2(\bar{\theta})\right)\right]}{\omega+\frac{1}{q}\,\langle 1|\epsilon\rangle+\tilde{\mathrm{J}}\left[\sigma(\bar{\theta})-\delta t\dot{\bar{\theta}}\sigma'(\bar{\theta})\right]}\\
\frac{\langle e_i|\varphi'\rangle}{\langle e_i|\varphi\rangle} &= \frac{\left[\frac{\langle e_i|\epsilon\rangle}{\langle e_i|\varphi\rangle}-\frac{\langle e_i|\epsilon\rangle}{\langle e_i|\varphi\rangle}\lambda_i\delta t\sigma'(\bar{\theta})\right]+\lambda_i\left[\sigma'(\bar{\theta})-\delta t\left(\dot{\bar{\theta}}\sigma''(\bar{\theta})+\lambda_i\sigma'^2(\bar{\theta})\right)\right]}{\omega+\frac{1}{q}\,\langle 1|\epsilon\rangle+\tilde{\mathrm{J}}\left[\sigma(\bar{\theta})-\delta t\dot{\bar{\theta}}\sigma'(\bar{\theta})\right]}
\end{aligned}$$

We then now let $T(\bar{\theta}) = \dot{\bar{\theta}} = \omega + \frac{1}{q}\,\langle 1|\epsilon\rangle + \tilde{\mathrm{J}}\left[\sigma(\bar{\theta})-\delta t\dot{\bar{\theta}}\sigma'\bar{\theta})\right]$ and we can obtain $T'(\bar{\theta})$

$$\begin{aligned}
T'(\bar{\theta}) = \frac{\mathrm{d}}{\mathrm{d}\bar{\theta}}T(\bar{\theta}) &= \tilde{\mathrm{J}}\left[\sigma'(\bar{\theta})-\delta t\left(\dot{\bar{\theta}}\sigma''(\bar{\theta})+\sigma'(\bar{\theta})T'(\bar{\theta})\right)\right]\\
&= \tilde{\mathrm{J}}\left[\sigma'(\bar{\theta})-\delta t\left(\dot{\bar{\theta}}\sigma''(\bar{\theta})+\tilde{\mathrm{J}}\sigma'^2(\bar{\theta})\right)\right]+\mathcal{O}(\delta t^2)
\end{aligned}$$

Hence,

$$\begin{aligned}
\frac{\langle e_i|\varphi'\rangle}{\langle e_i|\varphi\rangle} &= \frac{\lambda_i\left[\sigma'(\bar{\theta})-\delta t\left(\dot{\bar{\theta}}\sigma''(\bar{\theta})+\tilde{\mathrm{J}}\sigma'^2(\bar{\theta})\right)-\delta t\lambda_i\sigma'^2(\bar{\theta})+\tilde{\mathrm{J}}\delta t\sigma'^2(\bar{\theta})\right]}{T}\\
&\quad+\frac{1}{T}\left[\frac{\langle e_i|\epsilon\rangle}{\langle e_i|\varphi\rangle}-\frac{\langle e_i|\epsilon\rangle}{\langle e_i|\varphi\rangle}\lambda_i\delta t\sigma'(\bar{\theta})\right]\\
&= \frac{\lambda_i}{\tilde{\mathrm{J}}}\left[\frac{T'}{T}+\frac{-\tilde{\mathrm{J}}\delta t\lambda_i\sigma'^2(\bar{\theta})+\tilde{\mathrm{J}}^2\delta t\sigma'^2(\bar{\theta})}{T}\right]+\frac{1}{T}\left[\frac{\langle e_i|\epsilon\rangle}{\langle e_i|\varphi\rangle}-\frac{\langle e_i|\epsilon\rangle}{\langle e_i|\varphi\rangle}\lambda_i\delta t\sigma'(\bar{\theta})\right]
\end{aligned}$$

If we let $g(\bar{\theta}) = \frac{\lambda_i}{\tilde{\mathrm{J}}}\left[\frac{T'}{T}+\frac{-\tilde{\mathrm{J}}\delta t\lambda_i\sigma'^2(\bar{\theta})+\tilde{\mathrm{J}}^2\delta t\sigma'^2(\bar{\theta})}{T}\right]$ and the above equation will become

$$\langle e_i|\varphi'\rangle = \langle e_i|\varphi\rangle\,g(\bar{\theta})+\frac{1}{T}\left[\langle e_i|\epsilon\rangle-\langle e_i|\epsilon\rangle\,\lambda_i\delta t\sigma'(\bar{\theta})\right]\ .$$

Appendix B

Code for numerical implementations

B.1 Numerical implementation of Eigenvector-finding Method

```
#define FT_TYPE double
#define FT_OUT "%10.20g"
#define MALLOC(a,n) {if ((a=malloc((n)*sizeof(*(a))))==NULL) \
   {fprintf(stderr, "Fatal error (%s::%i) malloc(3)ing %i bytes for
      variable %s: %i (%s).\n", \
   __FILE__, __LINE__, (int)(n*sizeof(*(a))), #a, errno,
      strerror(errno)); exit(EXIT_FAILURE);}}
#define OUT(a) printf("# %s: " FT_OUT "\n", #a, (FT_TYPE)(a))

FT_TYPE **left_eigvec_matrix(FT_TYPE **J, FT_TYPE *lambda, int N){
  int i, j, k;
  FT_TYPE **eigen_matrix;
  FT_TYPE *left_ev;
  MALLOC(eigen_matrix,N);
  MALLOC(left_ev,N);
  for (i=0; i<N; i++){
    MALLOC(eigen_matrix[i],N);
  }

  for (k=0; k<N; k++){
    left_ev = left_eig_vectors(J,lambda[k],N);
```

```
    normalise_vector(left_ev,N);
    for (j=0; j<N; j++)  eigen_matrix[k][j] = left_ev[j];
    for (i=0; i<N; i++){
      for (j=0; j<N; j++) J[i][j] = ORIG_J[i][j];
    }
  }
  return(eigen_matrix);
}

FT_TYPE **right_eigvec_matrix(FT_TYPE **J, FT_TYPE *lambda, int N){
  int i, j, k;
  FT_TYPE **eigen_matrix;
  FT_TYPE *right_ev;
  MALLOC(eigen_matrix,N);
  MALLOC(right_ev,N);
  for (i=0; i<N; i++){
    MALLOC(eigen_matrix[i],N);
  }

  for (k=0; k<N; k++){
    right_ev = right_eig_vectors(J,lambda[k],N);
    normalise_vector(right_ev,N);
    for (j=0; j<N; j++)  eigen_matrix[j][k] = right_ev[j];
    for (i=0; i<N; i++){
      for (j=0; j<N; j++) J[i][j] = ORIG_J[i][j];
    }
  }
  return(eigen_matrix);
}

FT_TYPE *left_eig_vectors(FT_TYPE **J, FT_TYPE lambda, int N){
  int i;
  int cnt = 0;
  FT_TYPE tau;
  FT_TYPE *y;
```

```
  FT_TYPE *b;
  FT_TYPE **inv;
  MALLOC(y,N);
  MALLOC(b,N);
  MALLOC(inv,N);

  for (i=0; i<N; i++) MALLOC(inv[i],N);
  b = rand_vector(N);
  /* We need to divide drand48() by 1000;
   * since drand48() can return any number in the interval [0,1]. */
  tau = lambda + drand48()/1000.;
  for (i=0; i<N; i++) J[i][i] -= tau;

  inv = mat_inverse(J,N);
  y = vecmatmult(b,inv,N);
  /* Apprroximation of eigenvector after one iteration. */
  //print_vector(y,N);

  while (cnt<600){
    normalise_vector(y,N);
    for (i=0; i<N; i++) b[i] = y[i];
    //normalise_vector(y,N);
    y = vecmatmult(b,inv,N);
    cnt++;
  }

  return(y);
}

FT_TYPE *right_eig_vectors(FT_TYPE **J, FT_TYPE lambda, int N){
  int i;
  FT_TYPE tau, y_norm;
  FT_TYPE *y;
  FT_TYPE *y_old;
  FT_TYPE *b;
```

```
FT_TYPE **inv;
FT_TYPE deviation;
FT_TYPE sign;
int loop=0;

MALLOC(y,N);
MALLOC(y_old,N);
MALLOC(b,N);
MALLOC(inv,N);

for (i=0; i<N; i++) MALLOC(inv[i],N);
b = rand_vector(N);
/* We need to divide drand48() by 1000;
 * since drand48() can return any number in the interval [0,1]. */
if (lambda!=0.)
  tau = lambda * (1.+ drand48()/1000.);
else
  tau = drand48()/1000.;

for (i=0; i<N; i++) J[i][i] -= tau;

inv = mat_inverse(J,N);
y = matvecmult(inv,b,N);
/* Apprroximation of eigenvector after one iteration. */
//print_vector(y,N);

y_norm = norm(y,N);
for (i=0; i<N; i++) y[i]/=y_norm;

do {
  loop++;
  for (i=0; i<N; i++) y_old[i] = b[i] = y[i];
  y = matvecmult(inv,b,N);
  normalise_vector(y,N);
  /* To catch sign flipping: */
```

```
    for (sign=1, i=0; i<N; i++) if ((y[i]!=0) && (y_old[i]!=0)) {
        sign=y[i]/y_old[i]; break; }

    for (deviation=0., i=0; i<N; i++) {
      deviation+=SQUARE(y[i]*sign-y_old[i]);
      //printf("%i %g %g %g\n", loop, y[i], y_old[i], deviation);
    }
    deviation=sqrt(deviation);
    //printf("loop %i %g\n", loop, deviation);
  } while (deviation>EPS);

  return(y);
}

void normalise_vector(FT_TYPE *v, int N){
  int i;
  FT_TYPE v_norm;
  v_norm = norm(v,N);
  for (i=0; i<N; i++) v[i] /= v_norm;
}

FT_TYPE norm(FT_TYPE *v, int N){
  int i;
  FT_TYPE x = 0.;
  for (i=0; i<N; i++) x += SQUARE(v[i]);
  return(sqrt(x));
}

FT_TYPE *rand_vector(int N){
  int i;
  FT_TYPE *v;
  MALLOC(v,N);
  for (i=0; i<N; i++) v[i] = drand48();
  return(v);
}
```

```
FT_TYPE **mat_inverse(FT_TYPE **J, int N){
  int i, j, *indx;
  FT_TYPE d, *col;
  FT_TYPE **M, **tmp1, **tmp2;
  MALLOC(M,N);
  MALLOC(tmp1,N+1);
  MALLOC(tmp2,N+1);
  MALLOC(indx,N+1);
  MALLOC(col,N+1);
  for (i=0; i<N; i++){
    MALLOC(M[i],N);
  }
  for (i=0; i<=N; i++){
    MALLOC(tmp1[i],N+1);
    MALLOC(tmp2[i],N+1);
  }
  /* Brute force the matrix (J) to start at (1,1) as matrix tmp1. */
  for (i=1; i<N+1; i++) tmp1[i] = J[i-1]-1;
  ludcmp(tmp1,N,indx,&d);
  for (j=1; j<=N; j++){
    for (i=1; i<=N; i++) col[i] = 0.0;
    col[j] = 1.0;
    lubksb(tmp1,N,indx,col);
    for (i=1; i<=N; i++) tmp2[i][j] = col[i];
  }
  /* Here tmp2 is the inverse matrix of tmp1. */
  /* Replace the values of tmp2 into M, starting at (0,0). */
  for (i=0; i<N; i++) M[i] = tmp2[i+1]+1;
  //print_matrix(M,N,N);
  //printf("# After printing the inverse matrix. \n");
  return(M);
}
```

find_eigenvectors.c

B.2 Numerical implementation of Gaussian Noise

```
#define FT_TYPE long double
#define FT_OUT "%10.20Lg"

void gaussian_noise(FT_TYPE *eta, int iterations){
  int i, j;
  FT_TYPE x;
  for (i=0; i<NO_OF_OSCILLATORS; i++) eta[i] = 0;
  for (i=0; i<NO_OF_OSCILLATORS; i++){
    for (j=0; j<iterations; j++){
      x = (FT_TYPE)(rand()) / ((double)(RAND_MAX));
      eta[i] += x;
    }
    eta[i] -= (FT_TYPE)(iterations)/2;
    eta[i] *= sqrt(12/((FT_TYPE)(iterations)));
  }
}
```

gaussian_noise.c